

Elena S. Zhitova

Crystal Chemistry of Natural Layered Double Hydroxides

ABSTRACT

The thesis contains results of the first comprehensive crystal chemical study of natural layered double hydroxides (LDHs) from the Kovdor alkaline massif (Kola peninsula, Russia) and the Bazhenovo ultramafic massif (middle Urals, Russia). Various samples were studied by single crystal X-ray diffraction, powder X-ray diffraction, microprobe chemical analysis, and infrared spectroscopy. It has been shown that the studied samples from both deposits belong to quintinite, $[\text{Mg}_4\text{Al}_2(\text{OH})_{12}][(\text{CO}_3)(\text{H}_2\text{O})_3]$, and not manasseite or hydrotalcite as was thought previously. Studies have shown that quintinite has at least four structurally confirmed polytypic modifications: $2H\text{-}3c$ [$6R$], $1M$, $2H$ and $2H\text{-}1c$, three of which ($2H\text{-}3c$, $1M$, $2H$) are completely new and previously unknown, whereas the fourth polytype ($2H\text{-}1c$) is close to the one described previously. An improved scheme for the description of polytypes with stacking layers (in case of ordering of cations in the octahedral layers) is proposed.

Supervisor

Prof. Dr. Sergey V. Krivovichev
Department of Crystallography
Faculty of Geology
Saint-Petersburg State University, Russia

Opponents

Prof. Dr. Anatoly N. Zaitsev (Chairman)
Department of Mineralogy
Faculty of Geology
Saint-Petersburg State University, Russia

Prof. Dr. Vladimir G. Krivovichev
Department of Mineralogy
Faculty of Geology
Saint-Petersburg State University, Russia

Prof. Dr. Igor V. Pekov
Department of Mineralogy
Faculty of Geology
Moscow State University, Russia

Prof. Dr. Stanislav K. Filatov
Department of Crystallography
Faculty of Geology
Saint-Petersburg State University, Russia

Prof. Dr. Giovanni Ferraris
Department of Mineralogy and Petrology
University of Turin, Italy

Prof. Dr. Ronald Miletich-Pawliczek
Institute of Mineralogy and Crystallography
Faculty of Geosciences, Geography and Astronomy
University of Vienna, Austria

Prof. Dr. Olga V. Yakubovich
Department of Crystallography and Crystal Chemistry
Faculty of Geology
Moscow State University, Russia

ACKNOWLEDGEMENTS

I would like to thank my advisor and supervisor, Dr. Sergey V. Krivovichev, who introduced me to crystallography and crystal chemistry. It is a great piece of luck to work with such a talented, kind and understanding man, who is a wonderful exemplar as a scientist and as a person. This thesis would have been impossible without him.

I would like to express the deepest appreciation to Andrey A. Zolotarev who so patiently guided me during my Bachelor and Master works and still helps me in different research. I thank him for his friendly attitude. He spares no effort to teach me to work with different equipment and to educate me on various issues.

I would like to express my gratitude to Victor N. Yakovenchuk for his sustainable moral and scientific support, he was ever attentive to my life (maybe he is the most attentive person I have ever met). Special thanks to him for unique mineralogical collection of samples for this research, for his consultations, for fascinating field practices and for his hospitality.

I wish to thank Yakov A. Pakhomovsky, Grigory U. Ivanuk (Kola Science Centre, RAS) and Andrey A. Antonov (St. Petersburg State University) for their assistance.

Apart from the efforts of myself, the success of any project depends largely on the encouragement and guidelines of many others. I take this opportunity to express my gratitude to, to my family, friends and crystallography and mineralogy departments (St. Petersburg State University).

Last of all, I give a special recognition to Mineralogical Society of Great Britain & Ireland and Springer for the permission to republish articles.

Financial support was provided through the Federal Grant-in-Aid Program “Cadres” (agreement 8313), Russian Foundation for Basic Research (project no. 09-08-12000), and St. Petersburg State University (grant no. 3.37.84.2011). X-ray diffraction studies were partially done in the X-ray Diffraction Resource Centre of St.Petersburg State University.

LIST OF FIGURES

- FIGURE 1 Samples studied in this work from the Kovdor alkaline massif (*a*, *b*, *c*, *d*, *e*, *f*) and from Bazhenovo ultramafic complex (*d*).
- FIGURE 2 The (100) (*a*) and (001) (*b*) sections of reciprocal diffraction space (quintinite- $2H\text{-}3c[6R]$) containing both sharp and diffuse reflections; the latter can be separated into closely separated weak reflections as can be seen from the enlarged part of the (100) section(*c*). The relations between subcell and supercell in the reciprocal lattice section ($hk0$) is shown in *d*. Three-dimensional reconstruction of diffuse streak is shown in (*e*).
- FIGURE 3 The structure of quintinite- $2H\text{-}3c[6R]$ (Q1) (*a*), a projection of the double hydroxide layer (*b*) and the geometry of the $M(OH)_6$ octahedra (*c*).
- FIGURE 4 Reconstructed sections of reciprocal space obtained for quintinite- $1M$: $hk0$ section (*a*: note weak reflections with odd h and k indices), $h0l$ section (*b*: note the presence of sharp Bragg reflections), $h1l$ section (*c*: note the presence of only weakly discrete diffraction streaks elongated along the c^* axis), and enlarged part of the $h1l$ section showing the position of the 311 reflection (*d*). The scheme in (*e*) shows the choice of reciprocal space vectors and indexing of reflections in the $hk0$ section (the black and red colours indicate subcell and supercell vectors and indices, respectively).
- FIGURE 5 The $hk1$ (*a*) and $h0l$ (*b*) sections of reciprocal diffraction space obtained from quintinite- $2H$ crystals.
- FIGURE 6 (001) section of reciprocal diffraction space (left) and (010) section of reciprocal diffraction space (right) obtained from the quintinite- $2H\text{-}1c$ crystal.

LIST OF TABLES

TABLE 1 Crystallographic data and refinement parameters for quintinite polytypes.

CONTENTS

ABSTRACT

ACKNOWLEDGMENTS

LIST OF FIGURES

LIST OF TABLES

CONTENTS

LIST OF INCLUDED ARTICLES

1 INTRODUCTION

2 BRIEF DESCRIPTION OF RESULTS

2.1 OBJECTS AND METHODS

2.2 EXPERIMENTAL RESULTS AND DISCUSSION

2.2.1 QUINTINITE-2H-3c[6R] (KOVDOR)

2.2.2 QUINTINITE-1M (KOVDOR AND BAZHENOVO)

2.2.3 Mg-Al-DISORDERED QUINTINITE-2H (KOVDOR)

2.2.4 QUINTINITE-2H-1c (KOVDOR)

SUMMARY

REFERENCES

INCLUDED ARTICLES

LIST OF INCLUDED ARTICLES

- PI Krivovichev S.V., Yakovenchuk V.N., Zhitova E.S., Zolotarev A.A., Pakhomovsky Ya.A., Ivanyuk G.Yu.. Crystal chemistry of natural layered double hydroxides. 1. Quintinite- $2H$ - $3c$ from Kovdor alkaline massif, Kola peninsula, Russia // Mineralogical Magazine. 2010. Vol. 74(5). P. 821-832.
- PII Krivovichev S.V., Yakovenchuk V.N., Zhitova E.S., Zolotarev A.A., Pakhomovsky Ya.A., Ivanyuk G.Yu. Crystal chemistry of natural layered double hydroxides. 2. Quintinite- $1M$: first evidence of monoclinic polytype in M^{2+} - M^{3+} layered double hydroxides // Mineralogical Magazine. 2010. Vol. 74(5). P. 833-840.
- PIII Zhitova E.S., Yakovenchuk V.N., Krivovichev S.V., Zolotarev A.A., Pakhomovsky Ya.A., Ivanyuk G.Yu. Crystal chemistry of natural layered double hydroxides. 3. The crystal structure of Mg,Al-disordered quintinite- $2H$ // Mineralogical Magazine. 2010. Vol. 74(5). P. 841-848.
- PIV Krivovichev S.V., Antonov A.A., Zhitova E.S., Zolotarev A.A., Krivovichev V.G., Yakovenchuk V.N. Quintinite- $1M$ from Bazhenovskoe deposit (Middle Ural, Russia): crystal structure and properties // Bulletin of Saint-Petersburg State University. 2012. Ser. Geology and Geography (7). № 2. P. 3-9 (in Russian).
- PV Krivovichev S.V., Yakovenchuk V.N., Zhitova E.S. Natural double layered hydroxides: structure, chemistry, and information storage capacity// Minerals as Advanced Materials II (Ed. S.V.Krivovichev). Springer-Verlag, Berlin Heidelberg. 2012. P. 87-91.

OTHER PUBLICATIONS

- AI Zhitova E.S. Zolotarev A.A., Krivovichev S.V., Yakovenchuk V.N. Diffuse scattering and threefold superstructure of quintinite-2H from the Kovdor massif (Kola peninsula, Russia) // Minerals: structure, properties, research methods. Miass. 2009. P. 148-150. (in Russian)
- AII Zhitova E.S., Zolotarev A.A., Krivovichev S.V., Yakovenchuk V.N. Cation ordering and threefold superstructure in Quintinite-2H from the Kovdor alkaline massif, Kola peninsula, Russia // Clays, clay minerals and layered materials – CMLM2009. Moscow. 2009. P. 90.
- AIII Zhitova E.S. Zolotarev A.A., Krivovichev S.V., Yakovenchuk V.N., Pakhomovsky Ya.A. Crystal structure of Mg,Al-disordered quintinite-2H // Fedorov session 2010. Saint Petersburg. 2010. P. 90-91. (in Russian)
- IV Zhitova E.S. Zolotarev A.A., Krivovichev S.V., Yakovenchuk V.N. 2H-polytypes of quintinite from the Kovdor massif (Kola peninsula, Russia) // Minerals: structure, properties, and research methods. Miass. 2011. P. 138-140. (in Russian)
- AV Zolotarev A.A., Krivovichev S.V., Yakovenchuk V.N., Zhitova E.S., Pakhomovsky Ya.A., Ivanyuk G.Yu. Crystal chemistry of natural layered double hydroxides from the Kovdor alkaline massif, Kola Peninsula, Russia. Polytypes of quintinite: cation ordering and superstructures // Peralk-Carb 2011 (workshop on peralkaline rocks and carbonatites). Tubingen. 2011. P. 170-171.
- AVI Zhitova E.S. Zolotarev A.A., Krivovichev S.V., Yakovenchuk V.N. Crystal structure of quintinite-2H-1c from the Kovdor alkaline massif, Kola peninsula, Russia // Crystal chemistry, X-ray diffraction, spectroscopy. Saint Petersburg. 2011. P. 88-89. (in Russian)
- AVII Zolotarev A.A., Krivovichev S.V., Zhitova E.S., Yakovenchuk V.N., Pakhomovsky Ya.A., Ivanyuk G.Yu. Crystal chemistry of natural layered double hydroxides from the Kovdor alkaline massif – prototypes of new materials. Quintinite group // Scientific and practical problems in the field of chemistry and chemical technology. 2011. P. 18-20. (in Russian)
- AVIII Zhitova E.S. Zolotarev A.A., Krivovichev S.V., Yakovenchuk V.N. Crystal structure of quintinite-1M from the Kovdor massif (Kola peninsula, Russia) // 6th National conference on crystal chemistry. Suzdal. 2011. P.35-36. (in Russian)
- AIX Zhitova E.S. Zolotarev A.A., Krivovichev S.V. Crystal chemical study of quintinite from the Kovdor alkaline massif // 11th conference of student scientific society of geological faculty of SPbU. Saint Petersburg. 2011. P. 20-22. (in Russian)
- AX Zhitova E.S., Krivovichev S.V., Zolotarev A.A., Yakovenchuk V.N. Three generations of quintinite from the Kovdor alkaline massif (Kola peninsula, Russia): an X-ray single-crystal diffraction study // European mineralogical conference. 2012. P. 28-30.
- AXI Zhitova E.S. Zolotarev A.A., Krivovichev S.V., Yakovenchuk V.N., Pakhomovsky Ya.A. X-ray diffraction study of three structurally different quintinites from the Kovdor alkaline massif (Kola peninsula, Russia) // Fedorov session 2012. P. 115-116. (in Russian)
- AXII Zhitova E., Krivovichev S., Zolotarev A., Yakovenchuk V. Polytypes of natural layered mineral – quintinite from the Kovdor massif (Kola peninsula, Russia) // Clays, clay minerals and layered materials – CMLM2009. Saint Petersburg. 2013. P. 48.

1 INTRODUCTION

Layered Double Hydroxides (LDHs) are natural minerals and synthetic materials, which also commonly known as «hydrotalcites», «hydrotalcite-manasseite-group minerals» and «anionic clays». These compounds are characterized by structures based upon double brucite-like hydroxide layers $[M_n^{2+}M_n^{3+}(OH)_{2(m+n)}]^{m+}$, where $M^{2+} = Mg^{2+}, Fe^{2+}, Mn^{2+}, Zn^{2+}$, etc.; $M^{3+} = Al^{3+}, Fe^{3+}, Cr^{3+}, Mn^{3+}$, etc. The positive charge of the layer is balanced by interlayer species that may consist of anions ($CO_3^{2-}, Cl^{-}, SO_4^{2-}$, etc.) or both anions and cations (Na^+, Ca^{2+}, Sr^{2+} , etc.). Due to their layered character, LDHs display polytypism and layer stacking disorder. Polytype diversity of LDHs has been described in detail by Bookin and Drits (1993), Bookin *et al.* (1993), and Drits and Bookin (2001), who developed a structural nomenclature for the polytypes observed in this group.

Due to their crystal structures and physical properties LDHs have become important to industry and found applications in catalysis, drug delivery media, absorption of heavy ions and non-ionic organic compounds, photochemistry, electrochemistry, the reduction of oxidized pollutants such as nitrates and carbon dioxide sequestration (Duan and Evans, 2006; Kameda *et al.*, 2012a,b; Kameda and Yoshika, 2011; Newman and Jones, 1998; Génin *et al.*, 2006, 2008, Mills *et al.*, 2012). Another area of interest in LDHs is the theory of the origin of life on the Earth. It had been suggested that clay mineral complexes with organic molecules could constitute the first organisms (Bernal 1951, 1967; Cairns-Smith, 1982). For the MgAl LDHs similar to those studied in this work, Mg-Al cation order is important for catalytic activity correlated with the number and arrangement of adjacent Al^{3+} sites (Kim *et al.*, 2003). Different distribution of Al in a Mg hydroxide matrix also results in different charge distribution in the layer, which is critically important for intercalation reactions. Structural features of LDHs such as cation ordering, charge distribution and polytypism have an immediate influence upon their properties and have been under extensive experimental and theoretical investigations recently.

The archetype of LDHs is hydrotalcite $[Mg_6Al_2(OH)_{16}](CO_3)(H_2O)_4$, which was the first phase to be discovered by Hochstetter in Sweden in 1842 (Hochstetter, 1842) and it gave name firstly to the group of minerals than to the supergroup. A bit later pyroaurite $[Mg_6Fe_2(OH)_{16}](CO_3)(H_2O)_4$ was discovered in Lånban, Värmland, Sweden by Igelstörm (1865). The first chemical formula of hydrotalcite was determined by E. Manasse, professor of Mineralogy at the University of Florence (Italy) in 1915 and hydrotalcite was approved as mineral specie. The first X-ray investigation was conducted by Aminoff and Broomé on pyroaurite in 1931. Frondel (1941) published an X-ray study on hydrotalcite from four localities, including the sample from the type locality. For studied samples two phases were discovered: rhombohedral one with $a = 3.065$, $c = 23.07 \text{ \AA}$ and hexagonal phase $a = 3.06$, $c = 15.34 \text{ \AA}$. The name «hydrotalcite» was reserved for rhombohedral phase and hexagonal one was called manasseite what persisted. However it has been known since the study of Ingram and Taylor (1967), that the two minerals are in fact polytypic modifications (Mills *et al.*, 2012). The name «manasseite» was excluded in 2012 by Mills *et al.* (2012) and renamed to hydrotalcite-2H. Some fundamental works on crystal structures of «hydrotalcites» were published by Taylor (1969, 1973), Allmann (1968), Allmann and Donnay (1969), Allmann and Jepsen (1969). Since 1970 when the first patent for LDHs appeared the interest to those compounds has increased and they are still actively studied nowadays. Recently new nomenclature of 44 natural species of LDH phases was proposed (Mills *et al.*, 2012). This nomenclature combined all 44 minerals in hydrotalcite supergroup which includes 9 mineral groups.

Generally, LDH minerals are not frequent and they commonly found in small quantities and often intergrown, twinned or X-ray amorphous and doesn't form well-diffracting crystals, which makes working with them difficult. Due to this fact, most research on LDHs was done on synthetic materials. All the structural studies on synthetic LDHs deal with powder samples that

prevent elucidation of such fine details of structure architecture as formation of superstructures due to cation ordering. In contrast to synthetic materials, natural LDHs are known to form single crystals accessible to single-crystal X-ray diffraction analysis, which allowed to identify basic features of their crystal chemistry and to demonstrate peculiarities of cation and anion ordering. Structural features of LDHs such as cation ordering, charge distribution and polytypism have an immediate influence upon their properties and have been under extensive experimental and theoretical investigations recently.

This work is based on crystal chemical study of natural minerals, which occur in well formed crystals (up to several cm) within Kovdor alkaline massif (Kola peninsula, Russia) and ultramafic massif (Middle Urals, Russia), which makes them appropriate for X-ray single-crystal investigations.

New results are reported in this thesis for the crystal chemistry of natural LDHs obtained by application of area detectors of X-rays, which provide new opportunities for quantitative studies of commensurate, incommensurate and diffuse scattering features of diffraction patterns.

The main aim of this work is crystal chemical study of samples from the Kovdor alkaline (Kola peninsula, Russia) and Bazhenovo ultramafic (Middle Urals, Russia) massifs in order to study their mineralogical appurtenance, structure peculiarities (cation ordering), and polytypism.

2 BRIEF DESCRIPTION OF RESULTS

2.1 OBJECTS AND METHODS

Crystals studied in this work were found in the Kovdor alkaline (Kola peninsula, Russia) and Bazhenovo ultramafic (Middle Urals, Russia) massifs (Fig. 1). Quantitative chemical analyses were carried out using a Cameca MS-46 electron microprobe (Geological Institute of the Kola Science Centre of the Russian Academy of Sciences, Apatity, Russia) operating at 20 kV and 20-30 nA with a 20 μm beam diameter. Infra-red absorption spectra were recorded using a Bruker Vertex IR spectrometer. The measurements were taken at room temperature, using the KBr pellets technique. Powder X-ray diffraction data were obtained on a STOE-STADI P diffractometer using CuK_α radiation operating at 45 kV and 35 mA. The STOE-WINXPOW software package was used to process the diffraction data. The unit cell parameters refined from the powder data using STOE-WINXPOW.

Single-crystal X-ray diffraction data were collected using Stoe IPDS II Image-Plate-based X-ray diffractometer operated at 50 kV and 40 mA. More than a hemisphere of three-dimensional data were collected for each crystal using monochromatic MoK_α X-radiation. The unit-cell parameters were refined by least-squares methods. The SHELXTL program package was used for all structural calculations (Sheldrick, 2008). The final models included all atomic positional parameters, anisotropic-displacement parameters for atoms of the metal hydroxide layer and refinable weighting schemes of the structure factors. The structures were solved by direct methods and the final models were checked for missing symmetry operations using the PLATON program (Speck, 2003).

2.2 EXPERIMENTAL RESULTS AND DISCUSSION

It has been found that all samples studied in this work in fact correspond to quintinite and not hydrotalcite or manasseite as was thought previously. Crystallographic data and experimental parameters of data collection and structure refinement are listed in Table 1. Below we briefly summarize some peculiarities of diffraction patterns observed and provide their interpretation from the viewpoint of superstructures and polytypism.

2.2.1 Quintinite-2H-3c[6R] (Kovdor)

Inspection of the reconstructed reciprocal lattice slices showed presence of strong, sharp reflections and rows of weak reflections (Fig. 2). Indexing based on the strong set of sublattice reflections resulted in a small subcell with parameters $a = 3.045$ and $c = 15.12$ Å, which agree approximately with unit cell parameters of the $2H_1$ polytype of Mg-Al LDHs (Bookin and Drits, 1993). The weak superlattice reflections define a rhombohedral supercell with unit-cell parameters: $a = 5.2745(7)$, $c = 45.36(1)$ Å. The geometrical relationship between sublattice and superlattice reflections is shown in Fig. 2. Sublattice reflections correspond to conditions $h-k = 3n$ and $l = 3n$, whereas rows of weak intensity maxima extending parallel to c^* occur at $h-k \neq 3n$. Sharp Bragg reflections originate from basic layer stacking of metal hydroxide layers, while weak reflections indicate the formation of 3-D cation superlattices due to the Mg-Al ordering (Krivovichev *et al.*, 2010a; Krivovichev *et al.*, 2012). In the structure of quintinite-2H-3c[6R], Mg and Al are completely ordered on distinct sites, allowing formation of honeycomb structure (Fig. 3b) and resulting in a tripling of the c parameter. The effect of cation ordering in natural LDHs with $M^{2+} = Mg^{2+}$ and $M^{3+} = Al^{3+}$ is governed by the tendency to minimize $M^{3+}-M^{3+}$ repulsive interaction, what is energetically favored and in agreement with the cation avoidance rule (Loewenstein, 1954; Trave *et al.*, 2002). There are three symmetry-independent octahedrally coordinated cation sites in the structure. As the scattering factors of Mg^{2+} and Al^{3+} cations are nearly identical, the only way to distinguish between Mg and Al sites is to evaluate M-O bond lengths. The structure refinement indicates that one M site has bond lengths in the range 1.936-1.940 Å and two M sites have bond lengths of 2.042-2.045 and 2.070-2.077 Å (Fig. 3c). Thus, bond lengths distinguish two distinct types of site that are consistent with ordered occupancy by Al (shorter bonds) and Mg (longer bonds) (Krivovichev *et al.*, 2012a; Krivovichev *et al.*, 2012). The 2H-3c[6R] structure is a superstructure of 2H polytype produced by cation ordering in octahedral layers. According to the LDH polytype nomenclature (Bookin and Drits, 1993), the layer stacking in quintinite-2H-3c[6R] can be described as ...AC = CA = AC... (with A and C being positions of hydroxide ions and b position of cations) and corresponds to that of the two-layer $2H_1$ polytype, as observed for manasseite and quintinite-2H by Arakcheeva *et al.* (1996). However, in contrast to the Brazilian quintinite, the unit cell of our crystal contains six layers. The tripling of the c parameter is caused by the Mg-Al ordering in the $[Mg_2Al(OH)_6]^+$ layer (Fig. 3a).

2.2.2 Quintinite-1M (Kovdor and Bazhenovo)

The three-dimensional diffraction pattern of quintinite-1M contains weak diffuse discrete streaks which clearly indicated the formation of a 2-D superstructure due to Mg-Al ordering (Fig. 4) as it was observed for quintinite-2H-3c[6R]. The integration of weak superlattice reflections into indexing of the diffraction pattern, which was possible using Stoe Integration software (X-Area = 1.42; Stoe, 1997), gave a C-centred monoclinic cell (Table 1). Metal hydroxide layers in monoclinic quintinite have almost perfect Mg-Al ordering which can be inferred from average Mg-O (2.044 Å) and Al-O (1.944 Å) bond lengths. We infer that this cation ordering is responsible for the appearance of weak superstructure reflections, which correspond to the $h-k \neq 3n$ reflections of Mg-Al ordered quintinite-2H-3c[6R] (Krivovichev *et al.*, 2010a). The ordering of M^{2+} and M^{3+} cations in brucite-like layer for quintinite-1M results in symmetry reduction: from rhombohedral ($3R_1$ polytype) to monoclinic (1M) and the formation of superstructure. It is noteworthy that, before our work, monoclinic symmetry has never been observed previously in natural or synthetic LDHs having di- and trivalent cations. This symmetry reduction is induced by the Mg-Al ordering in metal hydroxide layers and the ordered stacking of these layers. Taking into account the small difference in Mg and Al scattering

factors, it is perhaps surprising that Mg-Al ordering is registered by the appearance of weak superstructure reflections.

2.2.3 Mg-Al-disordered quintinite-2H (Kovdor)

Initial indexing of diffraction patterns provided unit cells with parameters $a \approx 3.05$, $c \approx 15.1$ Å, characteristic of manasseite, Mg_3Al-CO_3 LDH (Table 1). Inspection of $hk1$ and $h0l$ sections of reciprocal space (Fig. 5) showed the almost complete absence of superstructure reflections which would indicate Mg-Al ordering in metal hydroxide layers, as has been observed for ordered quintinite polytypes (Krivovichev *et al.*, 2010a,b). The structures were solved in space group $P6_3/mmc$. The stacking sequence of layers can be expressed as ...=AC=CA=..., i.e. with hydroxide anions in A and C, and cations in the b positions. As the structure shows no signs of cation ordering, the studied crystals can be characterized as an Mg-Al-disordered 2H polytype of quintinite, in contrast to Mg,Al-ordered quintinite-2H-1c and quintinite-2H-3c reported by Arakcheeva *et al.* (1996) and Krivovichev *et al.* (2010a), respectively. The observed disorder is probably the result of a higher temperature of formation of the samples compared with the ordered polytypes. This suggestion is in general agreement with the previous observations that demonstrated, for the Mg-Al system, a higher temperature of formation of the hexagonal (or pseudo-hexagonal in the case of quintinite-2H-3c) 2H polytype compared with the rhombohedral (or pseudo-rhombohedral polytype in the case of quintinite-1M) 3R polytype (Bellotto *et al.*, 1996). Indeed, most syntheses of LDHs are carried out at near-ambient temperatures (coprecipitation is the usual synthesis technique) and the samples obtained display either rhombohedral or random layer stacking. As far as we know, no samples with pure hexagonal (manasseite-type) layer stacking have been reported yet. As was pointed out by Pausch *et al.* (1986), in nature, hydrotalcite and manasseite (Mg_3Al-CO_3 LDHs) are commonly intergrown, with manasseite forming the core and hydrotalcite the outer part of a mineral grain. Similar observations were reported by Allmann (1968) for the pyroaurite-sjögrenite ($Mg_3Fe^{3+}-CO_3$ LDHs) crystals from Långban: rhombohedral low-temperature polymorph (pyroaurite) is always found in the outermost shell of natural crystals.

2.2.4 Quintinite-2H-1c (Kovdor)

The diffraction pattern comprises both strong basic and weak superstructure Bragg reflections (Fig. 6), which indicated Mg-Al ordering in the metal hydroxide layers. Crystal structure of quintinite-2H was firstly described by Arakcheeva *et al.* (1996) on a Brazilian sample. The structure was solved in the space group $P-62m$, the unit cell parameters are $a = 5.283(3)$, $c = 15.150(9)$ Å. In addition to different space groups, the distinction between the structure described by Arakcheeva *et al.* (1996) and the structure of Kovdor quintinite-2H-1c lies in the architecture of the interlayer region. Arakcheeva *et al.* (1996) consider the crystal structure of Brazilian quintinite consisting of 3 types of layers. The first type is the $[Mg_2Al(OH)_6]$ octahedral layers. The second one is presented by the $[CO_3]^{2-}$ groups. The third layer contains water molecules only. The layers of the three types alternate along the hexagonal axis and form the sequence -1-2-1-3-1-. In contrast, layers in between octahedral layers in the Kovdor quintinite-2H-1c are identical to each other and consist of both carbonate groups and water molecules.

Mg^{2+} and Al^{3+} atoms occupy the same octahedral sites in every first and third metal-hydroxide layer, what in comparison to quintinite-2H-3c[6R] reduce the amount of layers within the unit cell from six to two. According to Bookin and Drits (1993) nomenclature, this polytype should be described as ...= AC = CA = ... what corresponds to the 2H₁ polytype (Bookin and Drits, 1993; Arakcheeva *et al.*, 1996) and doesn't reflect the difference between polytypes with ordered and disordered distribution of cations in brucite-like layers. It is obvious that for Mg-Al

disordered polytypes cation sites are unknown and layer stacking can be described only as ... = AC = CA = ..., while in Mg-Al-ordered polytype Al occupy b_1 and Mg may occupy b_2 and b_3 sites. Taking into account Mg-Al ordering, the full description of the layer sequence can be written as ... = $Ab_2C = Cb_3A = \dots$ This sequence corresponds to the two-layer polytype and completely characterizes the observed structure, taking into account layer stacking and cation ordering.

In order to distinguish the «classical» manasseite ($a \approx 3.06$, $c \approx 15.34$ Å, Q3 and Q4 in this work) and «classical» quintinite ($a \approx 5.28$, $c \approx 15.15$ Å, Q6-2 and Brazilian sample (Arakcheeva *et al.*, 1996)) unit cells, additional suffix indicating a value of the c parameter compared to the ‘standard’ polytype may be useful. Thus, by analogy with quintinite- $2H-3c$ the structures of the studied sample and Brazilian quintinite (Arakcheeva *et al.*, 1996) can be described as quintinite- $2H-1c$, indicating presence of the Mg-Al ordering and $c \approx 15$ Å. Quintinite- $2H-1c$ is the first cation-ordered polytype with quintinite unit cell for Kovdor samples.

SUMMARY

In this thesis, detailed study of natural LDH polytypes allowed to identify and structurally characterize four different polytypes of quintinite, from which two have been unknown before our work. Cation ordering and superstructures observed by us in quintinite polytypes are probably common to many natural and synthetic LDHs. In particular, it is noteworthy that many minerals previously identified as manasseite or hydrotalcite appeared to be different polytypes of quintinite. For example, the first structure determination of ‘hydrotalcite’ was done on the mineral with the formula $Mg_4Al_2(OH)_{12}(CO_3)(H_2O)_3$, which is obviously quintinite (Allmann and Jepsen, 1969). In 1987, Drits *et al.* reported results of powder XRD studies of ‘manasseite’, again with the formula $Mg_4Al_2(OH)_{12}(CO_3)(H_2O)_3$, which can now be identified as quintinite- $2H$. Distinction of quintinite from hydrotalcite and manasseite is by means of the Mg:Al ratio (2:1 vs. 3:1) (Chao and Gault, 1997). The Mg₂Al stoichiometry shows a strong tendency to cation ordering and the formation of superstructures, as we demonstrated in our papers given at the end of this thesis. However, the present work also demonstrated that Mg,Al-disordered quintinite also exists and it is not clear whether or not the Mg,Al disorder is specifically three-dimensional, i.e. concerns only stacking disorder of fully ordered layers, or is also present within the metal hydroxide layers.

In general, we point out that polytype formation and cation ordering are definitely the result of different temperature regime of growth of quintinite crystals with samples with high symmetry and disorder being formed under elevated temperatures compared to more ordered structures.

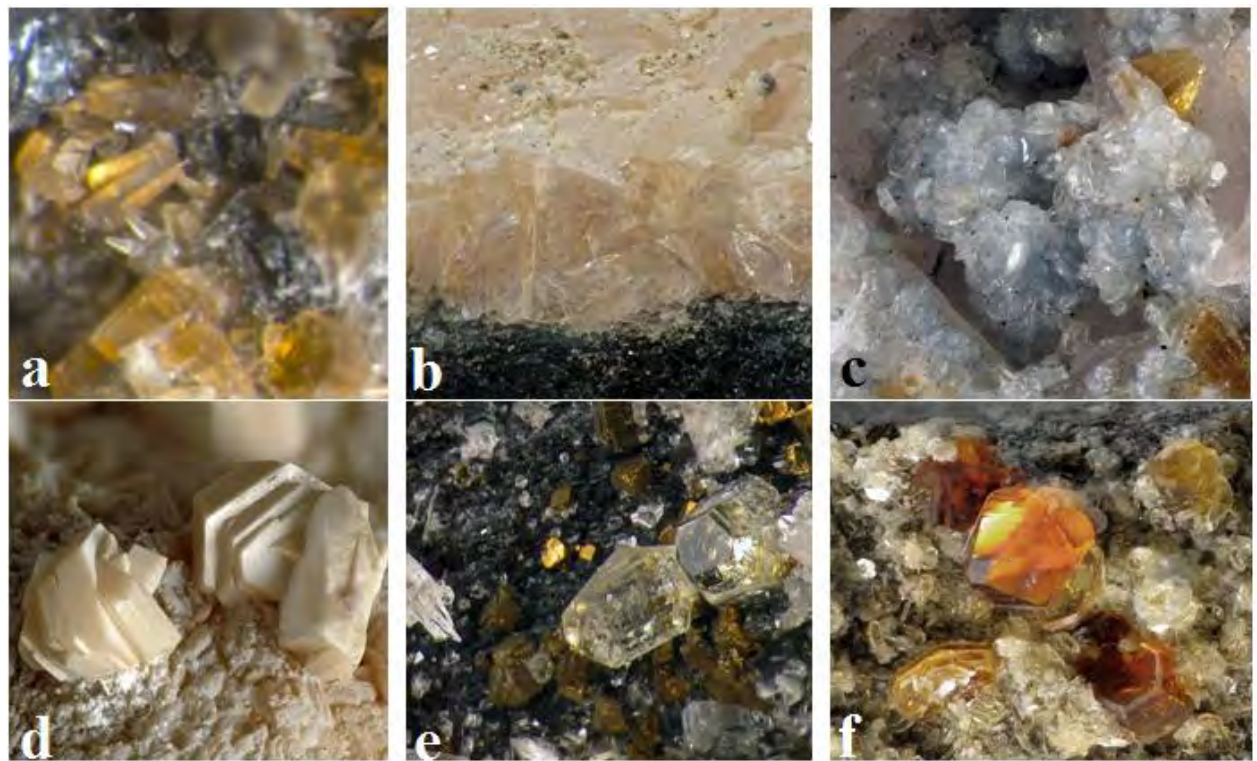


FIG. 1. Samples studied in this work from the Kovdor alkaline massif (*a, b, c, d, e, f*) and from Bazhenovo ultramafic complex (*d*).

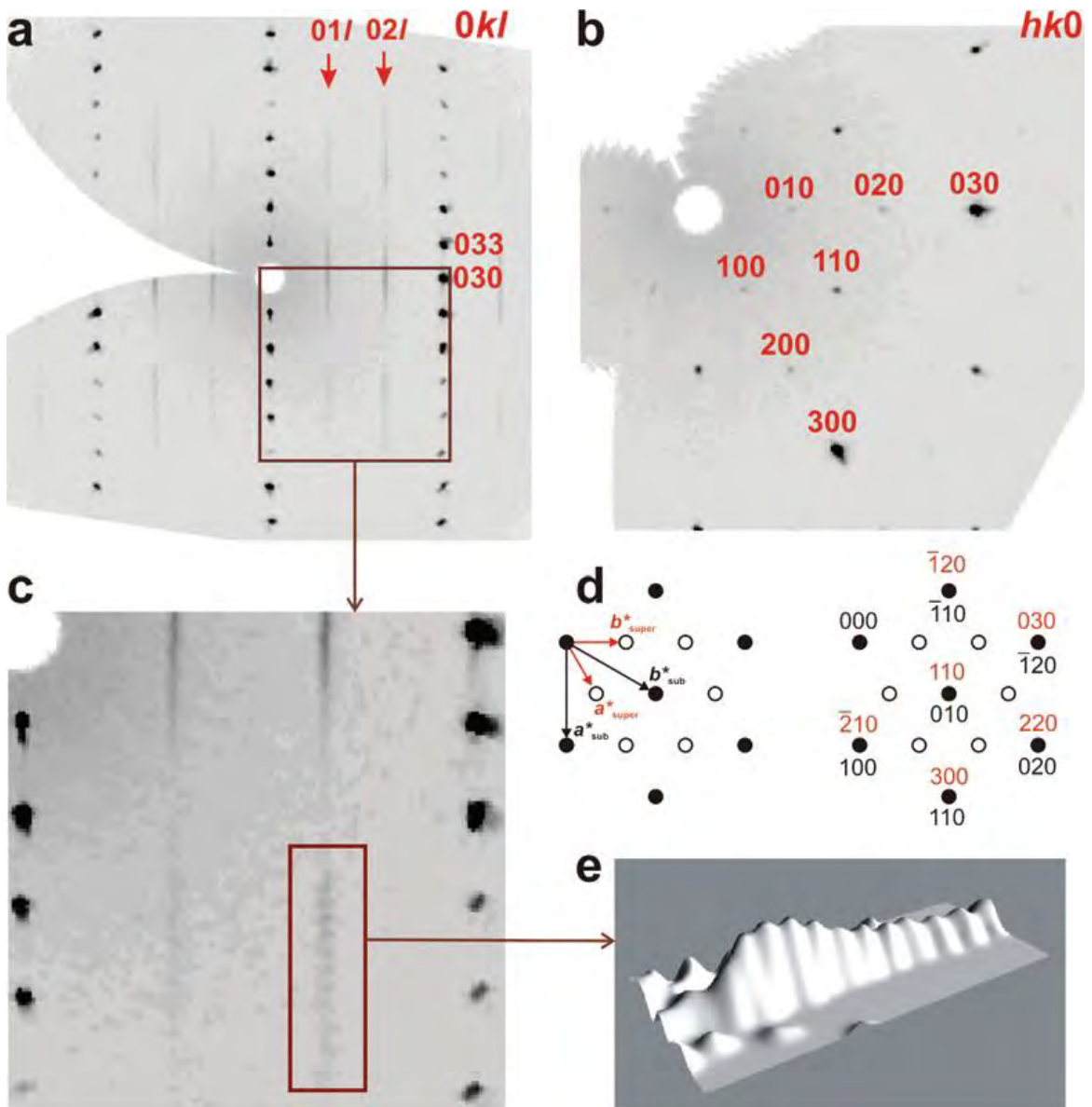


FIG. 2. The (100) (a) and (001) (b) sections of reciprocal diffraction space (quinitite- $2H\text{-}3c[6R]$) containing both sharp and diffuse reflections; the latter can be separated into closely separated weak reflections as can be seen from the enlarged part of the (100) section(c). The relations between subcell and supercell in the reciprocal lattice section ($hk0$) is shown in d. Three-dimensional reconstruction of diffuse streak is shown in (e).

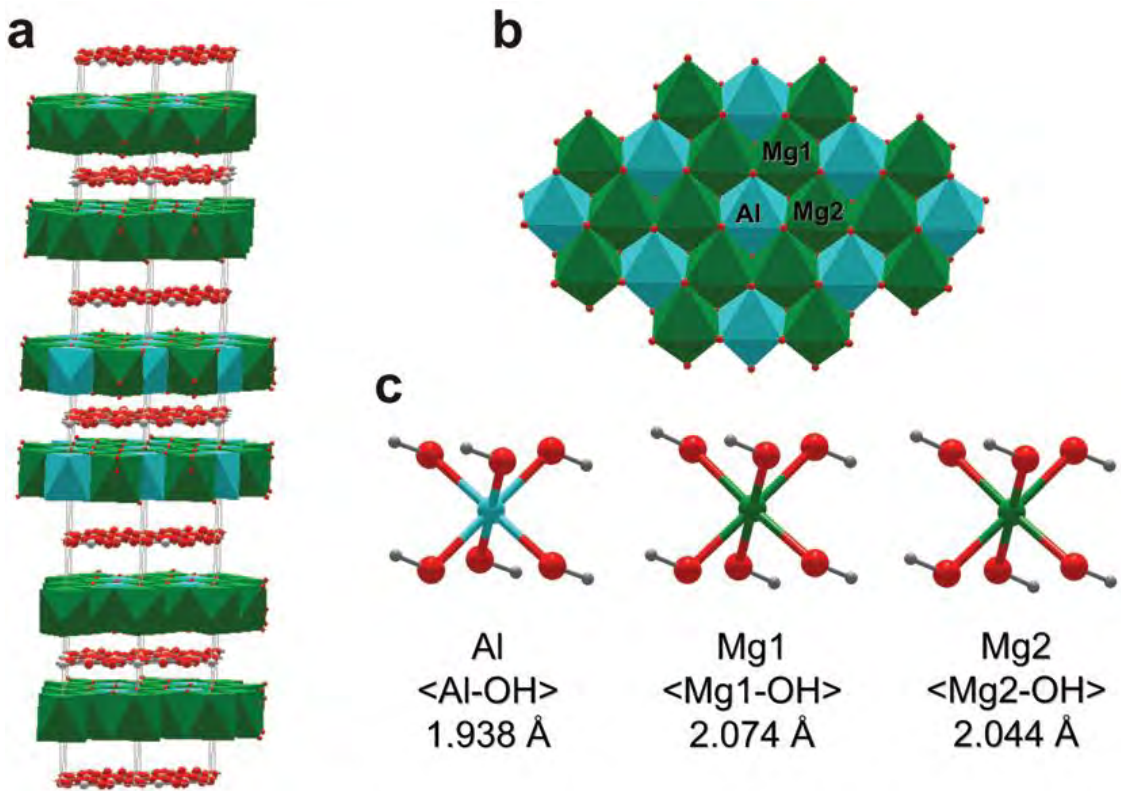


FIG. 3. The structure of quintinite-2H-3c[6R] (Q1) (*a*), a projection of the double hydroxide layer (*b*) and the geometry of the M(OH)₆ octahedra (*c*).

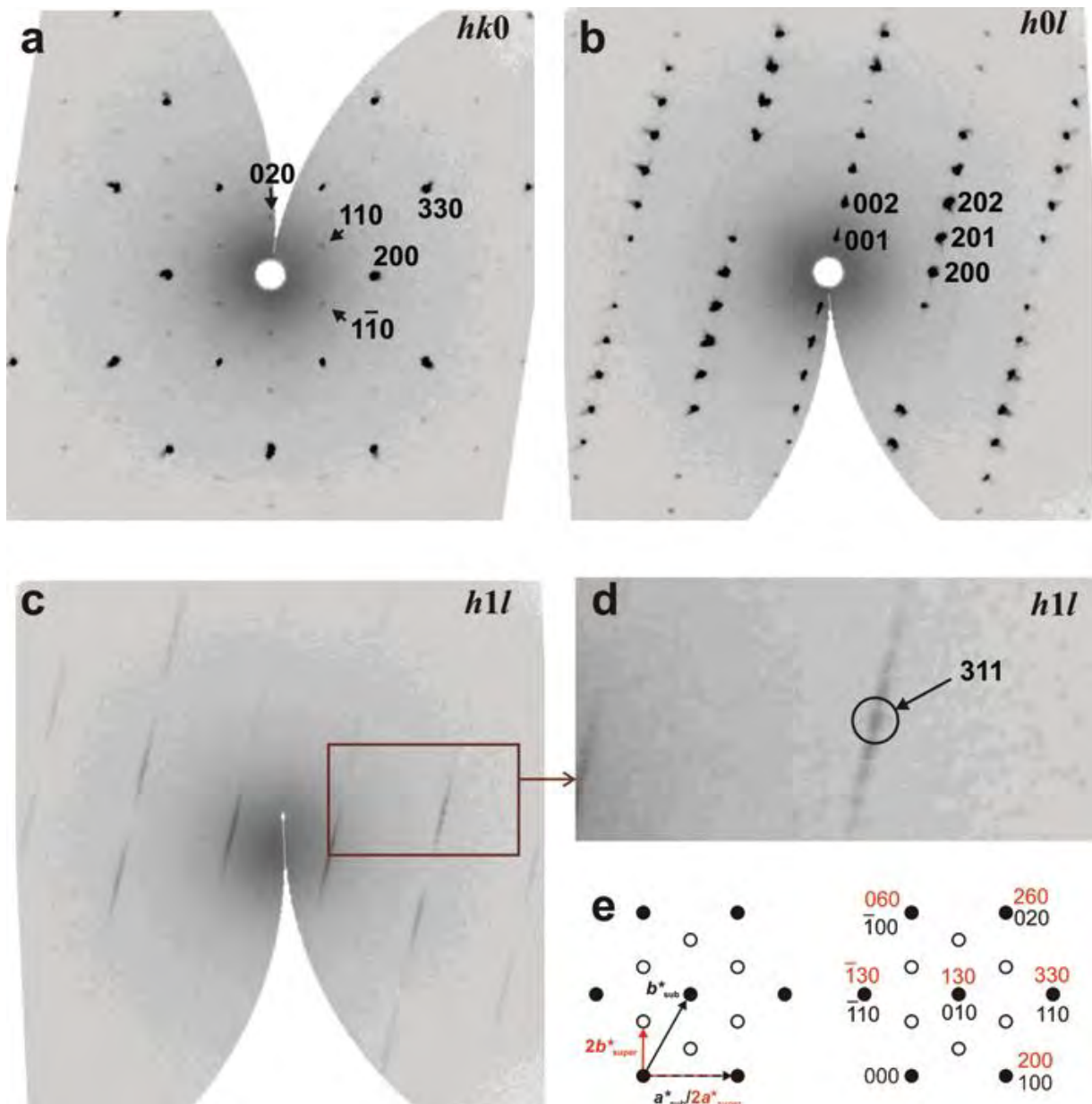


FIG. 4. Reconstructed sections of reciprocal space obtained for quintinite-1M: $hk0$ section (a: note weak reflections with odd h and k indices), $h0l$ section (b: note the presence of sharp Bragg reflections), $h1l$ section (c: note the presence of only weakly discrete diffraction streaks elongated along the c^* axis), and enlarged part of the $h1l$ section showing the position of the 311 reflection (d). The scheme in (e) shows the choice of reciprocal space vectors and indexing of reflections in the $hk0$ section (the black and red colours indicate subcell and supercell vectors and indices, respectively).

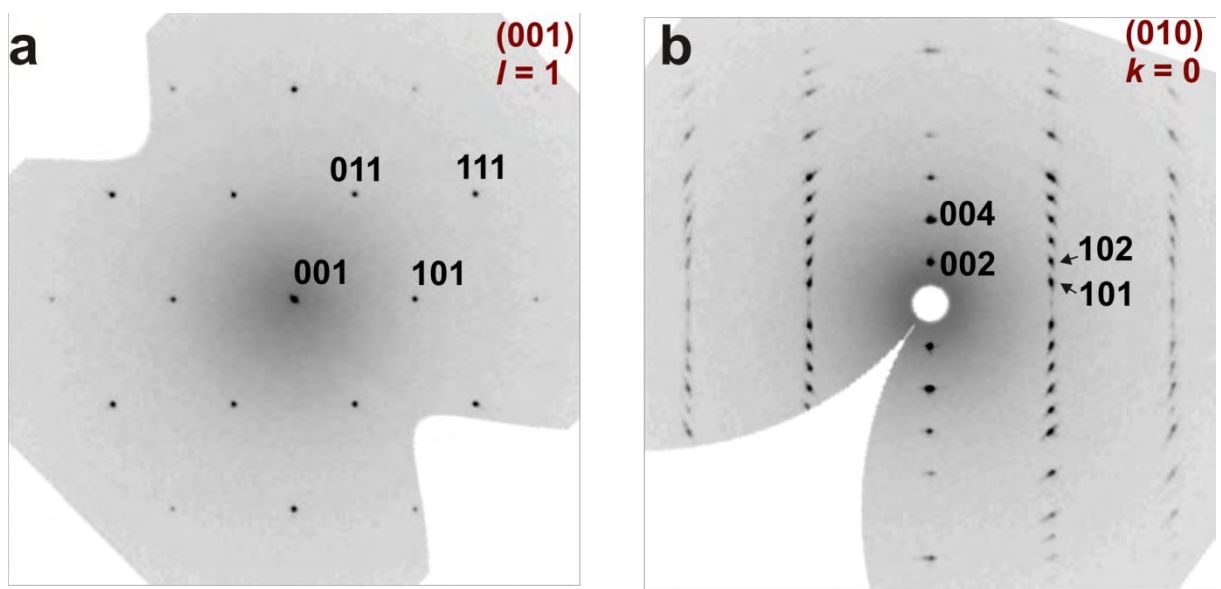


FIG. 5. The $hk1$ (a) and $h0l$ (b) sections of reciprocal diffraction space obtained from quintinite- $2H$ crystals.

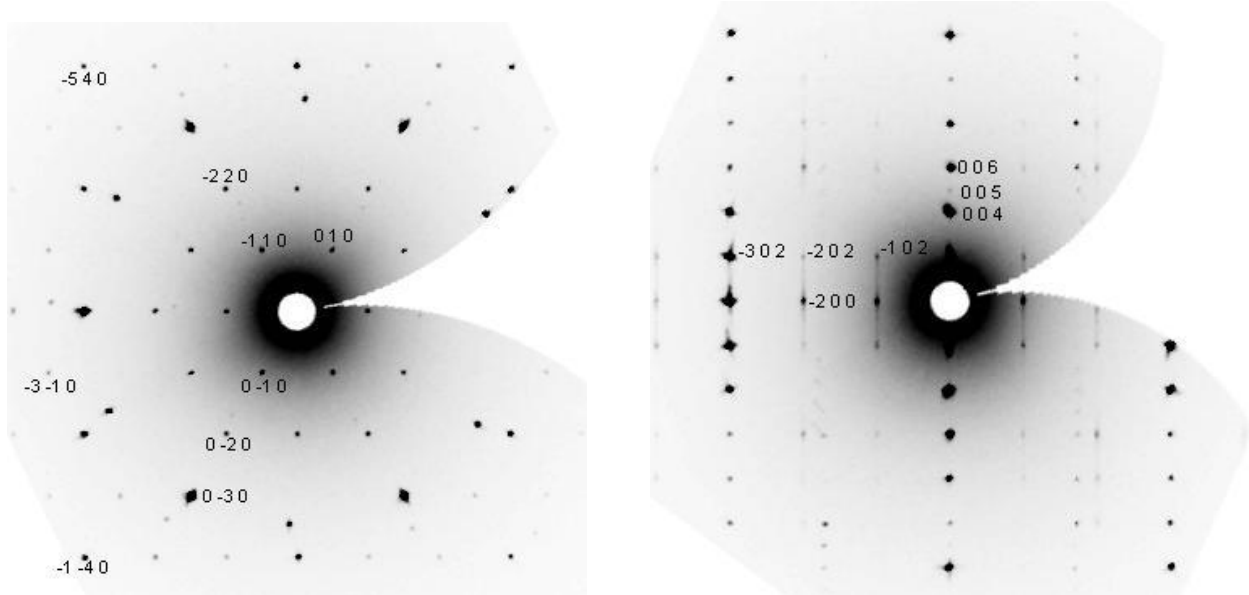


FIG. 6. (001) section of reciprocal diffraction space (left) and (010) section of reciprocal diffraction space (right) obtained from the quintinite- $2H$ - $1c$ crystal.

TABLE 1. Crystallographic data and refinement parameters for quintinite polytypes

Polytype	Quintinite-2H-3c	Quintinite-1M	Quintinite-2H	Quintinite-2H-1c
Crystallographic data				
Ideal formula	[Mg ₄ Al ₂ (OH) ₁₂](CO ₃)(H ₂ O) ₃			
Crystal system	Trigonal	Monoclinic	Hexagonal	Trigonal
Space group	R32	C2/m	P6 ₃ /mmc	P-3c1
Unit-cell parameters a, b, c (Å), β (°)	5.2745(6), 5.2745(6), 45.364(10), 90	5.266(2), 9.114(2), 7.766(3), 103.17(3)	3.0446(9), 3.0446(9), 15.178(5), 90	5.2720(6), -, 15.113(3)
Unit-cell volume (Å ³)	1093.0(3)	362.9(2)	121.84(6)	363.76(8)
Z	3	1	1	2
Data collection				
θ range (°)	2.69-29.10	4.47-29.16	2.69-29.26	2.29 - 29.76
h, k, l ranges	-7→6, -7 → 6, ±61	±7, 0 → 12, -10 → 0	-4→3, ±3, ±20	±7, -7 → 6, ±20
Total reflections collected	3414	511	829	3304
Unique reflections	668	511	84	330
Unique reflections $F > 4\sigma(F)$	484	304	76	304
Data completeness to θ_{\max} (%)	99.5	97.9	90.3	95.6
Structure refinement				
Refinement method	Full-matrix least-squares on F^2			
Weighting coefficients a, b	0.0877, 4.2621	0.0666, 0.2562	0.0185, 0.2743	0.0817, 0.6432
Extinction coefficient	0.006(2)	-	0.00(6)	0.17(3)
Data/restraints/parameters	668/0/59	511/2/65	84/1/19	330/0/38
R_1 [$F > 4\sigma(F)$], wR_2 [$F > 4\sigma(F)$],	0.055, 0.182	0.031, 0.102	0.046, 0.088	0.0603, 0.1778
R_1 all, wR_2 all	0.072, 0.203	0.055, 0.119	0.053, 0.088	0.0643, 0.1741
Goodness-of-fit on F^2	1.170	0.996	1.285	1.181
Largest diff. peak and hole (e Å ⁻³)	0.45, -0.80	0.32, -0.28	0.55, -0.26	0.95, -0.74

REFERENCES

- Allmann, R. (1968) The crystal structure of pyroaurite. *Acta Crystallographica*, B24, 972-977.
- Allmann, R. and Donnay, J.D.H. (1969) About the structure of iowaite. *American Mineralogist*, 54, 296-299.
- Allmann, R., Jepsen, H.P. (1969) Die Structur des Hydrotalkits. *Neues Jahrbuch für Mineralogie Monatshefte*, 1969, 544-551.
- Aminoff, G. and Broomé, B. (1931) Contributions to the mineralogy of Långban. III. Contributions to the knowledge of the mineral pyroaurite. *Kungliga Svenska vetenskapsakademiens handlingar*, 9, 23-48.
- Arakcheeva, A.V., Pushcharovskii, D.Yu., Atencio, D. and Lubman, G.U. (1996) Crystal structure and comparative crystal chemistry of $\text{Al}_2\text{Mg}_4(\text{OH})_{12}(\text{CO}_3)\times 3\text{H}_2\text{O}$, a new mineral from the hydrotalcite- manasseite group. *Crystallography Reports*, 41, 972-981.
- Bellotto, M., Rebours, B., Clause, O., Lynch, J., Bazin, D. and Elkaim, E. (1996) A reexamination of hydrotalcite crystal chemistry. *Journal of Physical Chemistry*, 100, 8527-8534.
- Bernal, J.D. (1951) *The physicabasis of life*. Routledge and Kegan Paul, London.
- Bernal, J.D. (1967) *The origin of life*. Weidenfeld and Nicolson, London.
- Bookin, A.S. and Drits, V.A. (1993) Polytype diversity of the hydrotalcite-like minerals. I. Possible polytypes and their diffraction patterns. *Clays and Clay Minerals*, 41, 551-557.
- Bookin, A.S. Cherkashin, V.I., Drits V.A. (1993) Polytype diversity of the hydrotalcite-like minerals. II. Determination of the polytypes of experimentally studied varieties. *Clays and Clay Minerals*, 41, 558-564.
- Cairns-Smith, A.G. (1982) *Genetic takeover and mineral origins of life*. Cambridge University Press, Cambridge.
- Chao, G.Y. and Gault, R.A. (1997) Quintinite- $2H$, quintinite- $3T$, charmarite- $2H$, charmarite- $3T$ and caresite- $3T$, a new group of carbonate minerals related to the hydrotalcite/manasseite group. *The Canadian Mineralogist*, 35, 1541-1549.
- Drits, V.A. and Bookin, A.S. (2001) Crystal structure and X-ray identification of layered double hydroxides. Pp. 39-92 in: *Layered Double Hydroxides: Present and Future* (V. Rives, editor). Nova Science Publishers Inc., New York.
- Duan, X., Evans, G.D. (2006) *Layered Double Hydroxides*. Springer, Berlin.
- Frondel, C. (1941) Constitution and polymorphism of the pyroaurite and sjögrenite groups. *American Mineralogist*, 26, 295-315.
- Génin, J.-M.R., Ruby, C. and Upadhyay, C. (2006) Structure and thermodynamics of ferrous, stoichiometric and ferric oxyhydroxycarbonate green rusts; redox flexibility and fougérite mineral. *Solid State Science*, 8, 1330-1343.
- Génin, J.-M.R., Renard A. and Ruby, C. (2008) Fougérite $\text{Fe}^{\text{II-III}}$ oxyhydroxycarbonate in environmental chemistry and nitrate reduction. *Hyperfine Interactions*, 186, 31-37.

Hochstetter, C. (1842) Untersuchung über die Zusammensetzung einiger Mineralien. *Journal für Praktische Chemie*, 27, 375-378.

Igelstörm, L.J. (1865) Nya och sällsynta mineralier från Vermalands och Örebro län. *Öfversigt af Kongliga Vetenskaps-Akademien Förhandlingar*, 16, 399-400.

Kameda, T. and Yoshika, T. (2011) Hybrid inorganic/organic composites of layered double hydroxides intercalated with organic acid anions for the uptake of hazardous substances from aqueous solution. In: Cupoletti J., (ed). Metal, ceramic and polymeric composites for various uses, 123-148.

Kameda, T., Fubasami, Y. and Yoshika, T. (2011a) Kinetics and equilibrium studies on the treatment of nitric acid with Mg-Al oxide obtained by thermal decompinsation of NO_3^- -intercalated Mg-Al layered double hydroxide. *Journal of Colloid and Interface Science*, 362, 497-502.

Kameda, T., Uchiyama, N. and Youshika, T. (2011b) Removal of HCl, SO_2 , and NO by treatment of acid gas with Mg-Al oxide slurry. *Chemosphere*, 82, 587-591.

Kim, D., Huang, C., Lee, H., Han, I., Kang, S., Kwon, S., Lee, J., Han, Y., Kim, H. (2003) Hydrotalcite-type catalysts for narrow-range oxyethylation of 1-dodecanol using ethyleneoxide. *Applied Catalysis*, A, 229-240.

Krivovichev, S.V., Yakovenchuk, V.N., Zhitova, E.S., Zolotarev, A.A., Pakhomovsky, Ya.A., Ivanyuk, G.Yu. (2010) Crystal chemistry of natural layered double hydroxides. 1. Quintinite- $2H\cdot3c$ from Kovdor alkaline massif, Kola peninsula, Russia. *Mineralogical Magazine*, 74(5), 821-832.

Krivovichev, S.V., Yakovenchuk, V.N., Zhitova, E.S., Zolotarev, A.A., Pakhomovsky, Ya.A., Ivanyuk, G.Yu. (2010) Crystal chemistry of natural layered double hydroxides. 2. Quintinite- $1M$: first evidence of monoclinic polytype in $\text{M}^{2+}\text{-M}^{3+}$ layered double hydroxides. *Mineralogical Magazine*, 74(5), 833-840.

Krivovichev, S.V., Antonov, A.A., Zhitova, E.S., Zolotarev, A.A., Krivovichev, V.G., Yakovenchuk, V.N. (2012) Quintinite- $1M$ from Bazhenovskoe deposit (Middle Ural, Russia): crystal structure and properties. *Bulletin of Saint-Petersburg State University, Ser. Geology and Geography* (7), № 2, 3-9 (in Russian).

Krivovichev, S.V., Yakovenchuk, V.N., Zhitova, E.S. (2012) Natural double layered hydroxides: structure, chemistry, and information storage capacity. *Minerals as Advanced Materials II* (Ed. S.V.Krivovichev) (2012). Springer-Verlag, Berlin Heidelberg, 87-91.

Loewenstein, W. (1954) The distribution of aluminum in the tetrahedral of silicates and aluminates. *American Mineralogist*, 39, 92-96.

Mills, S.J., Christy, A.G., Génin, J-M. R., Kameda, T., Colombo, F. (2012) Nomenclature of the hydrotalcite supergroup: natural layered double hydroxides. *Mineralogical Magazine*, 76, 1289-1336.

Newman, S.P. and Jones, W. (1998) Synthesis, characterization and applications of layered double hydroxides containing organic guests. *New Journal of Chemistry*, 22, 105-115.

- Pausch, I., Lohse, H.-H., Schurmann, K. and Allmann, R. (1986) Synthesis of disordered and Al-rich hydrotalcite-like compounds. *Clays and Clay Minerals*, 34, 507-510.
- Sheldrick, G.M. (2008) A short history of SHELX. *Acta Crystallographica*, A64 , 112-122.
- Speck, A. (2003) Single-crystal structure validation with the program PLATON. *Journal of Applied Crystallography*, 36, 7-13.
- Taylor, H.F.W. (1969) Segregation and cation-ordering in sjögrenite and pyroaurite. *Mineralogical Magazine*, 37, 338-342.
- Taylor, H.F.W. (1973) Crystal structures of some double hydroxide minerals. *Mineralogical Magazine*, 39, 377-389.
- Trave, A., Selloni, A., Goursot, A., Tichit, D. and Weber, J. (2002) First Principles Study of the Structure and Chemistry of Mg-Based Hydrotalcite-Like Anionic Clays. *Journal of Physical Chemistry*, 106, 12291-12296.
- Zhitova, E.S., Yakovenchuk, V.N., Krivovichev, S.V., Zolotarev, A.A., Pakhomovsky, Ya.A., Ivanyuk, G.Yu. (2010) Crystal chemistry of natural layered double hydroxides. 3. The crystal structure of Mg,Al-disordered quintinite- $2H$. *Mineralogical Magazine*, 74(5), 841-848.

INCLUDED ARTICLES

PI

QUINTINITE-2H-3c FROM KOVDOR ALKALINE MASSIF, KOLA PENINSULA, RUSSIA

The paper “Quintinite-2H-3c from Kovdor alkaline massif, Kola peninsula, Russia” was published in Mineralogical Magazine (2010, Vol. 74, No. 5, pp. 821-832) by Krivovichev S.V., Yakovenchuk V.N., Zhitova E.S., Zolotarev A.A., Pakhomovsky Ya.A., Ivanyuk G.Yu.

Reproduced, with the permission of the Mineralogical Society of Great Britain & Ireland, from Krivovichev *et al.* (2010), originally published in *Mineralogical Magazine*.

DOI: 10.1180/minmag.2010.074.5.821

Concept: Prof. Dr. S.V. Krivovichev, V.N. Yakovenchuk, E.S. Zhitova

Sampling and measurement: E.S. Zhitova, A.A. Zolotarev, Ya.A. Pakhomovsky

Data analysis: Prof. Dr. S.V. Krivovichev, E.S. Zhitova, A.A. Zolotarev, G.Yu. Ivanyuk

Writing the manuscript: Prof. Dr. S.V. Krivovichev, V.N. Yakovenchuk, E.S. Zhitova, G.Yu. Ivanyuk.

Crystal chemistry of natural layered double hydroxides. I. Quintinite-2H-3c from the Kovdor alkaline massif, Kola peninsula, Russia

S. V. KRIVOVICHEV^{1,2}, V. N. YAKOVENCHUK^{2,3}, E. S. ZHITOVA¹, A. A. ZOLOTAREV¹, Y. A. PAKHOMOVSKY^{2,3} AND G. YU. IVANYUK^{2,3}

¹ Department of Crystallography, Faculty of Geology, St. Petersburg State University, University Emb. 7/9, 199034 St. Petersburg, Russia

² Nanomaterials Research Center, Kola Science Center, Russian Academy of Sciences, Apatity, Russia

³ Geological Institute, Kola Science Center, Russian Academy of Sciences, Apatity, Russia

[Received 19 March 2010; Accepted 3 August 2010]

ABSTRACT

The crystal structure of quintinite-2H-3c, $[\text{Mg}_4\text{Al}_2(\text{OH})_{12}](\text{CO}_3)(\text{H}_2\text{O})_3$, from the Kovdor alkaline massif, Kola peninsula, Russia, was solved by direct methods and refined to an agreement index (R_1) of 0.055 for 484 unique reflections with $|F_o| \geq 4\sigma_F$. The mineral is rhombohedral, $R\bar{3}2$, $a = 5.2745(7)$, $c = 45.36(1)$ Å. The diffraction pattern of the crystal has strong and sharp Bragg reflections having $h-k = 3n$ and $l = 3n$ and lines of weak superstructure reflections extended parallel to ϵ^* and centred at $h-k \neq 3n$. The structure contains six layers within the unit cell with the layer stacking sequence of ...AC=CA=AC=CA=AC=CA... The Mg and Al atoms are ordered in metal hydroxide layers to form a honeycomb superstructure. The full superstructure is formed by the combination of two-layer stacking sequence and Mg-Al ordering. This is the first time that a long-range superstructure in carbonate-bearing layered double hydroxide (LDH) has been observed. Taking into account Mg-Al ordering, the unique layer sequence can be written as ...=Ab₁C=Cb₁A=Ab₂C=Cb₂A=Ab₃C=Cb₃A=... The use of an additional suffix is proposed in order to distinguish between LDH polytypes having the same general stacking sequence but with different c parameters compared with the ‘standard’ polytype. According to this notation, the quintinite studied here can be described as quintinite-2H-3c or quintinite-2H-3c[6R], indicating the real symmetry.

KEYWORDS: layered double hydroxides, quintinite, crystal structure, cation ordering, polytypism.

Introduction

LAYERED double hydroxides (LDHs) are an important group of inorganic materials with many applications ranging from catalysis and absorption to carriers in drug delivery, DNA intercalation and carbon dioxide sequestration (Choy *et al.*, 1999; Rives, 2001; Khan and O’Hare, 2002; Duan and Evans, 2006). Structural features of LDHs such as cation

ordering, charge distribution and polytypism have a direct influence upon their properties and have been under extensive experimental and theoretical investigations (Wang *et al.*, 2001, 2003; Kumar *et al.*, 2006; Génin *et al.*, 2006; Thyveetil *et al.*, 2008; Ruby *et al.*, 2008; Britto and Kamath, 2009; Johnsen and Norby, 2009; Christiansen *et al.*, 2009). However, all structural studies on synthetic LDHs have used powder samples which prevent elucidation of fine details of the structure architecture such as the formation of superstructures by cation and anion ordering. So-called $\text{Mg}_2\text{Al}-\text{CO}_3$ hydrotalcite (one of the most widely studied LDHs) reveals no signs of superstructures when studied by powder X-ray

* E-mail: sk@min.uni-kiel.de
DOI: 10.1180/minmag.2010.074.5.821

diffraction (XRD), though perfect short-range Mg-Al ordering has been detected by infrared (IR) and nuclear magnetic resonance (NMR) spectroscopies (Richardson and Braterman, 2007; Sideris *et al.* 2008). The hydrated character of LDHs precludes their study by the high-resolution electron microscopy techniques available at the moment (M. Ogawa, pers. comm.).

In contrast with synthetic materials, natural LDHs are known to form single crystals accessible to single-crystal XRD analysis, and this allows identification of basic features of their crystal chemistry (Ingram and Taylor, 1967; Allmann, 1968; Allmann and Donnay, 1969; Allmann and Jepsen, 1969; Taylor, 1973; Rius and Allmann, 1984; Braithwaite *et al.*, 1994). It is also possible to demonstrate peculiarities of cation and anion ordering (Arakcheeva *et al.*, 1996; Cooper and Hawthorne, 1996; Huminicki and Hawthorne, 2003). There are ~40 mineral species that belong to the LDH group, and many of them are important from both geochemical and environmental viewpoints. For example, green-blue iron hydroxide compounds known as ‘green rust’ are observed as corrosion products of steel (Stampfli, 1969), as constituents of waste sludges (Koch and Morup, 1991) and as soil minerals (Hansen, 2001; Trolard, 2006). Hydrotalcite-type LDHs have also been proposed as possible prebiotic information storage and transfer compounds (Arrhenius, 2003; Greenwell and Coveney, 2006).

New results are reported here for the crystal chemistry of natural LDHs obtained by application of area detectors of X-rays, which provide new opportunities for quantitative studies of commensurate, incommensurate and diffuse scattering features of diffraction patterns. The structure of rhombohedral quintinite from hydrothermal veins of the Kovdor alkaline massif, Kola peninsula, Russia are reported. Quintinite, $Mg_4Al_2(OH)_{12}(CO_3)(H_2O)_3$, has been described by Chao and Gault (1997) from the quarries at Mont Saint-Hilaire, Quebec, Canada, as a 3 T polytype (three-layer trigonal). Quintinite-2 H was found in vugs in dolomitic carbonatite at the Jacupiranga mine, São Paulo, Brazil, where it was originally described as manasseite (Menezes and Martins, 1984). The structure of quintinite-2 H was reported by Arakcheeva *et al.* (1996) as possessing complete ordering of interlayer anions and of Mg and Al cations in the double-hydroxide layer (see below). In the Kovdor alkaline massif, natural LDH minerals were first described by O.M. Rimskaya-Korsakova (Ivanyuk and

Yakovenchuk, 1997) and identified as manasseite, $Mg_6Al_2(OH)_{16}(CO_3)(H_2O)_4$. Detailed chemical and structural study demonstrated that, at least some of these minerals are in fact quintinite, which differs from manasseite in its Mg:Al ratio, anion and H_2O contents. It should also be noted that in the chemical literature, quintinite is usually specified as a “ Mg_2Al-CO_3 hydrotalcite” (Stanimirova *et al.* 2004).

Structural architecture of LDHs: general principles

The basic structural feature of natural and synthetic LDHs is the presence of a brucite-like double-hydroxide sheet $[M_n^{2+} M_m^{3+} (OH)_{2(m+n)}]^{m+}$, where $M^{2+} = Mg^{2+}, Fe^{2+}, Mn^{2+}, Zn^{2+}$, etc.; $M^{3+} = Al^{3+}, Fe^{3+}, Cr^{3+}, Mn^{3+}$, etc. The positive charge of the layer is compensated by interlayer species that may consist of anions (CO_3^{2-}, Cl^- , SO_4^{2-} , etc.) or both anions and cations (Na^+, Ca^{2+}, Sr^{2+} , etc.). Due to their layered character, LDHs display polytypism and layer stacking disorder. Polytype diversity of LDHs has been described in detail by Bookin and Drits (1993), Bookin *et al.* (1993), and Drits and Bookin (2001), who developed a structural nomenclature for the polytypes observed in this group, which we summarize below.

In the plane perpendicular to the direction of layer stacking, cations and anions may occupy three distinct sites: A, B and C (analogous to the sites of spheres in closest packing). The upper (A, B, C) and lower (a, b, c) case symbols are reserved for positions of hydroxyls and cations, respectively. If hydroxyl anions of the layer are in the A and C sites for example, the cations occupy the b sites, and the layer has a structural formula AbC (Fig. 1).

Stacking of two layers may result in the formation of two different types of interlayers (Fig. 2). In the case when the upper hydroxide sheet of the lower layer and lower hydroxide sheet of the upper layer have the same notations (e.g. A and A), the interlayer may be represented as consisting of trigonal prisms (Fig. 2b). This type of interlayer is referred to as a ‘P-type’ (P = prism) and denoted with an equal sign (=) (e.g. ...A=A...). In the alternative case, when the upper hydroxide sheet of the lower layer and lower hydroxide sheet of the upper layer have different notations (e.g. A and B), the interlayer may be represented as consisting of elongated octahedra (Fig. 2c). This type of interlayer is referred to as an ‘O-type’ (O = octahedron) and denoted with a dash (-) (e.g. ...A-B...). Using this simple

CRYSTAL STRUCTURE OF QUINTINITE

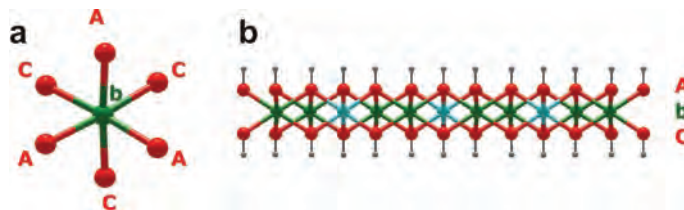


FIG. 1. Projection of metal-centred octahedron with identification of cation position as b and anion positions as A and C (a) and projection of a double hydroxide layer parallel to its extension (b).

notation, Bookin and Drits (1993) derived all two- and three-layer LDH polytypes and six-layer rhombohedral polytypes and calculated their powder XRD patterns. There are three two-layer polytypes, ...AC=CA=AC..., ...AC-AB-AC... and ...AC-BA=AC..., for example, denoted as $2H_1$, $2H_2$ and $2H_3$, respectively. Of these three polytypes, the $2H_1$ polytype appears to be the most common in Nature (e.g. it occurs in manasseite). In this polytype, all cations occupy the b sites and all interlayers are of the P-type. Among three-layer polytypes, the most common is the $3R_1$ polytype which has the structure ...AC=CB=BA=AC..., i.e. all its interlayers are of the P-type. On the basis of the nomenclature proposed by Bookin and Drits (1993), Bookin *et al.* (1993) investigated natural LDHs and reported the occurrence of $2H_1$ and $3R_1$ polytypes in CO_3 -bearing minerals. In sulphate-bearing LDHs, the

situation is more complex: one- and three-layer polytypes are observed with both P- and O-type interlayers. The nomenclature of LDHs was further illustrated and developed by Drits and Bookin (2001). However, despite its exhaustive and rigorous derivation of the polytypes, this nomenclature does not take into account some important structural features of LDHs, e.g. long-range ordering of M^{2+} and M^{3+} cations within the double-hydroxide layers.

The problem of long-range and short-range cation order-disorder in synthetic and natural LDHs was reviewed in great detail by Evans and Slade (2006). Those authors concluded that in LDHs with an $M^{2+}:M^{3+}$ ratio of 2:1, long-range cation order has sometimes been observed by single-crystal XRD, but in most cases, structural investigations are restricted to study by powder diffraction. Hofmeister and von Platen (1992)

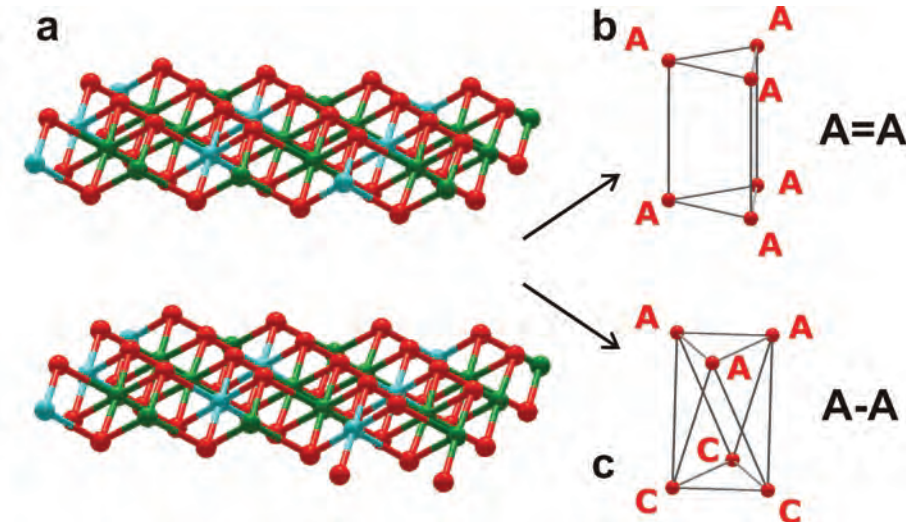


FIG. 2. The interlayer space in the structures of LDHs (a) may consist of either trigonal prisms (b: P-type interlayer) or octahedra (c: O-type interlayer).

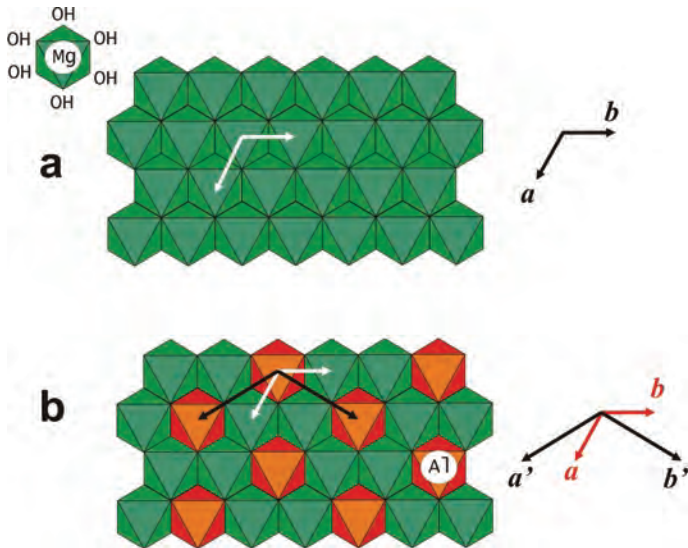


FIG. 3. The octahedral $[\text{Mg}(\text{OH})_2]$ layer in brucite (*a*) is characterized by a hexagonal unit cell with the *a* parameter, whereas the incorporation of Al results in the formation of an ordered $[\text{Mg}_2\text{Al}(\text{OH})_6]^+$ layer with a hexagonal unit cell where $a' = a \cdot 3^{1/2}$ (*b*).

suggested that the prevalence of $M^{2+}:M^{3+}$ ratio of 2:1 and 3:1 in natural and synthetic LDHs indicates a preference for cation order in the metal hydroxide layers, which is not always accompanied by ordered stacking of the layers.

In the case of the LDHs with a $M^{2+}:M^{3+}$ ratio of 2:1, the most uniform distribution of the cations in the layer corresponds to the formation of 2-D superstructure as shown in Fig. 3. If the $[\text{M}_2^{2+}\text{M}^{3+}(\text{OH})_6]^+$ layer with long-range disorder has a trigonal subcell with $a \approx 3 \text{ \AA}$ (Fig. 3*a*), its ordered equivalent has a supercell with $a' \approx a\sqrt{3} \approx 5.1 \text{ \AA}$ (Fig. 3*b*). Thus, in the case of perfect cation ordering in $\text{M}_2^{2+}\text{M}^{3+}$ LDHs, the diffraction pattern should contain superstructure reflections with non-integer indices relative to its subcell. However, the intensity of the superstructure reflections are rarely strong enough to detect by means of powder XRD and so can be overlooked during the structural studies. This is especially true for the LDHs with M^{2+} and M^{3+} cations with very similar site-scattering factors, such as Mg and Al (Bellotto *et al.* 1996).

There is a group of compounds known as the Ca_2Al -LDHs (Terzis *et al.* 1987; Francois *et al.*, 1998). The structures of these compounds are based upon fully ordered layers of octahedrally coordinated Al^{3+} and [7]-coordinated Ca^{2+} . Thus Ca_2Al -‘LDHs’ are not based on octahedral layers

and therefore cannot be considered in the framework of the classification system mentioned above.

Experimental methods

The sample of quintinite studied in this work comes from hydrothermal veins of the Kovdor alkaline massif, Kola peninsula, Russia. Here, quintinite occurs as druses of large (up to 1 cm) brown, yellow and colourless hexagonal pyramids with well developed (001) pinacoids



FIG. 4. Crystals of quintinite-2H-3c from the Kovdor alkaline massif.

CRYSTAL STRUCTURE OF QUINTINITE

(Fig. 4). The mineral was found in association with magnetite, greenish-blue phlogopite, johnaite, calcite and dolomite. The chemical composition was determined by wavelength dispersion spectrometry using a Cameca MS-46 electron microprobe operating at 20 kV and 20–30 nA. The average of eight analyses gave (wt.%) MgO 31.45, Al₂O₃ 21.02, FeO 3.67, CO₂ (calc.) 9.10, H₂O (calc.) 34.76, sum 100.00. The empirical formula derived, calculated on the basis of Mg + Al = 6, is [Mg_{4.01}Al_{1.99}(OH)₁₂] (CO₃)_{0.99}(H₂O)₃, which is in good agreement with the ideal formula [Mg₄Al₂(OH)₁₂] (CO₃)(H₂O)₃. An IR spectrum of quintinite was

recorded using a Bruker Vertex IR spectrometer and was found to be in general agreement with that reported for quintinite by Frost and Dickfos (2007) (see also Klopdroge *et al.*, 2002; Kirkpatrick *et al.*, 2005).

The crystal of quintinite selected for single-crystal XRD study was mounted on a Stoe IPDS II Image-Plate-based X-ray diffractometer operated at 50 kV and 40 mA. More than a hemisphere of three-dimensional data was collected using monochromatic Mo-K α X-radiation, with frame widths of 2° in ω , and with a 300 s count for each frame. The unit-cell parameters (Table 1) were refined by least-squares methods. The SHELXTL

TABLE 1. Crystallographic data and refinement parameters for quintinite-2H-3c.

Crystal data

Ideal formula	[Mg ₄ Al ₂ (OH) ₁₂] (CO ₃)(H ₂ O) ₃
Crystal system	Trigonal
Space group	<i>R</i> 32
Unit-cell dimensions <i>a</i> , <i>c</i> (Å)	5.2745(6), 45.364(10)
Unit-cell volume (Å ³)	1093.0(3)
<i>Z</i>	3
Calculated density (g/cm ³)	2.130
Absorption coefficient (mm ⁻¹)	0.42
Crystal size (mm)	0.14 × 0.14 × 0.02

Data collection

Diffractometer	Stoe IPDS II Image-Plate
Temperature (K)	293
Radiation, wavelength (Å)	Mo-K α , 0.71073
θ range (°)	2.69–29.10
<i>h</i> , <i>k</i> , <i>l</i> ranges	−7 → 6, −7 → 6, ±61
Axis, frame width (°), time per frame (s)	ω , 2, 300
Total reflections collected	3414
Unique reflections (<i>R</i> _{int})	668 (0.046)
Unique reflections <i>F</i> > 4σ(<i>F</i>)	484
Data completeness to θ _{max} (%)	99.5

Structure refinement

Refinement method	Full-matrix least-squares on <i>F</i> ²
Weighting coefficients <i>a</i> , <i>b</i> *	0.0877, 4.2621
Extinction coefficient	0.006(2)
Data/restraints/parameters	668/0/59
<i>R</i> ₁ [<i>F</i> > 4σ(<i>F</i>)], <i>wR</i> ₂ [<i>F</i> > 4 <i>s</i> (<i>F</i>)]	0.055, 0.182
<i>R</i> ₁ all, <i>wR</i> ₂ all	0.072, 0.203
Goodness-of-fit on <i>F</i> ²	1.170
Largest diff. peak and hole (e Å ^{−3})	0.45, −0.80

$$R_{\text{int}} = (n/n - 1)^{1/2} [F_o^2 - F_o \text{ (mean)}]^2 / \sum F_o^2$$

$$R_1 = \sum |F_o| - |F_c| / \sum |F_o|; wR_2 = \{ \sum [w(F_o^2 - F_c^2)^2] / \sum [w(F_o^2)^2] \}^{1/2};$$

$$* w = 1/[\sigma^2(F_o^2) + (aP)^2 + bP], \text{ where } P = (\max(F_o^2, 0) + 2F_c^2)/3;$$

$$\text{GooF} = \{ \sum [w(F_o^2 - F_c^2)^2] / (n - p) \}^{1/2}$$

where *n* is the number of reflections and *p* is the number of refined parameters.

TABLE 2. Atom coordinates, displacement parameters (\AA^2) and site-occupancies for quintinite- $2H\text{-}3c$.

Atom	Occupancy	<i>x</i>	<i>y</i>	<i>z</i>	<i>U</i> _{eq}
Octahedral sheet					
Al1	1	$\frac{1}{3}$	$\frac{2}{3}$	0.08335(4)	0.0144(6)
Mg1	1	$\frac{2}{3}$	$\frac{1}{3}$	0.08339(4)	0.0105(6)
Mg2	1	0	0	0.08338(4)	0.0099(6)
O(H)1	1	0.3286(4)	0.3488(4)	0.06154(5)	0.0182(7)
O(H)2	1	0.3293(4)	0.9811(4)	0.10512(5)	0.0139(7)
Interlayer anions and water molecules					
C1A	0.17*	$\frac{1}{3}$	$\frac{2}{3}$	$\frac{1}{6}$	0.022(11)
C2A	0.17*	$\frac{2}{3}$	$\frac{1}{3}$	0.1668(8)	0.034(11)
O1A	0.37(2)	0.437(3)	0.093(3)	0.1668(2)	0.046(4)
O2A	0.33(2)	$\frac{1}{3}$	0.892(4)	$\frac{1}{6}$	0.046(5)
H ₂ O(1)	0.13(2)	-0.014(6)	$\frac{2}{3}$	$\frac{1}{6}$	0.040*
C1B	0.17*	0	0.327(12)	0	0.10(5)
O1B	0.38(2)	0.435(3)	0.435(3)	0	0.037(4)
O2B	0.38(1)	0.235(3)	0.332(2)	0.00003(15)	0.039(3)
H ₂ O(2)	0.10(1)	0.328(5)	0.975(6)	0.1250(8)	0.040*

* fixed during refinement

program package was used for all structural calculations (Sheldrick, 2008). The final model included all atomic positional parameters, anisotropic-displacement parameters for atoms of the metal hydroxide layer and a refinable weighting scheme of the structure factors. The structure was solved in the space group $R\bar{3}$ and subsequently transformed into the space group $R\bar{3}2$ using PLATON (Speck, 2003). The final refinement converged to an agreement index (R_1) of 0.055, calculated for the 484 unique reflections with $|F_o| \geq 4\sigma_F$. The final atomic coordinates and anisotropic-displacement parameters are given in Table 2, and selected interatomic distances in Table 3. A list of observed and calculated structure factors can be downloaded from the journal's website at www.minersoc.org/pages/e_journals/dep_mat.html.

Results

Diffraction behaviour

The diffraction pattern comprises strong, sharp reflections and rows of weak reflections superimposed upon a background of modulated diffuse intensity (Fig. 5). Indexing based on the strong set of sublattice reflections resulted in a small subcell with parameters $a = 3.045$ and $c = 15.12 \text{ \AA}$, which agree approximately with unit-cell parameters of the $2H_1$ polytype of Mg-Al LDHs (Bookin *et al.*, 1993). The weak superlattice reflections define a rhombohedral supercell with unit-cell parameters: $a = 5.2745(7)$, $c = 45.36(1) \text{ \AA}$. The geometrical relationship between sublattice and superlattice reflections is shown in Fig. 5. The two reciprocal lattices are related by the matrix $(\frac{1}{3}\sqrt{3}/0 - \frac{1}{3}\sqrt{3}/3 0 0 0 \frac{1}{2})$. In terms of the supercell indices, sublattice reflec-

TABLE 3. Selected bond lengths (\AA) in the structure of quintinite- $2H\text{-}3c$.

Al1–O(H)1	1.936(2) 3 ×	Mg1–O(H)2	2.070(2) 3 ×	Mg2–O(H)2	2.042(2) 3 ×
Al1–O(H)2	1.940(2) 3 ×	Mg1–O(H)1	2.077(2) 3 ×	Mg2–O(H)1	2.045(2) 3 ×
C1A–O2A	1.190(19) 3 ×	C2A–O1A	1.239(15) 3 ×	C1B–O2B	1.23(3) 2 ×
				C1B–O1B	1.25(7)

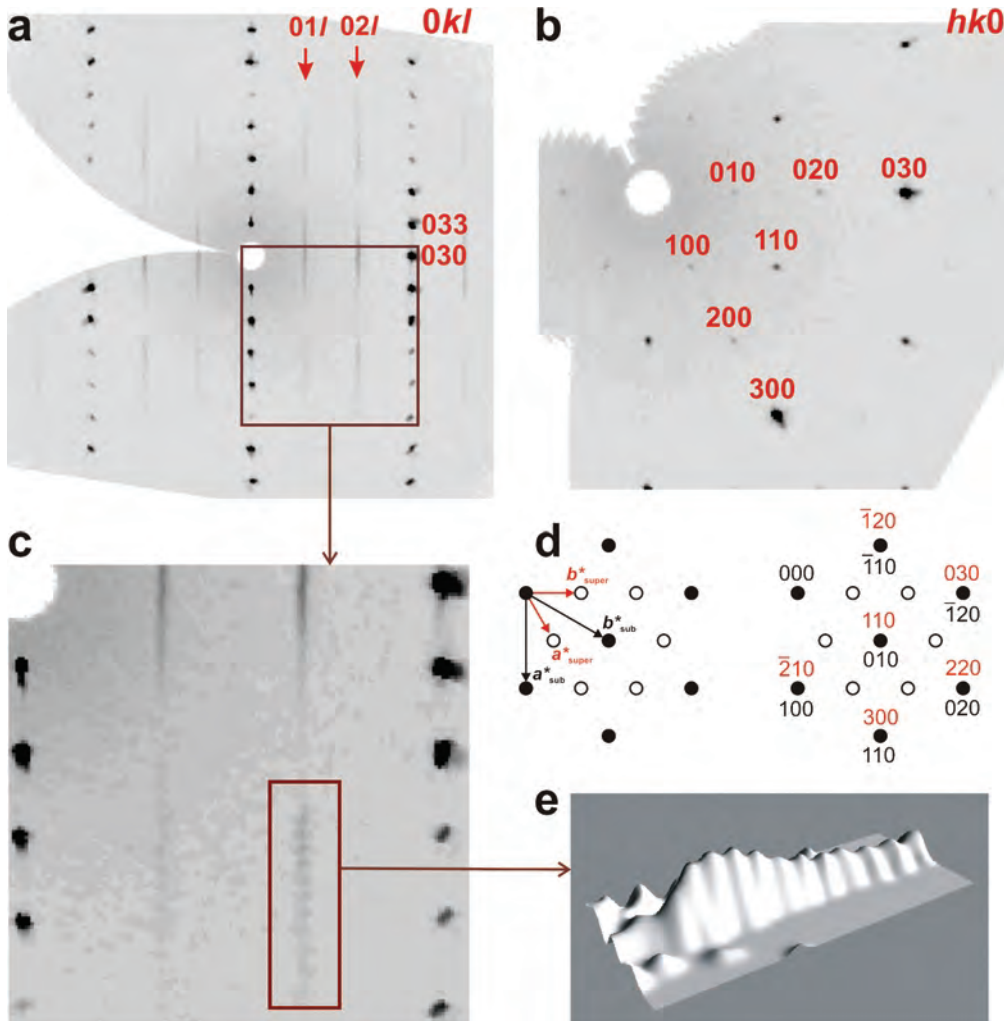


FIG. 5. The (100) (a) and (001) (b) sections of reciprocal diffraction space containing both sharp and diffuse reflections; the latter can be separated into closely separated weak reflections as can be seen from the enlarged part of the (100) section (c). The relations between subcell and supercell in the reciprocal lattice section ($hk0$) is shown in d.

Three-dimensional reconstruction of diffuse streak is shown in (e).

tions correspond to conditions $h-k = 3n$ and $l = 3n$, whereas rows of weak intensity maxima extending parallel to \mathbf{c}^* occur at $h-k \neq 3n$.

It should be noted that Chao and Gault (1997) reported space group $P6_322$ for quintinite- $2H$ and a cell with $a = 10.571(1)$, $c = 15.139(7)$ Å, which differs from our data by $2a$ and $\frac{1}{3}c$. Arakcheeva *et al.* (1996) found that a Brazilian quintinite- $2H$ had space group $P\bar{6}2m$ and $a = 5.283(3)$, $c = 15.150(9)$ Å.

Polytype identification

The structure of the quintinite polytype studied in this work consists of $[\text{Mg}_2\text{Al}(\text{OH})_6]^{+}$ hydroxide layers, and disordered interlayers (Fig. 6). According to the polytype nomenclature of Bookin and Drits (1993) (which does not consider intralayer cation ordering), the layer stacking is ...AC=CA=AC..., and corresponds to that of the two-layer $2H_1$ polytype, as observed for manasseite and quintinite- $2H$ by Arakcheeva *et al.*

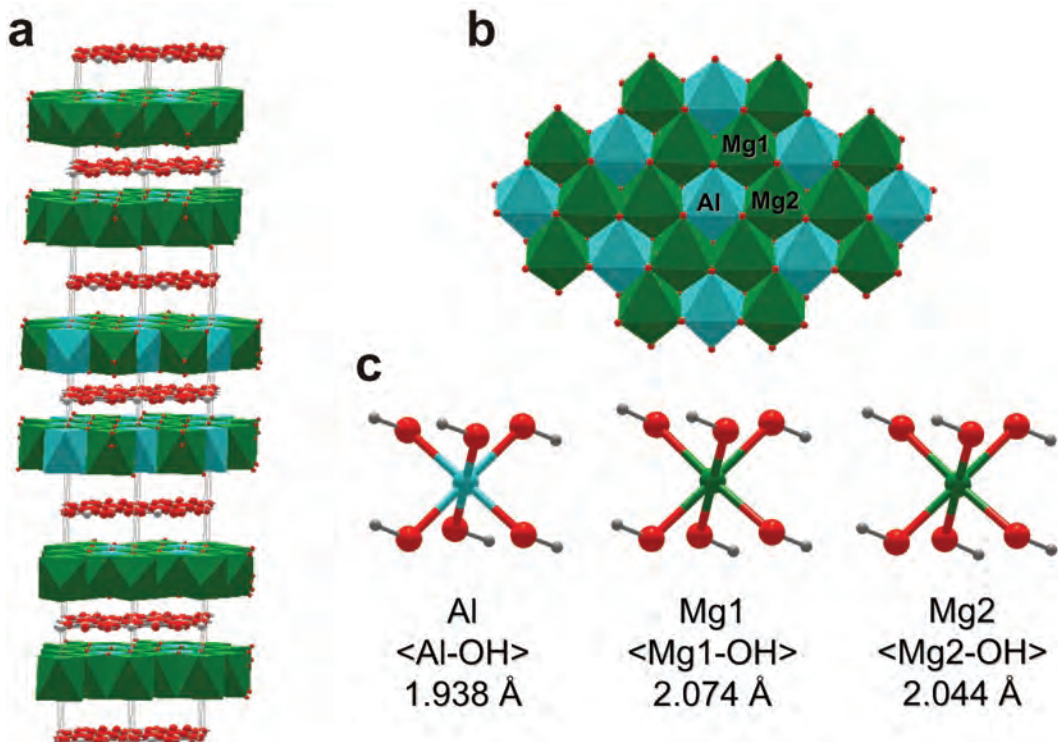


FIG. 6. The structure of quintinite-2H-3c (*a*), a projection of the double hydroxide layer (*b*) and the geometry of the $M(\text{OH})_6$ octahedra (*c*).

(1996). However, in contrast to Brazilian quintinite, the unit cell of our crystal contains six layers. The sequence of layers can be described as ...AC=CA=AC=CA=AC=CA...

Thus, in terms of layer-stacking sequence, the structure clearly has a pseudo-period with a *c* parameter of ~ 15.12 Å, which is one-third of that observed experimentally. The tripling of the *c*

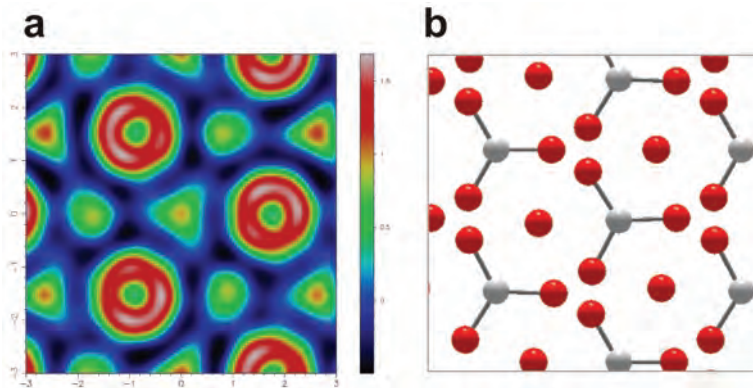


FIG. 7. Electron density Fourier map of the interlayer in quintinite-2H-3c (*a*) and a model of the disordered interlayer arrangement of carbonate anions and water molecules (*b*).

parameter is caused by Mg-Al ordering in the $[\text{Mg}_2\text{Al}(\text{OH})_6]^+$ layer.

Cation ordering

There are three non-equivalent, octahedrally-coordinated cation sites in the (super-) structure. As the scattering factors of Mg^{2+} and Al^{3+} cations are nearly identical, the only way to distinguish between Mg and Al sites is to evaluate $M-\text{O}$ bond lengths. The structure refinement (Table 2) indicates that one M site has bond lengths in the range 1.936–1.940 Å and two M sites have bond lengths of 2.042–2.045 and 2.070–2.077 Å. Thus, bond lengths distinguish two distinct types

of site that are consistent with ordered occupancy by Al (shorter bonds) and Mg (longer bonds). The site assignment given in Table 2 implies perfect Mg-Al ordering. However, the difference between $\text{Mg}-\text{O}$ bond lengths and bond-valence calculations implies that the ordering is not perfect, which also explains the diffuse component of reflections with $h-k \neq 3n$.

Interlayer structure

Characterization of the structure of the interlayer of quintinite is a challenge, because of the strong disorder usually observed for CO_3 groups and H_2O molecules in carbonate-bearing LDHs.

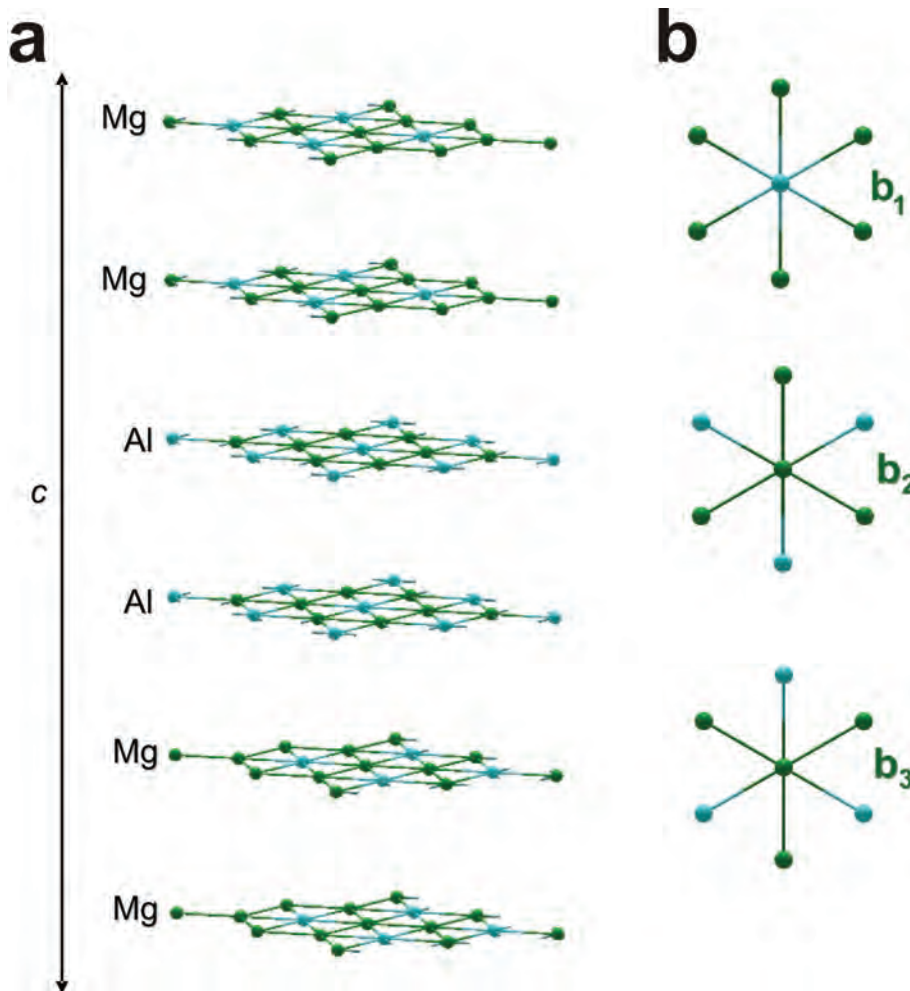


FIG. 8. Relative positions of Mg_2Al cation arrays in double hydroxide layers within the unit cell of quintinite-2H-3c (a) and three different positions of the Mg_2Al array with ordered distribution of Mg and Al cations (b).

Figure 7a shows a difference-Fourier electron density map calculated at the interlayer level, whereas Fig. 7b shows an approximate identification of the electron density peaks as proposed by the refinement. It can be seen that electron density maxima corresponding to the O atoms of carbonate groups are arranged into almost continuous toroidal regions, which makes refinement a very difficult task. As there is no evidence of any dynamic disorder effects in the structure (e.g. rotation of carbonate triangles), we assume that the observed continuous character of the tori is due to positional disorder. Clearly, a low-temperature single-crystal XRD study is needed to clarify this issue.

Discussion

The current study reports for the first time observation of long-range superstructure in carbonate-bearing LDH formed by combination of two-layer stacking sequence and Mg-Al cation ordering. This can be seen clearly in Fig. 8a which displays the relative positions of cation arrays in the structure under consideration. According to the Bookin and Drits (1993) nomenclature, all anions are either in A or C positions, whereas all cations are in the b positions. However, the sequence of the b positions if seen along the c axis can be occupied differently by Mg and Al cations. In general, this sequence can be written as [MgMgMgMgAlAl] or [Mg₄Al₂], taking into account that the content given in the square brackets corresponds to the c parameter repeat. Considering possible relative positions of the 2-D Mg-Al cation array, one may distinguish exactly three different Mg₂Al arrays related to each other by a or b translations (Fig. 8b). These arrays may be indicated as b₁, b₂ and b₃ (since all cations are in the b positions). Therefore the full description of the layer sequence (*i.e.* description that takes into account cation ordering) can be written as:

$$\dots = \text{Ab}_1\text{C} = \text{Cb}_1\text{A} = \text{Ab}_2\text{C} = \text{Cb}_2\text{A} = \text{Ab}_3\text{C} = \text{Cb}_3\text{A} = \dots$$

This sequence corresponds to the six-layer polytype and completely characterizes the observed structure, taking into account layer stacking and cation ordering.

As was mentioned above, the structure of Brazilian quintinite-2H was reported by Arakcheeva *et al.* (1996). Their structure model consists of a completely ordered [Mg₂Al(OH)₆]⁺ layer (which is manifest in the a parameter of

5.283 Å) and a two-layer sequence (c = 15.150 Å). The Mg and Al sites are segregated into lines along the c axis (the cation sequences along the c axis are either [Mg₂] or [Al₂]), which means that the Mg₂Al 2-D arrays are in the same relative position along the c direction. The full description of the layer sequence can be written as:

$$\dots = \text{Ab}_1\text{C} = \text{Cb}_1\text{A} = \dots$$

This sequence also indicates that our crystal of quintinite can be considered to have been built from two-layer quintinite-2H modules 15 Å thick and stacked in an ordered fashion along the c axis.

The results obtained in this study demonstrate that the current polytype notation (Bookin and Drits, 1993; Drits and Bookin, 2001) is insufficient to characterize the structural architecture of LDH polytypes completely, because it does not include the possibility of intralayer cation ordering. In order to distinguish between the stacking sequences with different cation distributions, certain additional descriptors should be included in the mineral formula. One possibility is to use a suffix indicating a value of the c parameter compared to the ‘standard’ polytype. For instance, quintinite studied by Arakcheeva *et al.* (1996) can be described as quintinite-2H-1c, whereas quintinite reported in this study can be described as quintinite-2H-3c. Though this does not characterize the structure completely, it would be sufficient to distinguish between the quintinite polytypes reported so far. As the real symmetry of the structure reported here is rhombohedral, an additional suffix can be added to the polytype name: quintinite-2H-3c[6R].

Acknowledgements

The authors are grateful to the Principal Editor, Mark Welch, for extensive and thorough editing of this manuscript. The research was supported by the Russian Foundation for Basic Research (grant 10-05-00431) and the President of Russian Federation Grant for Young Candidates of Sciences (to AAZ, grant MK-1783.2010.5).

References

- Allmann, R. (1968) The crystal structure of pyroaurite. *Acta Crystallographica*, **B24**, 972–977.
- Allmann, R. and Donnay, J.D.H. (1969) About the structure of iowaite. *American Mineralogist*, **54**, 296–299.
- Allmann, R. and Jepsen, H.P. (1969) Die struktur des

CRYSTAL STRUCTURE OF QUINTINITE

- Hydrotalkits. *Neues Jahrbuch für Mineralogie, Monatshefte*, **1969**, 544–551.
- Arakcheeva, A.V., Pushcharovskii, D.Yu., Atencio, D. and Lubman, G.U. (1996) Crystal structure and comparative crystal chemistry of $\text{Al}_2\text{Mg}_4(\text{OH})_{12}(\text{CO}_3)_3\text{H}_2\text{O}$, a new mineral from the hydrotalcite-manasite group. *Crystallography Reports*, **41**, 972–981.
- Arrhenius, G.O. (2003) Crystals and Life. *Helvetica Chimica Acta*, **86**, 1569–1586.
- Bellotto, M., Rebours, B., Clause, O., Lynch, J., Bazin, D. and Elkaim, E. (1996) A reexamination of hydrotalcite crystal chemistry. *Journal of Physical Chemistry*, **100**, 8527–8534.
- Bookin, A.S. and Drits, V.A. (1993) Polytype diversity of the hydrotalcite-like minerals. I. Possible polytypes and their diffraction patterns. *Clays and Clay Minerals*, **41**, 551–557.
- Bookin, A.S., Cherkashin, V.I. and Drits, V.A. (1993) Polytype diversity of the hydrotalcite-group minerals. II. Determination of the polytypes of experimentally studied varieties. *Clays and Clay Minerals*, **41**, 558–564.
- Braithwaite, R.S.W., Dunn, P.J., Pritchard, R.G. and Paar, W.H. (1994) Iowaite, a re-investigation. *Mineralogical Magazine*, **58**, 79–85.
- Britto, S. and Kamath, P.V. (2009) Structure of bayerite-based lithium-aluminum layered double hydroxides (LDHs): observation of monoclinic symmetry. *Inorganic Chemistry*, **48**, 11646–11654.
- Chao, G.Y. and Gault, R.A. (1997) Quintinite-2H, quintinite-3T, charmarite-2H, charmarite-3T and caresite-3T, a new group of carbonate minerals related to the hydrotalcite/manasite group. *The Canadian Mineralogist*, **35**, 1541–1549.
- Choy, J.-H., Kwak, S.-Y., Park, J.-S., Jeong, Y.-J. and Portier, J. (1999) Intercalative nanohybrids of nucleoside monophosphates and DNA in layered metal hydroxide. *Journal of the American Chemical Society*, **121**, 1399–1400.
- Christiansen, B.C., Balic-Zunic, T., Petit, P.O., Frandsen, C., Morup, S., Geckeis, H., Katerinopoulou, A. and Stipp, S.L.S. (2009) Composition and structure of an iron-bearing, layered double hydroxide (LDH) – Green rust sodium sulphate. *Geochimica et Cosmochimica Acta*, **73**, 3579–3592.
- Cooper, M.A. and Hawthorne, F.C. (1996) The crystal structure of shigaite, $[\text{AlMn}_2^{2+}(\text{OH})_6]_3(\text{SO}_4)_2 \text{Na}(\text{H}_2\text{O})_6\{\text{H}_2\text{O}\}_6$, hydrotalcite-group mineral. *The Canadian Mineralogist*, **34**, 91–97.
- Drits, V.A. and Bookin, A.S. (2001) Crystal structure and X-ray identification of layered double hydroxides. Pp. 39–92 in: *Layered Double Hydroxides: Present and Future* (V. Rives, editor). Nova Science Publishers Inc., New York.
- Duan, X. and Evans, D.G., editors (2006) *Layered Double Hydroxides. Structure and Bonding*, Vol. **119**, Springer, Berlin.
- Evans, D.G. and Slade, R.C.T. (2006) Structural aspects of layered double hydroxides. Pp. 1–87 in: *Layered Double Hydroxides* (X. Duan and D.G. Evans, editors). Springer, Berlin.
- Francois, M., Renaudin, G. and Evrard, O. (1998) A cementitious compound with composition $3\text{CaO}\cdot\text{Al}_2\text{O}_3\cdot\text{CaCO}_3\cdot 11\text{H}_2\text{O}$. *Acta Crystallographica, C***54**, 1214–1217.
- Frost, R.L. and Dickfos, M. (2007) Hydrated double carbonates – a Raman and infrared spectroscopic study. *Polyhedron*, **26**, 4503–4508.
- Génin, J.-M.R., Ruby, C. and Upadhyay, C. (2006) Structure and thermodynamics of ferrous, stoichiometric and ferric oxyhydroxycarbonate green rusts; redox exibility and fougere mineral. *Solid State Sciences*, **8**, 1330–1343.
- Greenwell, H.C. and Coveney, P.V. (2006) Layered double hydroxide minerals as possible prebiotic information storage and transfer compounds. *Origins of Life and Evolution of the Biosphere*, **36**, 13–37.
- Hansen, H.C.B. (2001) Environmental chemistry of iron(II)–iron(III) LDHs (Green Rusts). Pp. 413–434 in: *Layered Double Hydroxides: Present and Future* (V. Rives, editor). Nova Science Publishers Inc., New York.
- Hofmeister, W. and von Platen, H. (1992) Crystal chemistry and atomic order in brucite-related double-layer structures. *Crystallography Reviews*, **3**, 3–26.
- Huminicki, D.M.C. and Hawthorne, F.C. (2003) The crystal structure of nikischerite, $\text{NaFe}_6^{2+}\text{Al}_3(\text{SO}_4)_2(\text{OH})_{18}(\text{H}_2\text{O})_{12}$, a mineral of the shigaite group. *The Canadian Mineralogist*, **41**, 79–82.
- Ingram, L. and Taylor, H.F.W. (1967) The crystal structures of sjögrenite and pyroaurite. *Mineralogical Magazine*, **36**, 465–479.
- Ivanyuk, G.Yu. and Yakovenchuk, V.N. (1997) *Minerals of the Kovdor Massif*. Apatity, RAS Kola Science Center publishing, Russia, 116 pp. (in Russian).
- Johnsen, R.E. and Norby, P. (2009) A structural study of stacking disorder in the decomposition oxide of MgAl layered double hydroxide: a DIFFaX plus analysis. *Journal of Physical Chemistry*, **C113**, 19061–19066.
- Khan, A.I. and O’Hare, D. (2002) Intercalation chemistry of layered double hydroxides: recent developments and applications. *Journal of Materials Chemistry*, **12**, 3191–3198.
- Kirkpatrick, R.J., Kalinichev, A.G., Wang, J., Hou, X. and Amonette, J.E. (2005) Molecular modeling of the vibrational spectra of interlayer and surface

- species of layered double hydroxides. Pp. 239–285 in: *The Application of Vibrational Spectroscopy to Clay Minerals and Layered Double Hydroxides* (J.T. Klopdroge, editor). The Clay Minerals Society, Aurora, Colorado, USA.
- Klopdroge, J.T., Wharton, D., Hickey, L. and Frost, R.L. (2002) Infrared and Raman study of interlayer anions CO_3^{2-} , NO_3^- , SO_4^{2-} and ClO_4^- in Mg/Al hydrotalcite. *American Mineralogist*, **87**, 623–629.
- Koch, B.C. and Morup, S. (1991) Identification of green rust in an ochre sludge. *Clay Minerals*, **26**, 577–582.
- Kumar, P.P., Kalinichev, A.G. and Kirkpatrick, R.J. (2006) Hydration, swelling, interlayer structure, and hydrogen bonding in organolayered double hydroxides: insights from molecular dynamics simulation of citrate-intercalated hydrotalcite. *Journal of Physical Chemistry*, **B110**, 3841–3844.
- Menezes, L.A.D. and Martins, J.M. (1984) The Jacupiranga mine, São Paulo, Brazil. *Mineralogical Record*, **15**, 261–270.
- Richardson, M.C. and Braterman, P.S. (2007) Infrared spectra of oriented and nonoriented layered double hydroxides in the range from 4000 to 250 cm^{-1} , with evidence for regular short-range order in a synthetic magnesium-aluminum LDH with Mg:Al = 2:1 but not with Mg:Al = 3:1. *Journal of Physical Chemistry*, **C111**, 4209–4215.
- Rius, J. and Allmann, R. (1984) The superstructure of the double layer mineral wermelandite $[\text{Mg}_7(\text{Al}_{0.57}\text{Fe}_{0.43})_2(\text{OH})_{18}]^{2+}[(\text{Ca}_{0.6}\text{Mg}_{0.4})(\text{SO}_4)_2(\text{H}_2\text{O})_{12}]^{2-}$. *Zeitschrift für Kristallographie*, **168**, 133–144.
- Rives, V., editor (2001) *Layered Double Hydroxides: Present and Future*. Nova Science Publishers Inc., New York.
- Ruby, C., Abdelmoula, M., Aissa, R., Medjahdi, G., Brunelli, M. and François, M. (2008) Aluminium substitution in iron(II–III)-layered double hydroxides: formation and cationic order. *Journal of Solid State Chemistry*, **181**, 2285–2291.
- Sheldrick, G.M. (2008) A short history of SHELX. *Acta Crystallographica*, **A64**, 112–122.
- Sideris, P.J., Nielsen, U.G., Gan, Z.H. and Grey, C.P. (2008) Mg/Al ordering in layered double hydroxides revealed by multinuclear NMR spectroscopy. *Science*, **321**, 113–117.
- Speck, A. (2003) Single-crystal structure validation with the program PLATON. *Journal of Applied Crystallography*, **36**, 7–13.
- Stampfli, P.P. (1969) Ein basisches Eisen-II-III-Karbonat. *Corrosion Science*, **9**, 185–187.
- Stanimirova, T., Piperov, N., Petrova, N. and Kirov, G. (2004) Thermal evolution of Mg-Al- CO_3 hydrotalcites. *Clay Minerals*, **39**, 177–191.
- Taylor, H.F.W. (1973) Crystal structures of some double hydroxide minerals. *Mineralogical Magazine*, **39**, 377–389.
- Terzis, A., Filippakis, S., Kuzel, H.-J. and Burzlaff, H. (1987) The crystal structure of $\text{Ca}_2\text{Al}(\text{OH})_6\text{Cl}\cdot 2\text{H}_2\text{O}$. *Zeitschrift für Kristallographie*, **181**, 29–34.
- Thyveetil, M.-A., Coveney, P.V., Greenwell, H.C. and Suter J.L. (2008) Computer simulation study of the structural stability and materials properties of DNA-intercalated layered double hydroxides. *Journal of the American Chemical Society*, **130**, 4742–4756.
- Trolard, F. (2006) Fougerite: from field experiment to the homologation of the mineral. *Comptes Rendus Geoscience*, **338**, 1158–1166.
- Wang, J., Kalinichev, A.G., Kirkpatrick, R.J. and Hou, X. (2001) Molecular modeling of the structure and energetics of hydrotalcite hydration. *Chemistry of Materials*, **13**, 145–150.
- Wang, J., Kalinichev, A.G., Amonette, J. and Kirkpatrick, R.J. (2003) Interlayer structure and dynamics of Cl-bearing hydrotalcite: far infrared spectroscopy and molecular dynamics modeling. *American Mineralogist*, **88**, 398–409.

PII

QUINTINITE-1M: FIRST EVIDENCE OF MONOCLINIC POLYTYPE IN M^{2+} - M^{3+} LAYERED DOUBLE HYDROXIDES

The paper “Quintinite-1M: first evidence of monoclinic polytype in M^{2+} - M^{3+} layered double hydroxides” was published in Mineralogical magazine (2010, Vol. 74, No. 5, pp. 833-840) by Krivovichev S.V., Yakovenchuk V.N., Zhitova E.S., Zolotarev A.A., Pakhomovsky Ya.A., Ivanyuk G.Yu.

Reproduced, with the permission of the Mineralogical Society of Great Britain & Ireland, from Krivovichev *et al.* (2010), originally published in *Mineralogical Magazine*.

DOI: 10.1180/minmag.2010.074.5.833

Concept: Prof. Dr. S.V. Krivovichev and E.S. Zhitova

Sampling and measurement: E.S. Zhitova, A.A. Zolotarev, A.Ya. Pakhomovsky

Data analysis: E.S. Zhitova, Prof. Dr. S.V. Krivovichev

Writing the manuscript: Prof. Dr. S.V. Krivovichev, E.S. Zhitova, Dr. G.U. Ivanuk, V.N. Yakovenchuk

Crystal chemistry of natural layered double hydroxides. 2. Quintinite-1M: first evidence of a monoclinic polytype in M^{2+} - M^{3+} layered double hydroxides

S. V. KRIVOVICHEV^{1,2,*}, V. N. YAKOVENCHUK³, E. S. ZHITOVA¹, A. A. ZOLOTAREV¹, Y. A. PAKHOMOVSKY³ AND G. YU. IVANYUK^{2,3}

¹ Department of Crystallography, Faculty of Geology, St. Petersburg State University, University Emb. 7/9, 199034 St. Petersburg, Russia

² Nanomaterials Research Center, Kola Science Center, Russian Academy of Sciences, Apatity, Russia

³ Geological Institute, Kola Science Center, Russian Academy of Sciences, Apatity, Russia

[Received 19 March 2010; Accepted 8 September 2010]

ABSTRACT

Quintinite-1M, $[\text{Mg}_4\text{Al}_2(\text{OH})_{12}](\text{CO}_3)(\text{H}_2\text{O})_3$, is the first monoclinic representative of both synthetic and natural layered double hydroxides (LDHs) based on octahedrally coordinated di- and trivalent metal cations. It occurs in hydrothermal veins in the Kovdor alkaline massif, Kola peninsula, Russia. The structure was solved by direct methods and refined to $R_1 = 0.031$ on the basis of 304 unique reflections. It is monoclinic, space group $C2/m$, $a = 5.266(2)$, $b = 9.114(2)$, $c = 7.766(3)$ Å, $\beta = 103.17(3)^\circ$, $V = 362.9(2)$ Å³. The diffraction pattern of quintinite-1M contains sharp reflections corresponding to the layer stacking sequence characteristic of the 3R rhombohedral polytype, and rows of weak superlattice reflections superimposed upon a background of streaks of modulated diffuse intensity parallel to c^* . These superlattice reflections indicate the formation of a 2-D superstructure due to Mg-Al ordering. The structure consists of ordered metal hydroxide layers and a disordered interlayer. As the unit cell contains exactly one layer, the polytype nomenclature dictates that the mineral be called quintinite-1M. The complete layer stacking sequence can be described as ...=Ac₁B=Ba₁C=Cb₁A=... Quintinite-1M is isostructural with the monoclinic polytype of $[\text{Li}_2\text{Al}_4(\text{OH})_{12}](\text{CO}_3)(\text{H}_2\text{O})_3$.

KEYWORDS: layered double hydroxides, quintinite, crystal structure, polytypism, Kovdor alkaline massif, Russia.

Introduction

ALL known layered double hydroxides (LDHs) containing $[\text{M}_n^{2+}\text{M}_m^{3+}(\text{OH})_{2(m+n)}]^{m+}$ layers ($\text{M}^{2+} = \text{Mg}^{2+}$, Fe^{2+} , Mn^{2+} , Zn^{2+} , etc.; $\text{M}^{3+} = \text{Al}^{3+}$, Fe^{3+} , Cr^{3+} , Mn^{3+} , etc.) possess either trigonal (rhombohedral) or hexagonal symmetry. This is a direct consequence of the trigonal symmetry of metal hydroxide layers and the way the layers stack relative to each other. As indicated by Bookin and Drits (1993), layer stacking generates either

trigonal prismatic voids or octahedral voids that also have trigonal or hexagonal symmetry. Cation ordering may influence structure symmetry and results in the formation of superstructures (Krivovichev *et al.*, 2010). Here we report the first occurrence of a monoclinic polytype in LDHs with di- and trivalent metal cations.

There is a special class of LDHs that are formed by combination of mono- and trivalent metal cations, namely Li^+ and Al^{3+} . The structures of these LDHs are based on $[\text{Li}^+\text{Al}_2^{3+}(\text{OH})_6]^+$ layers that can be considered as dioctahedral, gibbsite-like, Al hydroxide layers with Li^+ cations inserted into octahedral voids. In order to compensate for the positive layer charge,

* E-mail: sk@min.uni-kiel.de
DOI: 10.1180/minmag.2010.074.5.833

anionic species such as CO_3^{2-} , Cl^- , Br^- and OH^- are incorporated. The first LiAl_2 LDH was prepared by Serna *et al.* (1982), and since then this class of compounds has received considerable attention due to their application in catalysis (Lei *et al.*, 2006) and shape-selective intercalation of anions (Fogg *et al.*, 1998, 1999, 2002). Serna *et al.* (1982) indexed the powder X-ray diffraction (XRD) pattern of the compound $[\text{Li}_2\text{Al}_4(\text{OH})_{12}](\text{CO}_3)(\text{H}_2\text{O})_3$ on an hexagonal cell, but Sissoko *et al.* (1985) suggested that it crystallizes in monoclinic space group $C2/m$, a result that was confirmed by Britto *et al.* (2008)



FIG. 1. Crystals of quintinite-1M on a magnetite surface (Kovdor alkaline massif, Kola peninsula, Russia).

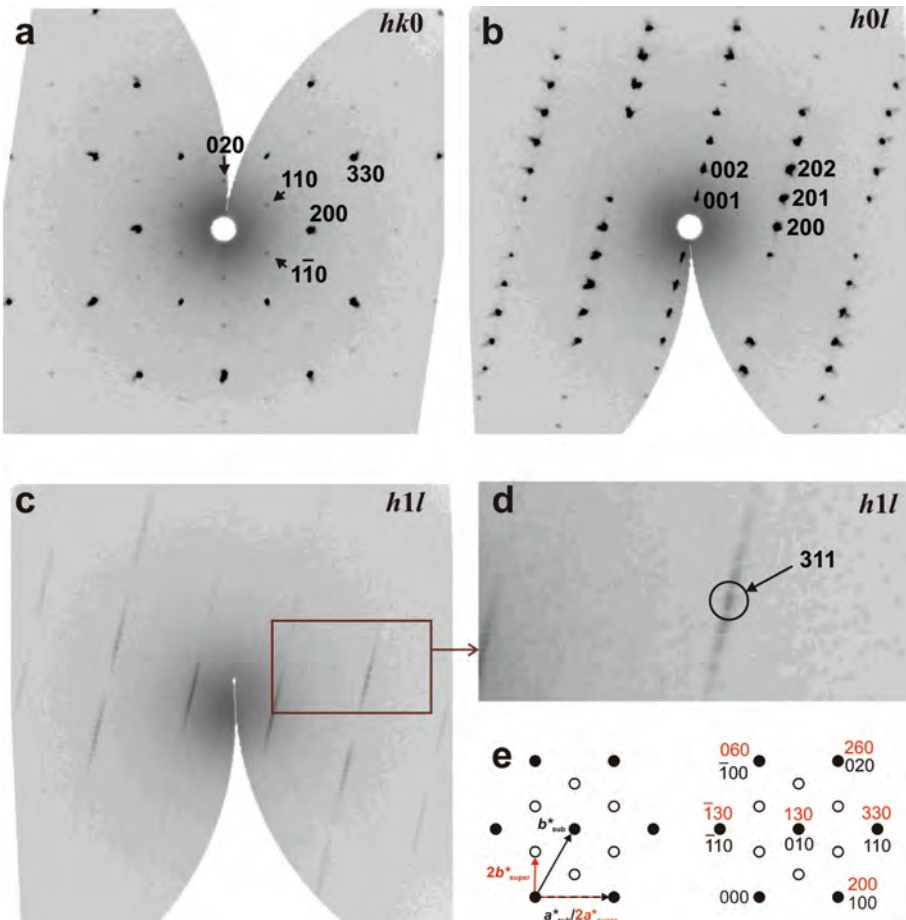


FIG. 2. Reconstructed sections of reciprocal space obtained for quintinite-1M: $hk0$ section (a: note weak reflections with odd h and k indices), $h0l$ section (b: note the presence of sharp Bragg reflections), $h1l$ section (c: note the presence of only weakly discrete diffraction streaks elongated along the c^* axis), and enlarged part of the $h1l$ section showing the position of the 311 reflection (d). The scheme in (e) shows the choice of reciprocal space vectors and indexing of reflections in the $hk0$ section (the black and red colours indicate subcell and supercell vectors and indices, respectively).

who reported a monoclinic C cell with the parameters $a = 5.0858$, $b = 8.8088$, $c = 7.758 \text{ \AA}$, $\beta = 102.62^\circ$. Similar results were reported for LiAl₂ LDHs with other interlayer anions by Thiel *et al.* (1993) and Britto and Kamath (2009). Monoclinic symmetry has not been reported for ‘classical’ M^{2+} - M^{3+} LDHs. In the present study we describe the characterization of the first monoclinic M^{2+} - M^{3+} LDH.

Experimental

The sample of quintinite studied here was obtained from hydrothermal veins of the Kovdor

alkaline massif, Kola peninsula, Russia, as was the sample of quintinite- $2H$ - $3c$ studied by Krivovichev *et al.* (2010). However, the appearance of the sample is quite different (Fig. 1): crystals of this quintinite form aggregates of colourless or greyish flakes on the surface of magnetite ore.

The chemical composition of quintinite was determined by the wave-length dispersive X-ray spectrometry using a Cameca MS-46 electron microprobe operated at 20 kV and 20–30 nA. The average of six spot analyses is (wt.%): MgO 34.20, Al₂O₃ 21.40, which gives Mg:Al = 2:1. The oxide total (55.60 wt.%) is consistent with an

TABLE 1. Crystallographic data and refinement parameters for quintinite- $1M$.

Crystal data

Ideal formula	$[\text{Mg}_4\text{Al}_2(\text{OH})_{12}](\text{CO}_3)(\text{H}_2\text{O})_3$
Crystal system	Monoclinic
Space group	$C2/m$
Unit-cell dimensions a , b , c , β (\AA , $^\circ$)	5.266(2), 9.114(2), 7.766(3), 103.17(3)
Unit-cell volume (\AA^3)	362.9(2)
Z	1
Calculated density (g/cm^3)	2.130
Absorption coefficient (mm^{-1})	0.42
Crystal size (mm)	0.08 \times 0.04 \times 0.01

Data collection

Diffractometer	Stoe IPDS II Image-Plate
Temperature (K)	293
Radiation, wavelength (\AA)	Mo- $K\alpha$, 0.71073
θ range for data collection ($^\circ$)	4.47–29.16
h , k , l ranges	± 7 , 0 \rightarrow 12, -10 \rightarrow 0
Axis, frame width ($^\circ$), time per frame (s)	ω , 2, 60
Reflections collected	511
Unique reflections	511
Unique reflections $F > 4\sigma(F)$	304
Data completeness to θ_{\max} (%)	97.9

Structure refinement

Refinement method	Full-matrix least-squares on F^2
Weighting coefficients a , b^*	0.0666, 0.2562
Extinction coefficient	—
Data/restraints/parameters	511/2/65
R_1 [$F > 4\sigma(F)$], wR_2 [$F > 4\sigma(F)$],	0.031, 0.102
R_1 all, wR_2 all	0.055, 0.119
Goodness-of-fit on F^2	0.996
Largest diff. peak and hole ($e \text{ \AA}^{-3}$)	0.32, -0.28

$$R_{\text{int}} = (n/n - 1)^{1/2} [F_{\text{o}}^2 - F_{\text{o}} \text{ (mean)}^2]/\Sigma F_{\text{o}}^2$$

$$R_1 = \sum |F_{\text{o}}| - |F_{\text{c}}| / \sum |F_{\text{o}}|; wR_2 = \{ \sum [w(F_{\text{o}}^2 - F_{\text{c}}^2)^2] / \sum [w(F_{\text{o}}^2)^2] \}^{1/2};$$

$$* w = 1/[\sigma^2(F_{\text{o}}^2) + (aP)^2 + bP], \text{ where } P = (\max(F_{\text{o}}, 0) + 2F_{\text{c}})/3;$$

$$\text{GooF} = \{ \sum [w(F_{\text{o}}^2 - F_{\text{c}}^2)^2] / (n - p) \}^{1/2}$$

where n is the number of reflections and p is the number of refined parameters.

ideal formula of $[\text{Mg}_4\text{Al}_2(\text{OH})_{12}](\text{CO}_3)(\text{H}_2\text{O})_3$. An infrared (IR) spectrum of quintinite was recorded using a Bruker Vertex IR spectrometer and was found to be in general agreement with that of quintinite- $2H\text{-}3c$.

The crystal of quintinite selected for single-crystal XRD study was mounted on a Stoe IPDS II Image-Plate-based X-ray diffractometer operated at 50 kV and 40 mA. More than a hemisphere of three-dimensional data was collected using monochromatic Mo- $K\alpha$ X-radiation, with frame widths of 2° in ω , and with a 60 s count for each frame. As was observed for quintinite- $2H\text{-}3c$ by Krivovichev *et al.* (2010) the three-dimensional diffraction pattern of the new sample contains weak diffuse discrete streaks which clearly indicated the formation of a 2-D superstructure due to Mg-Al ordering (Fig. 2). Using Stoe Integration software ($X\text{-Area} = 1.42$; Stoe, 1997), it was possible to integrate weak superlattice reflections into indexing of the diffraction pattern, which gave a *C*-centred monoclinic cell (Table 1) similar to that reported for $[\text{Li}_2\text{Al}_4(\text{OH})_{12}](\text{CO}_3)(\text{H}_2\text{O})_3$ (see above). A quadrant of unique data was collected ($h = \pm 7$, $k = 0 \rightarrow 12$, $l = -10 \rightarrow 0$).

The structure was solved in the space group $C2/m$. The *SHELXL* program package was used

for all structural calculations (Sheldrick, 2008). The final model included all atomic positional parameters, anisotropic-displacement parameters for atoms of the metal hydroxide layer and a refinable weighting scheme for structure factors. The final refinement converged to an agreement index $R_1 = 0.031$, calculated for the 304 unique reflections with $|F_o| \geq 4\sigma_F$. Final atom coordinates and anisotropic-displacement parameters are given in Table 2, and selected interatomic distances in Table 3. The list of observed and calculated structure factors can be downloaded from the journal's website at www.minersoc.org/pages/e_journals/dep_mat.html.

Results and discussion

As for quintinite- $2H\text{-}3c$ (Krivovichev *et al.*, 2010), metal hydroxide layers in monoclinic quintinite have almost perfect Mg-Al ordering which can be inferred from average Mg–O (2.044 Å) and Al–O (1.944 Å) bond lengths. We infer that this cation ordering is responsible for the appearance of weak superstructure reflections, which correspond to the $h-k \neq 3n$ reflections of Mg-Al ordered quintinite- $2H\text{-}3c$ (Krivovichev *et al.*, 2010).

TABLE 2. Atom coordinates, equivalent isotropic displacement parameters (\AA^2) and site occupancies for quintinite- $1M$.

Atom	Occupancy	<i>x</i>	<i>y</i>	<i>z</i>	U_{eq}
Octahedral sheet					
Al	1	$\frac{1}{2}$	$\frac{1}{2}$	$\frac{1}{2}$	0.0119(4)
Mg	1	$\frac{1}{2}$	0.16669(8)	$\frac{1}{2}$	0.0090(4)
O(H)1	1	0.6162(2)	0.33943(13)	0.36945(18)	0.0149(4)
O(H)2	1	0.1370(3)	$\frac{1}{2}$	0.3688(3)	0.0146(5)
H1	1	0.096(8)	$\frac{1}{2}$	0.2425(14)	0.05*
H2	1	0.568(6)	0.341(3)	0.2437(14)	0.05*
Interlayer anions and water molecules					
O11	0.16(3)	0.107(6)	$\frac{1}{2}$	-0.001(2)	0.027(8)
O12	0.163(15)	0.550(3)	0.3849(19)	0.0018(18)	0.031(5)
O21	0.151(13)	0.051(2)	0.442(2)	-0.0016(15)	0.020(4)
O22	0.195(16)	0.445(2)	0.2882(19)	0.0010(16)	0.036(4)
O23	0.15(2)	0.388(5)	0.338(3)	-0.0010(18)	0.031(7)
C1	0.081(9)	0.326(6)	$\frac{1}{2}$	-0.004(5)	0.014(8)
C2	0.084(4)	0.165(5)	0.328(3)	-0.005(3)	0.022(5)
Ow	0.09(4)	0	$\frac{1}{2}$	0	0.010(18)

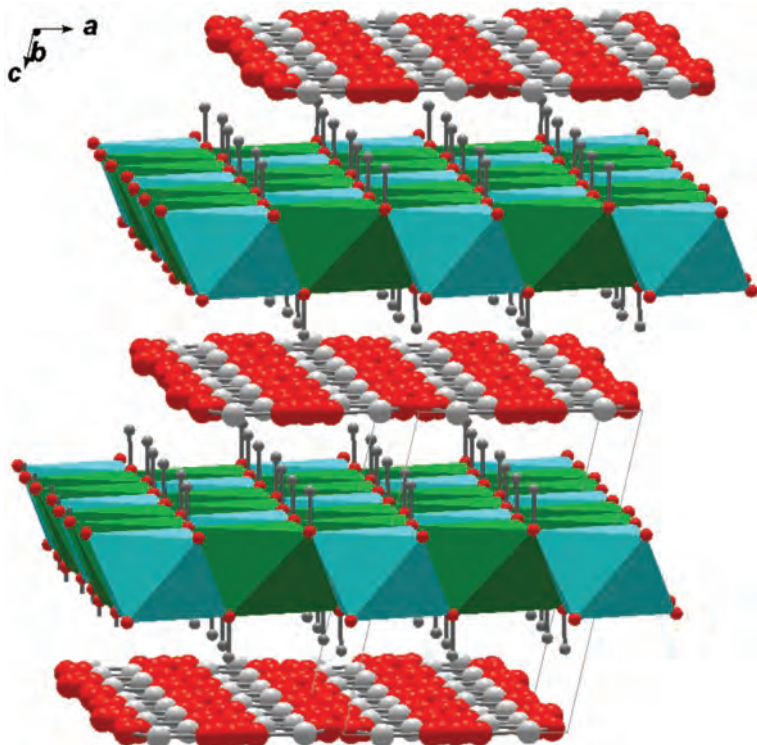
* fixed during refinement

TABLE 3. Selected bond lengths (\AA) in the structure of quintinite-1*M*.

Al—O(H)2	1.950(2)	2 ×	C1—O11	1.16(4)
Al—O(H)1	1.956(1)	4 ×	C1—O12	1.23(2)
MgO(H)1	2.041(1)	2 ×	C2—O21	1.20(3)
MgO(H)1	2.045(2)	2 ×	C2—O22	1.21(3)
MgO(H)2	2.0496(14)	2 ×	C2—O23	1.17(4)

The structure of monoclinic quintinite is shown in Fig. 3. It consists of ordered metal hydroxide layers and disordered interlayers. As the unit cell contains a one-layer repeat, polytype nomenclature dictates that the mineral be called quintinite-1*M* (monoclinic, one-layer). The analysis of layer stacking from the viewpoint of the theory outlined by Bookin and Drits (1993) leads to quintinite-1*M* being described by the layer sequence ...=AB=BC=CA=... (Krivovichev *et al.*, 2010). This sequence

corresponds to that of the 3*R*₁ polytype, which is characteristic of the ‘classical’ hydrotalcite structure. However, because of the cation ordering, the situation becomes more complex and can be deciphered from the analysis of the relative positions of the two-dimensional Mg₂Al cation arrays (Fig. 4). First, it is obvious that cations in quintinite-1*M* are located in all possible sites, a, b and c, so that the full description of the layer sequence should be written as: ...=AcB=BaC=CbA=...

FIG. 3. Crystal structure of quintinite-1*M*.

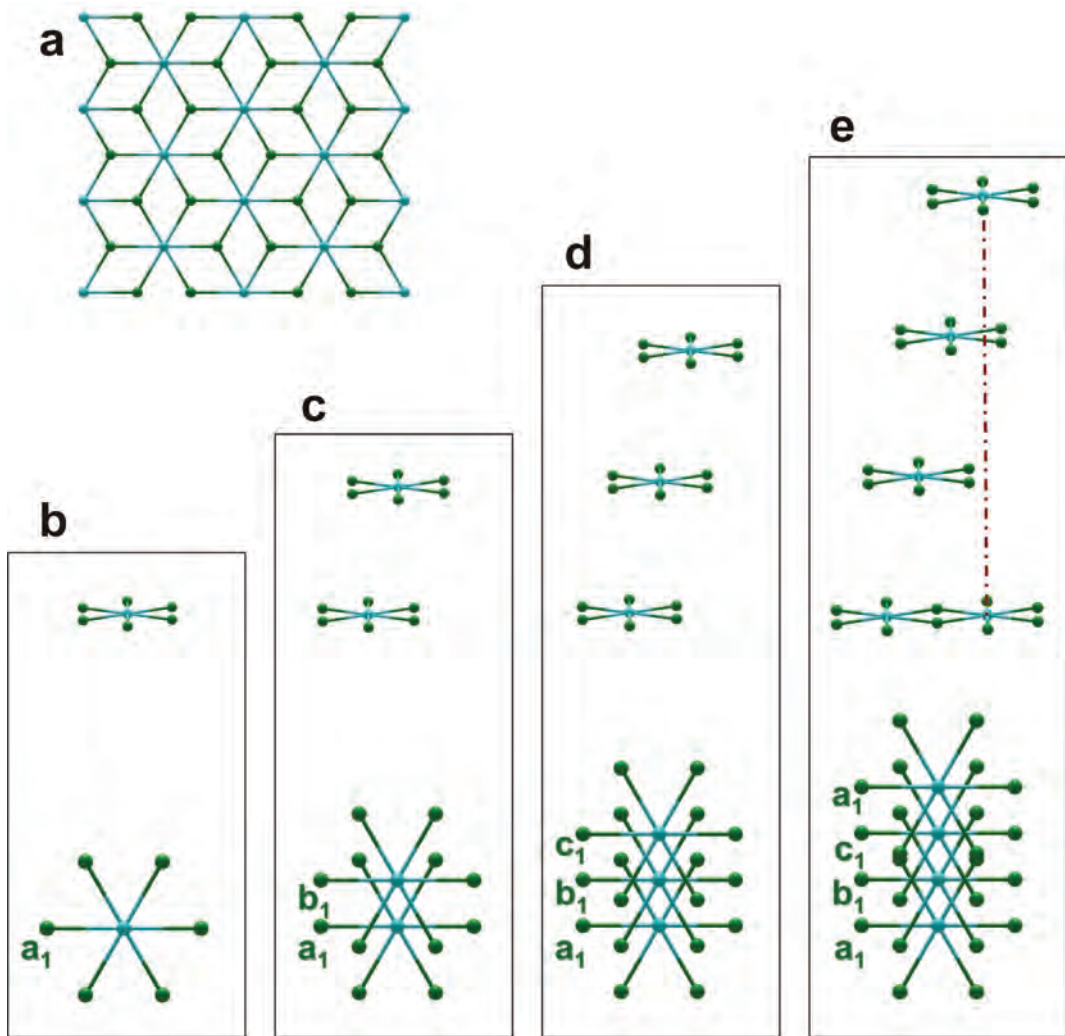


FIG. 4. Ordered Mg₂Al array in the structure of quintinite-1M (a) and relative positions of stacked Mg₂Al arrays: one (b), two (c), three (d) and four arrays (e). Note that the fourth array is equivalent to the first relative to the translation perpendicular to the layer plane.

In the case of complete Mg-Al disorder, a structure with this sequence would have a rhombohedral symmetry (space group *Rm*), but cation ordering results in lowering of symmetry and the formation of a superstructure. As can be seen from Fig. 4, Al cations in adjacent Mg₂Al arrays are located on a mirror plane *m* in the space group *C2/m*. This results in the disappearance of the threefold symmetry axis perpendicular to the layers and the transition from rhombohedral to monoclinic symmetry. In order to distinguish between *a*, *b* and *c* positions occupied by Mg and Al cations in the

Mg₂Al array, we identify them as *a*₁, *a*₂, *a*₃, etc., as for quintinite-2H-3c. Thus, the complete layer stacking sequence can be described as ...=Ac₁B=Ba₁C=Cb₁A=... It is of interest that the theoretical sequence ...=Ac₁B=Ba₁C=Cb₂A=... has trigonal symmetry with Al positions in adjacent layers related by a 3₁ axis, an arrangement not yet observed in natural LDHs. The theoretical derivation of possible polytypes in ordered M₂⁺M³⁺ LDHs will be the subject of a separate paper.

Figure 5a shows an electron-density distribution map of quintinite-1M at the level of the

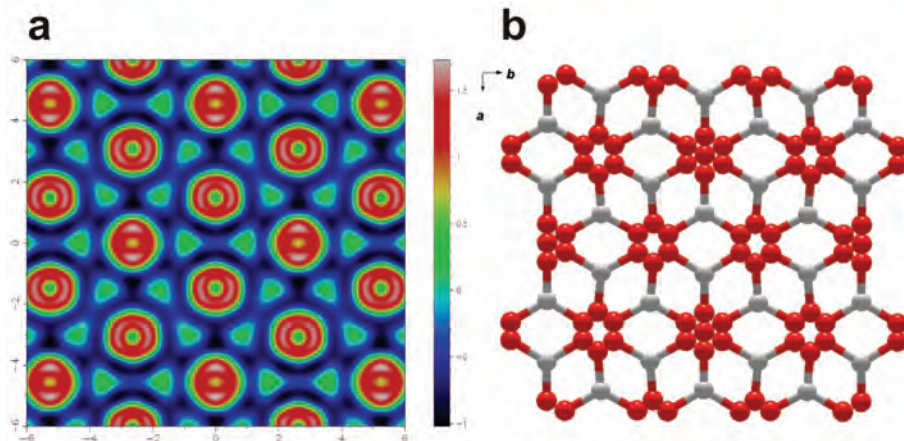


FIG. 5. Electron density Fourier map of the interlayer in quintinite-1M (*a*) and a model of the disordered interlayer arrangement of carbonate anions and water molecules (*b*).

$\text{CO}_3/\text{H}_2\text{O}$ interlayer. As with quintinite-2*H*-3*c* (Krivovichev *et al.*, 2010), this map has an almost continuous toroidal distribution of electron-density maxima, corresponding to the positions of O atoms of carbonate groups (Fig. 5*b*). However, in contrast to quintinite-2*H*-3*c*, these shapes are elliptical rather than circular, being either compressed or elongated relative to the *b* axis, a feature that is undoubtedly the consequence of symmetry reduction.

From the unit-cell parameters and the results of crystal-structure refinement, it is evident that quintinite-1*M* is isostructural with the monoclinic polytype of $[\text{Li}_2\text{Al}_4(\text{OH})_{12}](\text{CO}_3)(\text{H}_2\text{O})_3$ reported previously (Sissoko *et al.*, 1985; Britto *et al.*, 2008). However, monoclinic symmetry has never been observed previously in natural or synthetic LDHs having di- and trivalent cations. It is noteworthy that symmetry reduction is induced by the Mg-Al ordering in metal hydroxide layers and the ordered stacking of these layers. Taking into account the small difference in Mg and Al scattering factors, it is perhaps surprising that Mg-Al ordering is registered by the appearance of weak superstructure reflections.

Acknowledgements

The authors are grateful to the referees for their remarks and to the Principal Editor, Mark Welch, for extensive corrections. This work was supported by the Russian Foundation for Basic Research (grant # 10-05-00431) and the President

of Russian Federation Grant for Young Candidates of Sciences (to AAZ, grant MK-1783.2010.5).

References

- Bookin, A.S. and Drits, V.A. (1993) Polytype diversity of the hydrotalcite-like minerals. I. Possible polytypes and their diffraction patterns. *Clays and Clay Minerals*, **41**, 551–557.
- Britto, S. and Kamath, P.V. (2009) Structure of bayerite-based lithium–aluminum layered double hydroxides (LDHs): observation of monoclinic symmetry. *Inorganic Chemistry*, **48**, 11646–11654.
- Britto, S., Thomas, G.S., Kamath, P.V. and Kannan, S. (2008) Polymorphism and structural disorder in the carbonate containing layered double hydroxide of Li with Al. *Journal of Physical Chemistry*, **C112**, 9510–9515.
- Fogg, A.M., Dunn, J.S., Shyu, S.-G., Cary, D.R. and O’Hare, D. (1998) Selective ion-exchange intercalation of isomeric dicarboxylate anions into the layered double hydroxide $[\text{LiAl}_2(\text{OH})_6]\text{Cl}\cdot\text{H}_2\text{O}$. *Chemistry of Materials*, **10**, 351–355.
- Fogg, A.M., Green, V.M., Harvey, H.G. and O’Hare, D. (1999) New separation science using shape-selective ion exchange intercalation chemistry. *Advanced Materials*, **11**, 1466–1469.
- Fogg, A.M., Freij, A.J. and Parkinson, G.M. (2002) Synthesis and anion exchange chemistry of rhombohedral Li/Al layered double hydroxides. *Chemistry of Materials*, **14**, 232–234.
- Krivovichev, S.V., Yakovenchuk, V.N., Zhitova, E.S., Zolotarev, A.A., Pakhomovsky, Ya.A. and Ivanyuk,

- G.Yu. (2010) Crystal chemistry of natural layered double hydroxides. 1. Quintinite- $2H\text{-}3c$ from the Kovdor alkaline massif, Kola peninsula, Russia. *Mineralogical Magazine*, **74**, 821–832.
- Lei, L., Zhang, L., Hu, M. and Zheng, H. (2006) Alkaline hydrolysis of dimethyl terephthalate in the presence of $[\text{LiAl}_2(\text{OH})_6]\text{Cl}\cdot 2\text{H}_2\text{O}$. *Journal of Solid State Chemistry*, **179**, 3562–3567.
- Serna, C.J., Rendon, J.L. and Iglesias, J.E. (1982) Crystal-chemical study of layered $[\text{Al}_2\text{Li}(\text{OH})_6]^{+}$
 $\text{X}^{-}\cdot n\text{H}_2\text{O}$. *Clays and Clay Minerals*, **30**, 180–184.
- Sheldrick, G.M. (2008) A short history of SHELX. *Acta Crystallographica*, **A64**, 112–122.
- Sissoko, I., Iyagba, E.T., Sahai, R. and Biloen, P. (1985) Anion intercalation and exchange in $\text{Al}(\text{OH})_3$ -derived compounds. *Journal of Solid State Chemistry*, **60**, 283–288.
- Stoe (1997) *X-Area 1.42*.
- Thiel, J.P., Chiang, C.K. and Poeppelmeier, K.R. (1993) Structure of lithium aluminum hydroxide dihydrate $\text{LiAl}_2(\text{OH})_7\cdot 2\text{H}_2\text{O}$. *Chemistry of Materials*, **5**, 297–304.

PIII

THE CRYSTAL STRUCTURE OF Mg,Al-DISODERED QUINTINITE-2H

The paper “The crystal structure of Mg,Al-disordered quintinite-2H” by Zhitova E.S., Yakovenchuk V.N., Krivovichev S.V., Zolotarev A.A., Pakhomovsky Ya.A., Ivanyuk G.Yu. was published in Mineralogical Magazine (2010, Vol. 74 , No. 5, pp. 841-848).

Reproduced, with the permission of the Mineralogical Society of Great Britain & Ireland, from Zhitova *et al.* (2010), originally published in *Mineralogical Magazine*.

DOI: 10.1180/minmag.2010.074.5.841

Concept: E.S. Zhitova, Prof. Dr. S.V. Krivovichev, V.N. Yakovenchuk

Sampling and measurement: E.S. Zhitova, A.A. Zolotarev, A.Ya. Pakhomovsky, G.Yu. Ivanuk

Data analysis: E.S. Zhitova, A.A. Zolotarev, Prof. Dr. S.V. Krivovichev

Writing the manuscript: E.S. Zhitova, Prof. Dr. S.V. Krivovichev.

Crystal chemistry of natural layered double hydroxides. 3. The crystal structure of Mg,Al-disordered quintinite-2H

E. S. ZHITOVA¹, V. N. YAKOVENCHUK^{2,3}, S. V. KRIPOVICHEV^{1,3,*}, A. A. ZOLOTAREV¹, Y. A. PAKHOMOVSKY^{2,3} AND G. YU. IVANYUK^{2,3}

¹ Department of Crystallography, Faculty of Geology, St. Petersburg State University, University Emb. 7/9, 199034 St. Petersburg, Russia

² Geological Institute, Kola Science Center, Russian Academy of Sciences, Apatity, Russia

³ Nanomaterials Research Center, Kola Science Center, Russian Academy of Sciences, Apatity, Russia

[Received 19 March 2010; Accepted 8 September 2010]

ABSTRACT

Two crystals of Mg,Al-disordered quintinite-2H (Q1 and Q2), $[\text{Mg}_4\text{Al}_2(\text{OH})_{12}](\text{CO}_3)(\text{H}_2\text{O})_3$, from the Kovdor alkaline massif, Kola peninsula, Russia, have been characterized chemically and structurally. Both crystals have hexagonal symmetry, $P6_3/mcm$, $a = 3.0455(10)/3.0446(9)$, $c = 15.125(7)/15.178(5)$ Å, $V = 121.49(8)/121.84(6)$ Å³. The structures of the two crystals have been solved by direct methods and refined to $R_1 = 0.046$ and 0.035 on the basis of 76 and 82 unique observed reflections for Q1 and Q2, respectively. Diffraction patterns obtained using an image-plate area detector showed the almost complete absence of superstructure reflections which would be indicative of the Mg-Al ordering in metal hydroxide layers, as has been observed recently for other quintinite polytypes. The crystal structures are based on double hydroxide layers $[\text{M}(\text{OH})_2]$ with an average disordered distribution of Mg^{2+} and Al^{3+} cations. Average $\langle M-\text{OH} \rangle$ bond lengths for the metal site are 2.017 and 2.020 Å for Q1 and Q2, respectively, and are consistent with a highly Mg-Al disordered, average occupancy. The layer stacking sequence can be expressed as ...=AC=CA=..., corresponding to a Mg-Al-disordered 2H polytype of quintinite. The observed disorder is probably the result of a relatively high temperature of formation for the Q1 and Q2 crystals compared to ordered polytypes. This suggestion is in general agreement with the previous observations which demonstrated, for the Mg-Al system, a higher-temperature regime of formation of the hexagonal (or pseudo-hexagonal in the case of quintinite-2H-3c) 2H polytype in comparison to the rhombohedral (or pseudo-rhombohedral in the case of quintinite-1M) 3R polytype.

KEYWORDS: layered double hydroxides, quintinite, crystal structure, disorder, polytypism.

Introduction

ONE of the important aspects of crystal chemistry of layered double hydroxides (LDHs) containing $[\text{M}_n^{2+}\text{M}_m^{3+}(\text{OH})_{2(m+n)}]^{m+n}$ layers ($\text{M}^{2+} = \text{Mg}^{2+}$, Fe^{2+} , Mn^{2+} , Zn^{2+} , etc.; $\text{M}^{3+} = \text{Al}^{3+}$, Fe^{3+} , Cr^{3+} , Mn^{3+} , etc.) is the degree of order of di- and trivalent metal cations in metal hydroxide layers. This structural feature is especially important for technological applications of synthetic LDH

materials, as Mg and Al ordering results in different catalytic activity of MgAl LDHs (correlated with the numbers of Al^{3+} sites closest to other Al^{3+} sites) (Kim *et al.*, 2003). In addition, different distributions of Al in a Mg hydroxide matrix results in different charge distribution, which is critically important for intercalation reactions. In minerals with $\text{M}^{2+}:\text{M}^{3+} = 2:1$, the $\text{M}^{2+}-\text{M}^{3+}$ ordering was confirmed experimentally in LDH sulphates: motukoreite, $[\text{Mg}_6\text{Al}_3(\text{OH})_{18}]$ $[\text{Na}(\text{SO}_4)_2(\text{H}_2\text{O})_{12}]$ (Rius and Plana, 1986), shigaite, $[\text{Mn}_6^{2+}\text{Al}_3(\text{OH})_{18}]$ $[\text{Na}(\text{SO}_4)_2(\text{H}_2\text{O})_{12}]$ (Cooper and Hawthorne, 1996), and $[\text{Fe}_6^{2+}\text{Al}_3(\text{OH})_{18}]$ $[\text{Na}(\text{SO}_4)_2(\text{H}_2\text{O})_{12}]$ (Huminicki

* E-mail: sk@min.uni-kiel.de

DOI: 10.1180/minmag.2010.074.5.841

and Hawthorne, 2003); Sb(OH)₆-intercalated LDH: zincalstibite, [Zn₂Al(OH)₆][Sb(OH)₆], and cualstibite, [Cu₂Al(OH)₆][Sb(OH)₆] (Bonaccorsi *et al.*, 2007). The only reports of natural LDH carbonates with confirmed M^{2+} - M^{3+} order are the structures of quintinite-2H-1c (Arakcheeva *et al.*, 1996), quintinite-2H-3c (Krivovichev *et al.*, 2010a) and quintinite-1M (Krivovichev *et al.*, 2010b). In zaccagnaite, [Zn₄Al₂(OH)₁₂](CO₃)(H₂O)₃, Merlini and Orlandi (2001) reported the occurrence of diffuse streaks that are indicative of the formation of a Zn-Al superstructure component, but this could not be incorporated into the refinement. It is also noteworthy that Mg-Al/Fe ordering has been observed in wermlandite, [Mg₇(Al,Fe³⁺)₂(OH)₁₈][(Ca,Mg)(SO₄)₂(H₂O)₁₂], the mineral with the M^{2+} : M^{3+} ratio = 7:2 (Rius and Allmann, 1984).

Detection of the cation ordering is especially problematic in synthetic powder samples due to the weakness of the superlattice reflections and, in particular, in synthetic quintinites (i.e. Mg₂Al-CO₃ LDHs). Richardson and Braterman (2007) investigated short-range order in Mg-Al LDHs with Mg:Al = 2:1 and 3:1 by infrared (IR) spectroscopy in the region between 400 and 250 cm⁻¹. They studied both fresh and annealed (for 24 h) Mg₂Al LDHs and found that the annealed specimen had a sharp 447 cm⁻¹ band assigned to the coupling between two adjacent (OH)Mg₂Al groups, which is diagnostic of lattice ordering and which is absent in the IR spectra of fresh Mg₂Al and both fresh and annealed Mg₃Al samples. On this basis, Richardson and Braterman (2007) concluded that an initial disordered Mg₂Al material produced by a solution-precipitation process transforms into a phase with regular Mg-Al order. The driving force for the ordering is the avoidance of edge-sharing between Al(OH)₆ octahedra (overbonded shared oxygens), which, in Mg₂Al LDHs, is possible only through the formation of a regular honeycomb superstructure. In contrast, in Mg₃Al LDHs, Al-Al avoidance may be achieved in a disordered fashion, without the formation of a superstructure.

Sideris *et al.* (2008) investigated Mg-Al ordering in Mg-Al carbonate LDHs with the Mg:Al ratio of ~5:1, 4:1 and 2:1 by means of combined ¹H magic angle spinning and ²⁵Mg triple-quantum magic angle spinning nuclear magnetic resonance (NMR) spectroscopy and found that the Mg²⁺ and Al³⁺ are not randomly distributed in the metal hydroxide sheets and that in Mg₂Al LDH they are ordered in a honeycomb

arrangement. In an earlier study, which is somewhat in disagreement with the Nuclear Magnetic Resonance (NMR) spectroscopic data, Steeds and Morniroli (1992) studied synthetic Mg₂Al-CO₃ LDH by means of selected area electron diffraction (SAED) and showed that, for a few crystals from the sample, the (00l) diffraction patterns indicated evidence of a honeycomb superlattice, although this was not the case for the majority of the sample (see also Evans and Slade, 2006).

Here we report the results of a single-crystal diffraction study of two quintinite crystals from the Kovdor alkaline massif, which, in contrast to other known quintinite samples (Chao and Gault, 1997; Arakcheeva *et al.*, 1996; Krivovichev *et al.*, 2010a,b), show no evidence of superstructures induced by Mg-Al cation ordering.

Experimental

In order to investigate the crystal chemistry of quintinite from different localities in the Kovdor alkaline massif, two quintinite crystals (Q1 and Q2) from different samples were selected. The sample from which crystal Q1 was taken consists of transparent yellowish hexagonal pyramids, whereas the Q2 sample contained transparent bluish hexagonal plates (Fig. 1). The chemical compositions of the samples were determined by wavelength dispersive spectrometry using a Cameca MS-46 electron microprobe operated at 20 kV and 20–30 nA. Analytical data (average of eight analyses) and empirical formulae are given in Table 1. Both samples contain essential amounts of Fe. Infrared (IR) spectra were recorded using a Bruker Vertex IR spectrometer and were found to be basically the same as those obtained for quintinite-2H-3c and quintinite-1M from the same locality.

The crystals of quintinite selected for single-crystal X-ray diffraction (XRD) study were mounted on a Stoe IPDS II X-ray diffractometer with an image-plate detector and operated at 50 kV and 40 mA. More than a hemisphere of three-dimensional intensity data was collected using monochromatic Mo-K α X-radiation, frame widths of 2° in ω and a 60 s counting time for each frame. Initial indexing of diffraction patterns provided unit cells with parameters $a \approx 3.05$, $c \approx 15.1$ Å, characteristic of manasseite, Mg₃Al-CO₃ LDH (Table 2). Inspection of h k 1 and h 0 1 sections of reciprocal space (Fig. 2) showed the almost complete absence of

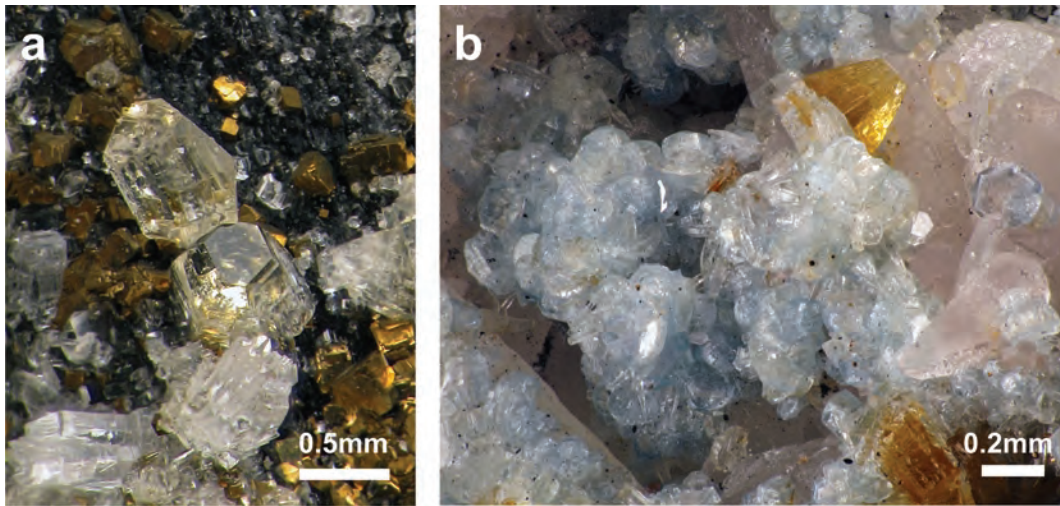


FIG. 1. Crystals of disordered quintinite-2H from the Kovdor alkaline massif: (a) yellowish crystals of sample Q1; (b) transparent blue plates of sample Q2.

superstructure reflections which would indicate Mg-Al ordering in metal hydroxide layers, as has been observed for ordered quintinite polytypes (Krivovichev *et al.*, 2010*a,b*). The structures were solved in space group $P6_3/mcm$. The *SHELXTL* program package was used for all structure calculations (Sheldrick, 2008). The final refinements for the two crystals converged to an agreement index R_1 of 0.046 (Q1) and 0.035

(Q2), calculated for 76 (Q1) and 82 (Q2) unique reflections with $|F_o| \geq 4\sigma_F$. Final atom coordinates and equivalent-isotropic-displacement parameters are given in Table 3, and selected interatomic distances in Table 4. A table of anisotropic displacement parameters and the lists of observed and calculated structure factors can be downloaded from the journal's website at www.minersoc.org/pages/e_journals/dep_mat.html.

TABLE 1. Chemical composition of quintinite crystals Q1 and Q2.

	Q1	Q2
Wt.%		
MgO	33.61	34.05
Al ₂ O ₃	21.00	20.19
Fe ₂ O ₃	2.82	2.23
CO ₂ (calc.)	9.84	9.32
H ₂ O (calc.)	28.82	28.54
Sum	96.09	94.33
a.p.f.u.		
Mg	3.91	4.00
Al	1.93	1.87
Fe	0.16	0.13
CO ₃	1.05	1.00
H ₂ O	3.00	3.00

Results and discussion

The crystal structure of Q1 is shown in Fig. 3. It is based on double hydroxide layers $[M(OH)_2]$ with an average disordered distribution of Mg²⁺ and Al³⁺ cations. The average $\langle M-OH \rangle$ bond lengths are equal to 2.017 and 2.020 Å for Q1 and Q2, respectively, which are between the values observed for $\langle M-O \rangle$ and $\langle Al-O \rangle$ bond lengths in ordered quintinite crystals (Krivovichev *et al.*, 2010*a,b*).

An electron-density distribution map at the level of the interlayer at $z = \frac{1}{4}$, and the modelled distribution of carbonate ions are shown in Fig. 4. In contrast to quintinite-2H-3c and quintinite-1M (Krivovichev *et al.*, 2010*a,b*), no toroidal density distributions were observed in either structure but instead, a rather broad plateau, ~0.8 Å wide.

The stacking sequence of layers can be expressed as ...=AC=CA=..., i.e. with hydroxide

TABLE 2. Crystallographic data and refinement parameters for two crystals of disordered quintinite-2H.

	Crystal Q1	Crystal Q2
Crystal data		
Ideal formula	[Mg ₄ Al ₂ (OH) ₁₂](CO ₃)(H ₂ O) ₃	[Mg ₄ Al ₂ (OH) ₁₂](CO ₃)(H ₂ O) ₃
Crystal system	hexagonal	hexagonal
Space group	P6 ₃ /mcm	P6 ₃ /mcm
Unit-cell dimensions <i>a</i> , <i>c</i> (Å)	3.0455(10), 15.125(7)	3.0446(9), 15.178(5)
Unit-cell volume (Å ³)	121.49(8)	121.84(6)
<i>Z</i>	1	1
Calculated density (g/cm ³)	2.138	2.132
Absorption coefficient (mm ⁻¹)	0.47	0.47
Crystal size (mm)	0.08 × 0.08 × 0.02	0.06 × 0.04 × 0.01
Data collection		
Diffractometer	Stoe IPDS II Image-Plate	Stoe IPDS II Image-Plate
Temperature (K)	293	293
Radiation, wavelength (Å)	Mo-K α , 0.71073	Mo-K α , 0.71073
θ range for data collection (°)	2.69–29.26	2.68–29.11
<i>h</i> , <i>k</i> , <i>l</i> ranges	−4 → 3, ±3, ±20	−4 → 3, ±4, ±20
Axis, frame width (°), time per frame (s)	ω , 2, 60	ω , 2, 60
Reflections collected	829	791
Unique reflections (<i>R</i> _{int})	84 (0.081)	90 (0.037)
Unique reflections <i>F</i> > 4σ(<i>F</i>)	76	82
Data completeness to θ_{\max} (%)	90.3	100
Structure refinement		
Refinement method	Full-matrix least-squares on <i>F</i> ²	Full-matrix least-squares on <i>F</i> ²
Weighting coefficients <i>a</i> , <i>b</i> *	0.0185, 0.2743	0.0525, 0.0483
Extinction coefficient	0.00(6)	0.00(7)
Data/restraints/parameters	84/1/19	90/3/19
<i>R</i> ₁ [<i>F</i> > 4σ(<i>F</i>)], <i>wR</i> ₂ [<i>F</i> > 4σ(<i>F</i>)],	0.046, 0.086	0.035, 0.085
<i>R</i> ₁ all, <i>wR</i> ₂ all	0.053, 0.088	0.044, 0.090
Goodness-of-fit on <i>F</i> ²	1.285	1.331
Largest diff. peak and hole (e Å ^{−3})	0.55, −0.26	0.31, −0.27

$$R_{\text{int}} = (n/n - 1)^{1/2} [F_o^2 - F_o \text{ (mean)}]^2 / \Sigma F_o^2$$

$$R_1 = \sum |F_o| - |F_c| / \sum |F_o|; wR_2 = \{\sum [w(F_o^2 - F_c^2)] / \sum [w(F_o^2)^2]\}^{1/2};$$

* *w* = 1/[σ²(*F*_o²) + (aP)² + bP], where P = (max(*F*_o², 0) + 2*F*_c²)/3;

$$\text{GooF} = \{\sum [w(F_o^2 - F_c^2)]^2 / (n - p)\}^{1/2}$$

where *n* is the number of reflections and *p* is the number of refined parameters.

anions in A and C, and cations in the b positions. As the structure shows no signs of cation ordering, the studied crystals can be characterized as an Mg-Al-disordered 2H polytype of quintinite, in contrast to Mg-Al-ordered quintinite-2H-1c and quintinite-2H-3c reported by Arakcheeva *et al.* (1996) and Krivovichev *et al.* (2010a), respectively. The observed disorder is probably the result of a higher temperature of formation of the Q1 and Q2 samples compared with the ordered polytypes. This suggestion is in general agreement with the previous observations that demon-

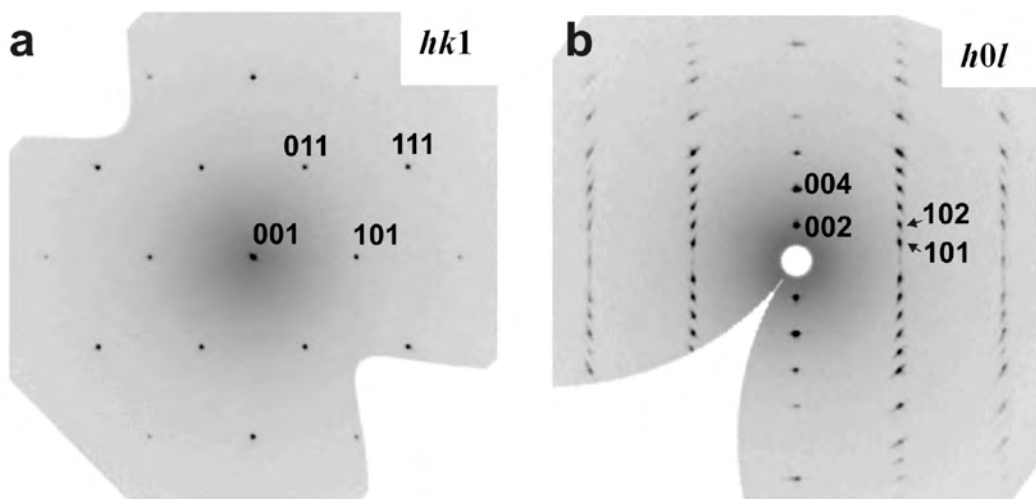
strated, for the Mg-Al system, a higher temperature of formation of the hexagonal (or pseudo-hexagonal in the case of quintinite-2H-3c) 2H polytype compared with the rhombohedral (or pseudo-rhombohedral polytype in the case of quintinite-1M) 3R polytype (Bellotto *et al.*, 1996). Indeed, most syntheses of LDHs are carried out at near-ambient temperatures (coprecipitation is the usual synthesis technique) and the samples obtained display either rhombohedral or random layer stacking. As far as we know, no samples with pure hexagonal (manasseite-type) layer

TABLE 3. Atom coordinates, equivalent isotropic displacement parameters (\AA^2) and site occupancies for crystals Q1 and Q2 of disordered quintinite- $2H$.

Atom	Crystal	Occupancy	<i>x</i>	<i>y</i>	<i>z</i>	<i>U</i> _{eq}
Octahedral sheet						
<i>M</i>	Q1	$\text{Mg}_{2/3}\text{Al}_{1/3}$	0	0	$1/2$	0.0194(9)
	Q2	$\text{Mg}_{2/3}\text{Al}_{1/3}$	0	0	$1/2$	0.0108(7)
O(H)	Q1	1	$1/3$	$2/3$	0.5654(3)	0.0282(13)
	Q2	1	$1/3$	$2/3$	0.56559(16)	0.0197(10)
H	Q1	1	$1/3$	$2/3$	0.621(5)	0.05*
	Q2	1	$1/3$	$2/3$	0.6278(14)	0.05*
C1	Q1	0.08(2)	$1/3$	$2/3$	$1/4$	0.03*
	Q2	0.07(1)	$1/3$	$2/3$	$1/4$	0.017(7)**
C2	Q1	0.09(2)	0	0	$1/4$	0.03*
	Q2	0.09(1)	0	0	$1/4$	0.017(7)**
O1	Q1	0.14(5)	0.562(6)	0.123(13)	$1/4$	0.038(18)
	Q2	0.19(3)	0.5636(19)	0.127(4)	$1/4$	0.049(10)
O2	Q1	0.20(5)	0.766(6)	0.234(6)	$1/4$	0.052(15)
	Q2	0.16(3)	0.7693(18)	0.2307(18)	$1/4$	0.027(9)

* fixed during refinement.

** constrained to be equal during refinement.

FIG. 2. The $hk1$ (a) and $h0l$ (b) sections of reciprocal diffraction space obtained from the Q1 crystal.

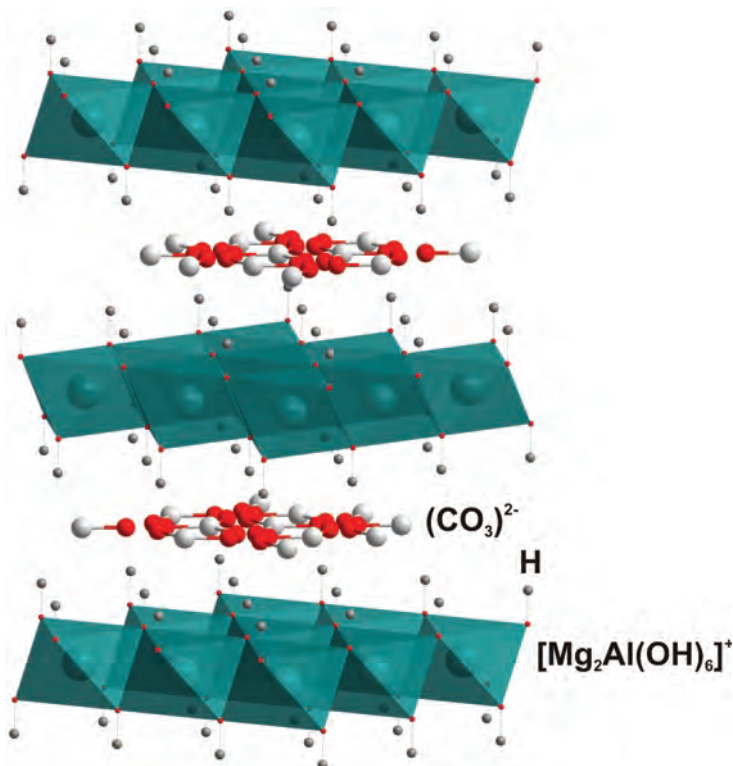


FIG. 3. Crystal structure of disordered quintinite-2H from the Kovdor alkaline massif, sample Q1.

stacking have been reported yet. As was pointed out by Pausch *et al.* (1986), in nature, hydrotalcite and manasseite (Mg_3Al-CO_3 LDHs) are commonly intergrown, with manasseite forming the core and hydrotalcite the outer part of a mineral grain. Similar observations were reported by Allmann (1968) for the pyroaurite-sjögrenite ($Mg_3Fe^{3+}-CO_3$ LDHs) crystals from Långban: rhombohedral low-temperature polymorph (pyroaurite) is always found in the outermost shell of natural crystals.

TABLE 4. Selected bond lengths (Å) in crystals of disordered quintinite-2H.

Bond	Q1	Q2
M—OH	2.017(2)	2.020(1) 6 ×
C1—O1	1.20(3)	1.21(1) 3 ×
C2—O2	1.24(3)	1.22(1) 3 ×

Finally, the cation ordering and superstructures observed in quintinite polytypes as reported by Krivovichev *et al.* (2010*a,b*), are probably common to many natural and synthetic LDHs. In particular, it is noteworthy that many minerals previously identified as manasseite or hydrotalcite are in fact different polytypes of quintinite. For example, the first structure determination of ‘hydrotalcite’ was done on the mineral with the formula $Mg_4Al_2(OH)_{12}(CO_3)(H_2O)_3$, which is obviously quintinite (Allmann and Jepsen, 1969). In 1987, Drits *et al.* reported results of powder XRD studies of “manasseite”, again with the formula $Mg_4Al_2(OH)_{12}(CO_3)(H_2O)_3$, which can now be identified as quintinite-2H. Distinction of quintinite from hydrotalcite and manasseite is by means of the Mg:Al ratio (2:1 vs. 3:1) (Chao and Gault, 1997). The Mg₂Al stoichiometry shows a strong tendency to cation ordering and the formation of superstructures. However, the present work also demonstrated that Mg,Al-disordered quintinite also exists and it is not clear whether or not the Mg,Al disorder is

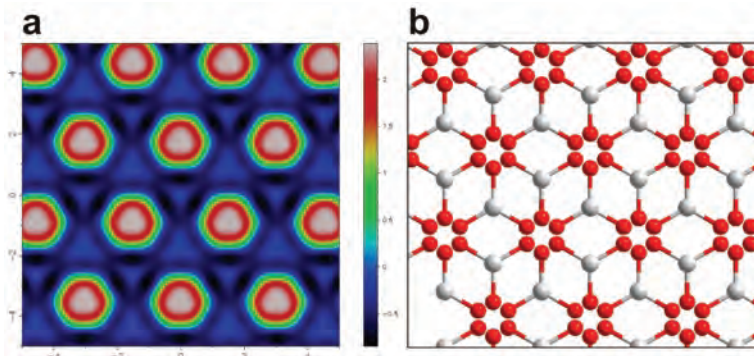


FIG. 4. Electron density distribution map at the level $z = \frac{1}{4}$ (a) and modelled distribution of carbonate ions in the interlayer (b).

specifically three-dimensional, i.e. concerns only stacking disorder of fully ordered layers, or is also present within the metal hydroxide layers.

Acknowledgements

The authors are grateful to the referees for their remarks and to the Principal Editor, Mark Welch, for extensive corrections. This work was supported by the Russian Foundation for Basic Research (grant # 10-05-00431) and the President of Russian Federation Grant for Young Candidates of Sciences (to AAZ, grant MK-1783.2010.5).

References

- Allmann, R. (1968) The crystal structure of pyroaurite. *Acta Crystallographica*, **B24**, 972–979.
- Allmann, R. and Jepsen, H.P. (1969) Die struktur des Hydrotalkits. *Neues Jahrbuch für Mineralogie, Monatshefte*, **1969**, 544–551.
- Arakcheeva, A.V., Pushcharovskii, D.Yu., Atencio, D. and Lubman, G.U. (1996) Crystal structure and comparative crystal chemistry of $\text{Al}_2\text{Mg}_4(\text{OH})_{12}(\text{CO}_3)_3\text{H}_2\text{O}$, a new mineral from the hydrotalcite–manasseite group. *Crystallography Reports*, **41**, 972–981.
- Bellotto, M., Rebours, B., Clause, O., Lynch, J., Bazin, D. and Elkaim, E. (1996) A reexamination of hydrotalcite crystal chemistry. *Journal of Physical Chemistry*, **100**, 8527–8534.
- Bonaccorsi, E., Merlino, S. and Orlandi, P. (2007) Zincalstibite, a new mineral, and cualstibite: crystal chemical and structural relationships. *American Mineralogist*, **92**, 198–203.
- Chao, G.Y. and Gault, R.A. (1997) Quintinite- $2H$, quintinite- $3T$, charmarite- $2H$, charmarite- $3T$ and caresite- $3T$, a new group of carbonate minerals related to the hydrotalcite/manasseite group. *The Canadian Mineralogist*, **35**, 1541–1549.
- Cooper, M.A. and Hawthorne, F.C. (1996) The crystal structure of shigaite, $[\text{AlMn}_2^{2+}(\text{OH})_6]_3(\text{SO}_4)_2\text{Na}(\text{H}_2\text{O})_6\{\text{H}_2\text{O}\}_6$, hydrotalcite-group mineral. *The Canadian Mineralogist*, **34**, 91–97.
- Drits, V.A., Sokolova, T.N., Sokolova, G.V. and Cherkashin, V.I. (1987) New members of the hydrotalcite–manasseite group. *Clays and Clay Minerals*, **35**, 401–417.
- Evans, D.G. and Slade, R.C.T. (2006) Structural aspects of layered double hydroxides. Pp. 1–87 in: *Layered Double Hydroxides* (X. Duan and D.G. Evans, editors). Springer, Berlin.
- Huminicki, D.M.C. and Hawthorne, F.C. (2003) The crystal structure of nikischerite, $\text{NaFe}_6^{2+}\text{Al}_3(\text{SO}_4)_2(\text{OH})_{18}(\text{H}_2\text{O})_{12}$, a mineral of the shigaite group. *The Canadian Mineralogist*, **41**, 79–82.
- Kim, D., Huang, C., Lee, H., Han, I., Kang, S., Kwon, S., Lee, J., Han, Y. and Kim, H. (2003) Hydrotalcite-type catalysts for narrow-range oxyethylation of 1-dodecanol using ethyleneoxide. *Applied Catalysis A: General*, **249**, 229–240.
- Krivovichev, S.V., Yakovenchuk, V.N., Zhitova, E.S., Zolotarev, A.A., Pakhomovsky, Ya.A. and Ivanyuk, G.Yu. (2010a) Crystal chemistry of natural layered double hydroxides. 1. Quintinite- $2H$ - $3c$ from Kovdor alkaline massif, Kola peninsula, Russia. *Mineralogical Magazine*, **74**, 821–832.
- Krivovichev, S.V., Yakovenchuk, V.N., Zhitova, E.S., Zolotarev, A.A., Pakhomovsky, Ya.A., Ivanyuk, G.Yu. (2010b) Crystal chemistry of natural layered double hydroxides. 2. Quintinite- $1M$: first evidence of monoclinic polytype in $M^{2+}\text{-}M^{3+}$ layered double hydroxides. *Mineralogical Magazine*, **74**, 833–840.
- Merlino, S. and Orlandi, P. (2001) Carraraite and

- zaccagnaite, two new minerals from the Carrara marble quarries: their chemical compositions, physical properties, and structural features. *American Mineralogist*, **86**, 1293–1301.
- Pausch, I., Lohse, H.-H., Schurmann, K. and Allmann, R. (1986) Synthesis of disordered and Al-rich hydrotalcite-like compounds. *Clays and Clay Minerals*, **34**, 507–510.
- Richardson, M.C. and Braterman, P.S. (2007) Infrared spectra of oriented and nonoriented layered double hydroxides in the range from 4000 to 250 cm⁻¹, with evidence for regular short-range order in a synthetic magnesium-aluminum LDH with Mg:Al = 2:1 but not with Mg:Al = 3:1. *Journal of Physical Chemistry*, **C111**, 4209–4215.
- Rius, J. and Allmann, R. (1984) The superstructure of the double layer mineral wermlandite $[\text{Mg}_7(\text{Al}_{0.57}\text{Fe}_{0.43})_2(\text{OH})_{18}]^{2+}[(\text{Ca}_{0.6}\text{Mg}_{0.4})(\text{SO}_4)_2(\text{H}_2\text{O})_{12}]^{2-}$.
- Zeitschrift für Kristallographie*, **168**, 133–144.
- Rius, J. and Plana, F. (1986) Contribution to the superstructure resolution of the double layer mineral motukoreaita. *Neues Jahrbuch für Mineralogie*, **6**, 263–272.
- Sheldrick, G.M. (2008) A short history of SHELX. *Acta Crystallographica*, **A64**, 112–122.
- Sideris, P.J., Nielsen, U.G., Gan, Z.H. and Grey, C.P. (2008) Mg/Al ordering in layered double hydroxides revealed by multinuclear NMR spectroscopy. *Science*, **321**, 113–117.
- Steeds, J.W. and Morniroli, J.P. (1992) Selected area electron diffraction (SAED) and convergent beam electron diffraction (CBED). Pp. 37–84 in: *Minerals and Reactions at the Atomic Scale* (P.R. Buseck, editor). Reviews in Mineralogy, **27**, Mineralogical Society of America, Washington, D.C.

PIV

NATURAL DOUBLE LAYERED HYDROXIDES: STRUCTURE, AND INFORMATION STORAGE CAPACITY

The paper “Natural double layered hydroxides: structure, chemistry, and information storage capacity” by Krivovichev S.V., Yakovenchuk V.N., Zhitova E.S. was published in Minerals as Advanced Materials II (Ed. S.V.Krivovichev), Springer Verlag (2012, pp. 87-91).

Reprinted with kind permission of Springer Science and Business Media.

DOI: 10.1007/978-3-642-20018-2_9

Concept: Prof. Dr. S.V. Krivovichev

Sampling and measurement: E.S. Zhitova, Prof. Dr. S.V. Krivovichev, V.N. Yakovenchuk

Data analysis: Prof. Dr. S.V. Krivovichev, E.S. Zhitova, V.N. Yakovenchuk

Writing the manuscript: Prof. Dr. S.V. Krivovichev, E.S. Zhitova

Natural Double Layered Hydroxides: Structure, Chemistry, and Information Storage Capacity

Sergey V. Krivovichev, Victor N. Yakovenchuk, and Elena S. Zhitova

1 Introduction

Layered double hydroxides (LDHs) constitute an important group of materials with many applications ranging from catalysis and absorption to carriers for drug delivery, DNA intercalation and carbon dioxide sequestration (Rives 2001; Duan and Evans 2006). The structures of LDHs are based upon double brucite-like hydroxide layers $[M_n^{2+}M_m^{3+}(OH)_{2(m+n)}]^{m+}$, where $M^{2+} = Mg^{2+}$, Fe^{2+} , Mn^{2+} , Zn^{2+} , etc.; $M^{3+} = Al^{3+}$, Fe^{3+} , Cr^{3+} , Mn^{3+} , etc. The positive charge of the layer is compensated by interlayer species that may consist of anions (CO_3^{2-} , Cl^- , SO_4^{2-} , etc.) or both anions and cations (Na^+ , Ca^{2+} , Sr^{2+} , etc.). Structural features of LDHs such as cation ordering, charge distribution and polytypism have an immediate influence upon their properties and have been under extensive experimental and theoretical investigations recently. In particular, Mg-Al cation order is important for catalytic activity of MgAl LDHs correlated with the numbers of Al^{3+} sites at the closest distance from an Al^{3+} site (Kim et al. 2003). Different distribution of Al in a Mg hydroxide matrix also results in different charge distribution in the interlayer, which is critically important for intercalation reactions.

Another area of interest in LDHs is the theory of the origin of life on Earth. Bernal (1951, 1967) first proposed that minerals played a crucial importance in the origin of life and, along this line, Cairns-Smith (1982) suggested that clay mineral

S.V. Krivovichev (✉)

Nanomaterials Research Center, Kola Science Center, the Russian Academy of Sciences,
14 Fersman Street, 184209 Moscow, Russia
and

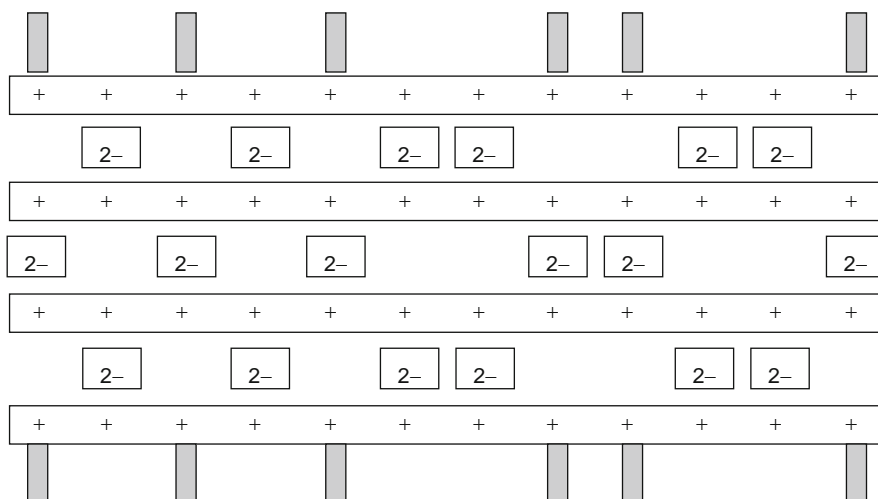
Department of Crystallography, Faculty of Geology, St. Petersburg State University,
University Emb. 7/9, 199034 St. Petersburg, Russia
e-mail: skrivovi@mail.ru

V.N. Yakovenchuk • E.S. Zhitova

Department of Crystallography, Faculty of Geology, St. Petersburg State University,
University Emb. 7/9, 199034 St. Petersburg, Russia

complexes with organic molecules could have constituted the first organisms, capable of self-assemblage, replication and mutation, and that carbon based life may have gradually evolved from such an organic–inorganic hybrid state. In his concept identified as a ‘genetic takeover’, Cairns-Smith proposed that the mechanisms of replication, information storage and transfer were first adapted by crystals of clay minerals, where bits of information were ciphered in crystal defects. Due to excellent intercalation properties of clays, they accommodated in their interlayers variety of biologically active molecules that took over replication mechanisms from mineral crystals and transferred them to biological systems.

Kuma et al. (1989) and Arrhenius (2003) proposed that, instead of clays, LDHs may serve as matrices for the origin of life in prebiotic systems. In particular, he noted that LDHs easily form as hydration products at ocean weathering of basalts, at serpentinization, etc. Of special interest is the fougereite or green rust, a mixed-valent Fe^{2+} – Fe^{3+} LDH, that could have a widespread occurrence in the Archean ocean. In development of these ideas, Greenwell and Coveney (2006) proposed mechanism of prebiotic information storage and transfer in LDH matrices on the basis of replication and conservation of M^{3+} – M^{2+} cation arrangements. According to their proposal (Fig. 1), pattern of M^{3+} sites in one layer may be transferred through the crystal by controlled location of interlayer anions (CO_3^{2-} , SO_4^{2-}). Information is stored in LDH by the arrangement of trivalent cation sites. The presence of this site is denoted ‘1’ and its absence as ‘0’. In the model shown in Fig. 1, the sequence of the sites provides a string of binary data. When entering into



Both top and bottom surfaces are: [101010011001]

Fig. 1 Schematic to show information encoded at the external surfaces of LDH polytypes with a three-layer repeat structure. The ‘+’ signs indicate positions of trivalent metal sites, ‘2-’ in boxes are divalent anions. See text for details (Reproduced with permission from Greenwell and Coveney (2006))

interlayer space, divalent anions will position into sites located around the positive charge ('1'). Thus the arrangement of the positive sites in the next layer will be exactly complementary to that of the previous layer. In the absence of stacking faults, defects and impurities, the alternating sequences of bit strings will propagate along the direction perpendicular to the layers. When LDH crystal gets too large and cleaves, it will replicate itself either by splitting or by epitaxial growth of another crystal.

If the proposed mechanism is realized in natural systems, it can be exploited by humans under laboratory conditions for creation of new subnanometer matrices for information storage and transfer. Thus the purpose of this contribution is to investigate possibility of this mechanism on the basis of current knowledge on natural LDHs. First, we briefly summarize basic chemical and structural factors affecting chemical and structural diversity of LDH minerals. Then we shall discuss the reliability of cation ordering in the information transfer and storage on the basis of our recent experimental studies in this field.

2 Natural LDHs: Structure and Chemistry

There are at least 38 minerals that can be considered as direct analogs of LDH materials with octahedrally coordinated metal cations (Table 1).

The main factors affecting their chemical diversity are:

1. Chemical nature of the M^{2+} and M^{3+} cations;
2. The $M^{2+}:M^{3+}$ ratio with the ratios 2:1 and 3:1 being the most common, which is the result of most preferable cation ordering patterns (Fig. 2); in minerals with $M^{2+}:M^{3+} = 2:1$, the $M^{2+}-M^{3+}$ ordering was experimentally confirmed in LDH sulfates (motukoreite, shigaite, and nikisherite), LDH antimonates (zincalstibite and cualstibite) and LDH carbonates (quintinites, see below); it is also noteworthy that Mg-Al/Fe ordering has been observed in wermlandite, the only mineral with the ratio $M^{2+}:M^{3+} = 7:2$ (Rius and Allmann 1984);
3. Chemical nature of interlayer anions and cations (if any): there are minerals that contain Na^+ or Ca^{2+} cations in the interlayer space.

Another important aspect of the crystal chemistry of LDHs is polytypism.

Polytype diversity of LDHs has been considered in details by Bookin and Drits (1993), Bookin et al. (1993), and Drits and Bookin (2001), who elaborated a structural nomenclature for the polytypes observed in this group, which is summarized below.

In the plane perpendicular to the direction of layer stacking, cations and anions may occupy three distinct sites: **A**, **B** and **C** (similar to the sites of spheres in closest packings). The upper (**A**, **B**, **C**) and lower (**a**, **b**, **c**) case symbols are reserved for positions of hydroxyls and cations, respectively. For instance, if hydroxyl anions of the layer are in the **A** and **C** sites, the cations occupy the **b** sites, and the layer has

Table 1 Natural double layered hydroxides and their crystal chemical parameters

M ²⁺ :M ³⁺	Mineral name	Chemical formula	Space group	Unit-cell parameters	Ref
LDHs with monovalent interlayer anions					
3:1	Iowaite	[Mg ₃ Fe ³⁺ (OH) ₈][Cl(H ₂ O) ₂]	R-3m	3.118–24.113	1
3:1	Woodallite	[Mg ₃ Cr ³⁺ (OH) ₈][Cl(H ₂ O) ₂]	R-3m	3.103–24.111	2
3:1	Meixnerite	[Mg ₃ Al(OH) ₈][(OH)(H ₂ O) ₂]	R-3m	3.046–22.93	3
	Droninoite	[Ni ₃ Fe ³⁺ (OH) ₈][Cl(H ₂ O) ₂]	R-3m	6.206–46.184	4
2:1	Chlormagaluminite	[Mg ₄ Al ₂ (OH) ₁₂][Cl ₂ (H ₂ O) ₂]	P6 ₃ /mmc	5.29–15.46	5
?	Jamborite	[Ni ²⁺ ,Ni ³⁺ ,Fe](OH) ₂ [OH, S,H ₂ O]	hex	3.07–23.3	6
LDH carbonates					
3:1	Pyroaurite	[Mg ₆ Fe ₂ ³⁺ (OH) ₁₆] [(CO ₃) (H ₂ O) ₄]	R-3m	3.111–23.504	7
	Sjögrenite	[Mg ₆ Fe ₂ ³⁺ (OH) ₁₆] [(CO ₃) (H ₂ O) ₄]	P6 ₃ /mmc	3.113–15.61	8
	Hydrotalcite	[Mg ₆ Al ₂ (OH) ₁₆] [(CO ₃) (H ₂ O) ₄]	R-3m	3.054–22.81	9
	Manasseite	[Mg ₆ Al ₂ (OH) ₁₆] [(CO ₃) (H ₂ O) ₄]	n.d.	6.12–15.34	7
	Stichtite	[Mg ₆ Cr ₂ ³⁺ (OH) ₁₆] [(CO ₃) (H ₂ O) ₄]	R-3m	3.096–23.507	10
	Barbertonite	[Mg ₆ Cr ₂ ³⁺ (OH) ₁₆] [(CO ₃) (H ₂ O) ₄]	P6 ₃ /mmc	3.097–15.619	10
	Desautelsite	[Mg ₆ Mn ₂ ³⁺ (OH) ₁₆] [(CO ₃) (H ₂ O) ₄]	R-3m	3.114–23.39	11
	Reevesite	[Ni ₆ Fe ₂ ³⁺ (OH) ₁₆] [(CO ₃) (H ₂ O) ₃]	R-3m	3.085–23.355	12
	Takovite	[Ni ₆ Al ₂ (OH) ₁₆] [(CO ₃) (H ₂ O) ₃]	R-3m	3.025–22.595	13
2:1	Comblainite	[Mg ₄ Co ₂ ³⁺ (OH) ₁₂] [(CO ₃) (H ₂ O) ₄] ?	R-3m	3.038–22.79	14
	Caresite-3T	[Fe ₄ ²⁺ Al ₂ (OH) ₁₂] [(CO ₃) (H ₂ O) ₃]	P6 ₃ 22	10.985–15.10	15
	Quintinite-2H	[Mg ₄ Al ₂ (OH) ₁₂] [(CO ₃) (H ₂ O) ₃]	P-62m	5.283–15.150	16
	Quintinite-3T	[Mg ₄ Al ₂ (OH) ₁₂] [(CO ₃) (H ₂ O) ₃]	P3 ₁ 2 ₁ ?	10.558–22.71	15
	Charmarite-2H	[Mn ₄ ²⁺ Al ₂ (OH) ₁₂] [(CO ₃) (H ₂ O) ₃]	P6 ₃ 22	10.985–15.10	15
	Charmarite-3T	[Mn ₄ ²⁺ Al ₂ (OH) ₁₂] [(CO ₃) (H ₂ O) ₃]	P3 ₁ 2 ₁ ?	10.985–22.63	15
2:1	Karchevskyite	[Mg ₁₈ Al ₉ (OH) ₅₄][Sr ₂ (CO ₃ , PO ₄) ₉ (H ₂ O,H ₃ O) ₁₁]	trigonal	16.055–25.66	32
	Zaccagnaite	[Zn ₄ Al ₂ (OH) ₁₂] [(CO ₃) (H ₂ O) ₃]	P6 ₃ /mmc	3.073–15.114	17
5:1	Coalingite	[Mg ₁₀ Fe ₂ ³⁺ (OH) ₂₄] [(CO ₃) (H ₂ O) ₂]	R-3m	3.12–37.4	18
6:1	Brugnatellite	[Mg ₆ Fe ³⁺ (OH) ₁₄] [(CO ₃) _{0.5} (H ₂ O) ₄] ?	n.d.	5.47–15.97	19

(continued)

Table 1 (continued)

M ²⁺ :M ³⁺	Mineral name	Chemical formula	Space group	Unit-cell parameters	Ref
LDH sulfates					
5:4	Carrboydite	[Ni ₅ Al ₄ (OH) ₁₈] [(SO ₄) ₂ (H ₂ O) ₁₀]	n.d.	9.14–10.34	20
5:3	Glaucoberinitite	[Zn ₁₀ Al ₆ (OH) ₃₂] [(SO ₄) ₃ (H ₂ O) ₁₈]	n.d.	3.070–32.65	21
3:1	Honessite	[Ni ₆ Fe ₂ ³⁺ (OH) ₁₆] [(SO ₄) ₂ (H ₂ O) ₄]	n.d.	3.083–26.71	22
	Hydrohonessite	[Ni ₆ Fe ₂ ³⁺ (OH) ₁₆] [(SO ₄) ₂ (H ₂ O) ₇]	n.d.	3.087–33.4	22
2:1	Motukoreaita	[Mg ₆ Al ₃ (OH) ₁₈] [Na _{0.6} (SO ₄) ₂ (CO ₃) ₂ (H ₂ O) ₁₂]	R-3m	9.172–33.51	23
11:3	Mountkeithite	[Mg ₁₁ Fe ₃ ³⁺ (OH) ₂₈] [(SO ₄) _{1.5} (H ₂ O) ₁₁ ?]	n.d.	10.698–22.545	24
2:1	Shigaite	[Mn ₆ Al ₃ (OH) ₁₈] [Na _{0.6} (SO ₄) ₂ (H ₂ O) ₁₂]	R-3	9.512–33.074	25
	Nikisherite	[Fe ₆ ²⁺ Al ₃ (OH) ₁₈] [Na _{0.6} (SO ₄) ₂ (H ₂ O) ₁₂]	R-3	9.347–33.000	26
7:2	Wermlandite	[Mg ₇ Al ₂ (OH) ₁₈] [Ca _{0.5} (SO ₄) ₂ (H ₂ O) ₁₂]	P-3c1	9.303–22.57	27
2:1	Woodwardite	[Cu ₄ Al ₂ (OH) ₁₂] [(SO ₄) ₂ (H ₂ O) _{2–4}]	R-3m	5.306–26.77	28
5:4	Hydrowoodwardite	[Cu ₅ Al ₄ (OH) ₁₈] [(SO ₄) ₂ (H ₂ O) _n]	R-3m	3.070–31.9	29
1:1 ?	Zincowoodwardite	[Zn ₂ Al ₂ (OH) ₈] [(SO ₄) ₂ (H ₂ O) _n]	P-3	3.036–8.85	30
5:3	Natroglaucocerinitite	[Zn ₂₀ Al ₁₂ (OH) ₆₄] [Na ₆ (SO ₄) ₉ (H ₂ O) ₃₆]	n.d.	n.d.	31
LDH antimonites					
2:1	Zincalstibite	[Zn ₂ Al(OH) ₆][Sb(OH) ₆]	P-3	5.321–9.786	33
	Cualstibite	[Cu ₂ Al(OH) ₆][Sb(OH) ₆]	P-3	9.150–9.745	33
LDH with variable interlayer content					
?	Fougerite	[Fe _{1-x} ²⁺ Fe _x ³⁺ Mg _y (OH) _{2+2y}] [_{x/nAⁿ⁻m(H₂O)}] with x/(1 + y) = 0.25–0.33 and m ≤ (1 – x + y)	variable	variable	34

n.d. = not determined

References: (1) Braithwaite et al. 1994; (2) Grguric et al. 2001; (3) Koritník and Suesse 1975; (4) Chukanov et al. 2009; (5) Kashaev et al. 1982; (6) Morandi and Dalrio 1973; (7) Taylor 1973; (8) Ingram and Taylor 1967; (9) Allmann and Jepsen 1969; (10) Mills et al. 2011; (11) Dunn et al. 1979; (12) Song and Moon 1998; (13) Bish and Brindley 1977; (14) Piret and Deliens 1980; (15) Chao, Gault, 1997; (16) Arakcheeva et al. 1996; (17) Merlino and Orlandi 2001; (18) Pastor-Rodriguez and Taylor 1971; (19) Fenoglio 1938; (20) Nickel and Clarke 1976; (21) Raade et al. 1985; (22) Bish and Livingstone 1981; (23) Rius and Plana 1986; (24) Hudson and Bussell (1981); (25) Cooper and Hawthorne 1996; (26) Huminicki and Hawthorne 2003; (27) Rius and Allmann 1984; (28) Nickel 1976; (29) Witzke 1999; (30) Witzke and Raade 2000; (31) mineral approved in 1995, but description has not yet been published; (32) Britvin et al. 2008; (33) Bonaccorsi et al. 2007; (34) Trolard et al. 2007

Fig. 2 2D M^{2+} - M^{3+} cation superstructures in natural LDHs (M^{2+} and M^{3+} sites are shown as green and orange hexagons, respectively):
(a) ideal brucite-like layer;
(b) layer with M^{2+} : $M^{3+} = 2:1$;
(c) layer with M^{2+} : $M^{3+} = 3:1$;
(d) layer with M^{2+} : $M^{3+} = 7:2$

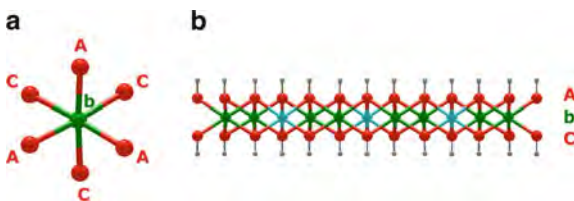
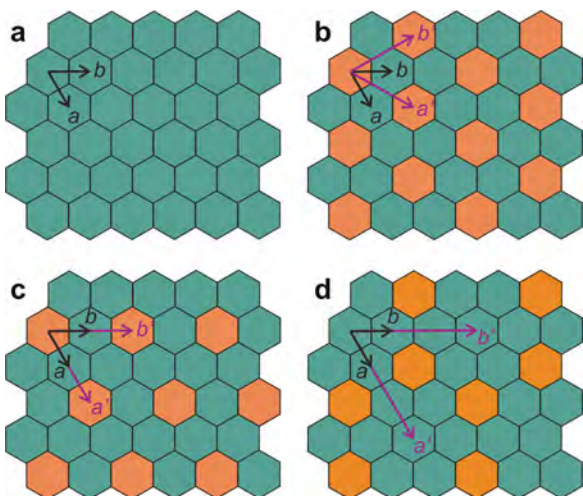
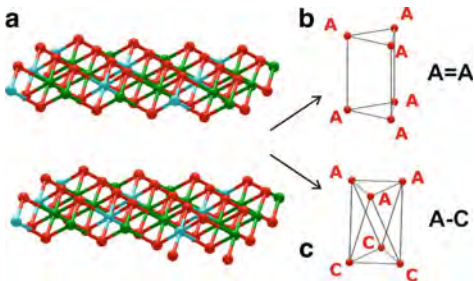


Fig. 3 Projection of metal-centered octahedron with identification of cation position as b and anion positions as A and C (a) and projection of double hydroxide layer parallel to its extension (b)

Fig. 4 The interlayer space in the structures of LDHs (a) may consist either from trigonal prisms (b): P-type interlayer or octahedra (c): O-type interlayer



a structural formula \mathbf{AbC} (Fig. 3). Since positions of the cations within the layer are uniquely determined by the hydroxyl positions, they can be omitted.

Stacking of two layers may result in formation of two different types of interlayers (Fig. 4). In the case when upper hydroxide sheet of the lower layer and lower hydroxide sheet of the upper layer have the same notations (e.g., A and A), interlayer may be represented as consisting of trigonal prisms (Fig. 4b). This type of

interlayer is referred to as a P-type and denoted with an equal sign (=) (e.g., ...A = A...). In the case when upper hydroxide sheet of the lower layer and lower hydroxide sheet of the upper layer have different notations (e.g., A and B), interlayer may be represented as consisting of elongated octahedra (Fig. 4c). This type of interlayer is referred to as a O-type and denoted with a dash (–) (e.g., ...A–B...).

Using this simple and elegant scheme of notations, Bookin and Drits (1993) derived all two- and three-layer LDH polytypes and six-layer rhombohedral polytypes and calculated their powder X-ray diffraction patterns. For instance, there are exactly three two-layer polytypes, ...AC = CA = AC..., ...AC-AB-AC..., and ...AC-BA = AC..., denoted as 2H₁, 2H₂, and 2H₃, respectively. Out of these three polytypes, 2H₁ polytype appears to be the most common in minerals (it is obviously one observed for manasseite). In this polytype, all cations occupy the **b** sites and all interlayers are of the P-type. Among three-layer polytypes, the most common is the 3R₁ polytype that has the structure ...AC = CB = BA = AC..., i.e. all its interlayers are of the P-type. On the basis of the nomenclature proposed by Bookin and Drits (1993), Bookin *et al.* (1993) investigated experimentally studied natural LDHs and reported occurrence of two- and three-layer polytypes 2H₁ and 3R₁ in CO₃-bearing minerals. In contrast, in sulfate-bearing LDHs, the situation is more complex: both one- and three-layer polytypes are observed with both P- and O-type interlayers. The nomenclature was further illustrated and exemplified by Drits and Bookin (2001). However, despite its exhaustive and rigorous character in derivation of the polytypes, this nomenclature does not take into account such important structural feature of LDHs as an ordering of M²⁺ and M³⁺ cations within the double hydroxide layers.

3 Cation Ordering in Natural Mg₂Al LDHs: Recent Results

All the structural studies on synthetic LDHs deal with powder samples that prevent elucidation of such fine details of structure architecture as formation of superstructures due to cation ordering.

Detection of the cation ordering is especially problematic in synthetic powder samples and, in particular, in synthetic quintinites (Mg₂Al-CO₃ LDHs). Richardson and Braterman (2007) investigated short-range order in Mg-Al LDHs with Mg: Al = 2:1 and 3:1 by infrared (IR) spectroscopy in the region between 400 and 250 cm⁻¹. They studied both fresh and aged (for 24 h) LDHs and found out that aged Mg₂Al specimen shows a sharp 447 cm⁻¹band, which is diagnostic of lattice ordering and which is absent in the IR spectra of fresh Mg₂Al and both fresh and aged Mg₃Al samples. On this basis, Richardson and Braterman (2007) concluded that a disorderly as-formed Mg₂Al material through a solution-precipitation process transforms into material with regular Mg-Al order. The driving force for the ordering is to avoid direct contacts of Al(OH)₆ octahedra, which, in Mg₂Al LDHs,

is possible only through formation of a regular honeycomb superstructure. In contrast, in Mg_3Al LDHs, Al-Al avoidance may be achieved in a disordered fashion, i.e. without formation of a periodic superstructure.

Sideris et al. (2008) investigated Mg-Al ordering in Mg-Al carbonate LDHs with the Mg:Al ratio of ca. 5:1, 4:1 and 2:1 by means of combined ^1H magic angle spinning and ^{25}Mg triple-quantum magic angle spinning nuclear magnetic resonance (NMR) spectroscopy and found that the Mg^{2+} and Al^{3+} are not randomly distributed in the metal hydroxide sheets and that in Mg_2Al LDH they are ordered in a honeycomb arrangement.

As to our knowledge, the only evidence of formation of 2D cation superstructures in LDHs with $\text{M}^{2+}:\text{M}^{3+} = 3:1$ comes from nanoscale imaging of surfaces of hydrotalcite crystals with ordering pattern shown in Fig. 2c. It is worthy to note that, though other superstructures can also be theoretically constructed, the one shown in Fig. 2c has the most uniform distribution of trivalent cations over octahedral layer.

When compared to the monocation $[\text{M}(\text{OH})_2]$ octahedral layer (Fig. 2a), cation ordering results in formation of 2D supercells related to the a_{br} parameter ($\sim 3.1\text{--}3.2 \text{ \AA}$) of the brucite-like layer as following: (1) for the hexagonal layer with $\text{M}^{2+}:\text{M}^{3+} = 2:1$ (Fig. 2b): $a' = b' = 3^{1/2}a_{\text{br}}$ ($\sim 5.2\text{--}5.4 \text{ \AA}$); (2) for the hexagonal layer with $\text{M}^{2+}:\text{M}^{3+} = 2:1$ (Fig. 2c): $a' = b' = 2a_{\text{br}}$ ($\sim 6.3\text{--}6.4 \text{ \AA}$); (3) for the hexagonal layer with $\text{M}^{2+}:\text{M}^{3+} = 7:2$ (Fig. 2d): $a' = b' = 3a_{\text{br}}$ ($\sim 9.3 \text{ \AA}$).

In contrast to synthetic materials, natural LDHs are known to form single crystals accessible to single-crystal X-ray diffraction analysis, which allowed to identify basic features of their crystal chemistry and to demonstrate peculiarities of cation and anion ordering. Figure 5 show crystals of quintinite ($\text{Mg}_2\text{Al}-\text{CO}_3$ LDHs) varieties from Kovdor alkaline massifs, Kola peninsula, Russia (Krivovichev et al. 2010a, b; Zhitova et al. 2010). In this mineral deposit, LDH-group minerals form at the late stages of hydrothermal activity as a result of secondary hydrothermal alteration of spinel crystals. Chemical composition of the samples studied by the wave-length dispersion spectrometry using a Cameca MS-46 electron microprobe and infrared spectroscopy provided the same (within standard errors) chemical formula, $[\text{Mg}_4\text{Al}_2(\text{OH})_{12}](\text{CO}_3)(\text{H}_2\text{O})_3$. Single-crystal X-ray diffraction study revealed that the diffraction pattern of the samples quintinite- $2H\text{-}3c$ and quintinite- $1M$ was characterized by the presence of strong and sharp Bragg reflections and weakly discrete diffuse-like lines. Whereas sharp Bragg reflections originate from basic layer stacking of metal hydroxide layers, weak reflections are indicative of formation of 3-D cation superlattices due to the Mg-Al ordering. For instance, diffuse streaks in diffraction pattern of quintinite- $2H\text{-}3c$ are extended along \mathbf{c}^* and centered at $h-k \neq 3n$ relative to a supercell indexing (R -cell, $a = 5.2745(7)$, $c = 45.36(1) \text{ \AA}$). Indexing of sharp Bragg reflections only resulted in a small subcell with parameters $a = 3.045$, $c = 15.12 \text{ \AA}$, which are approximately in agreement with unit-cell parameters of the $2H_1$ polytype of Mg-Al LDHs. In the large supercell, indices of the sharp Bragg reflections correspond to conditions $h-k = 3n$ and $l = 3n$ (Fig. 6a, b). Similar situation is observed also for quintinite- $1M$.



Fig. 5 Crystals of quintinite (natural $\text{Mg}_2\text{Al}-\text{CO}_3$ LDH) polytypes from hydrothermal veins of the Kovdor alkaline massif, Kola peninsula, Russia: (a) quintinite- $2H$ - $3c$, (b) quintinite- $1M$, (c, d) quintinite- $2H$ - $1c$

The unit-cell parameters obtained for the two samples are given in Table 2. It is noteworthy that, in quintinite- $2H$ - $3c$, Mg-Al ordering results in formation of threefold superstructure relative to the usual hexagonal $2H$ polytype, whereas, in quintinite- $1M$, cation ordering and superlattice formation results in dramatic reduction of symmetry: from rhombohedral (as in $3R$ polytype) to monoclinic (and thus the sample should be qualified as a $1M$ polytype).

The structures of all studied LDH crystals consists of metal hydroxide layers, $[\text{Mg}_2\text{Al}(\text{OH})_6]^+$, and disordered interlayer (Fig. 7a). According to LDH polytype nomenclature (see above), the layer stacking in quintinite- $2H$ - $3c$ can be described as $\dots \text{AC} = \text{CA} = \text{AC} \dots$, with **A** and **C** being positions of hydroxide ions and **b** position of cations (in the same manner as in closest packing of equal spheres). The sequence of layers within the unit cell can be described as $\dots \text{AC} = \text{CA} = \text{AC} = \text{CA} = \text{AC} = \text{CA} \dots$, since the unit cell contains exactly six double hydroxide layers.

Thus, in terms of layer stacking sequence, the structure clearly has a pseudo-period with *c* parameter of about 15.12 Å, i.e. three times smaller than one observed experimentally. The reason for tripling the *c* parameter is Mg-Al ordering in the $[\text{Mg}_2\text{Al}(\text{OH})_6]^+$ layer. There are three symmetry-independent octahedral cation

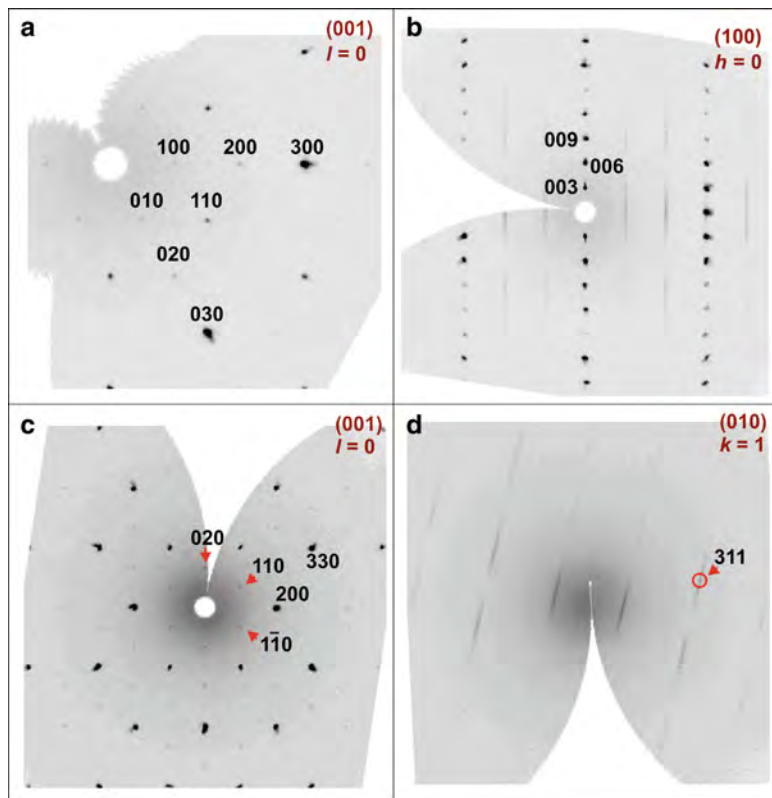


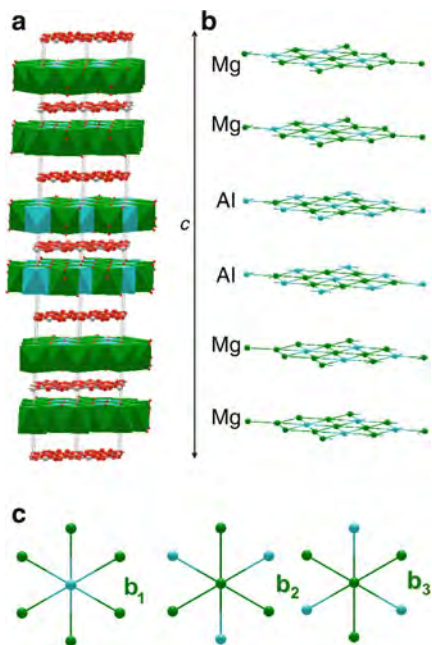
Fig. 6 Reconstructed sections of reciprocal diffraction space showing sharp and strong Bragg reflections and weak diffuse-like superstructure reflections for crystal quintinite-2H-3c (**a** and **b**) and quintinite-1M (**c** and **d**). Superstructure reflections are indicated by red arrows

Table 2 Crystallographic data for natural $\text{Mg}_2\text{Al}-\text{CO}_3$ LDHs (quintinites)

Sample	Quintinite-2H-3c	Quintinite-1M
Symmetry	Rhombohedral	Monoclinic
Space group	$R\bar{3}2$	$C2/m$
a [Å]	5.2745	5.2662
b [Å]	—	9.114
c [Å]	45.364	7.766
β [$^\circ$]	—	103.17
V [Å 3]	1093.0	362.9

sites in the structure of quintinite-2H-3c. Since the site-scattering factors of Mg^{2+} and Al^{3+} cations are nearly identical, the only way to distinguish between Mg and Al sites is to analyse distribution of the M-O bond lengths. The structure refinement indicates one M site with the M bond lengths in the range of 1.936–1.940 Å

Fig. 7 Crystal structure of quintinite- $2H\text{-}3c$ (a) and stacking of Mg_2Al cation arrays with the $[\text{Mg}_4\text{Al}_2]$ repeat sequence (b) and three different positions of the arrays (c)



(assigned to Al) and two M sites with the M-O bond lengths of 2.042–2.045 and 2.070–2.077 Å (assigned to Mg). According to the Bookin and Drits (1993) nomenclature, in $2H$ polytype, all anions are either in **A** or **C** positions, whereas all cations are in the **b** positions. However, the sequence of the **b** positions if seen along the *c* axis is occupied by Mg and Al cations differently. This sequence can be written as $[\text{MgMgMgMgAlAl}]$ or $[\text{Mg}_4\text{Al}_2]$, taking into account that the content given in the square brackets corresponds to the *c* parameter repeat. Considering possible relative positions of the 2-D Mg_2Al cation array, one may distinguish exactly three different Mg_2Al arrays related to each other by either *a* or *b* translations (Fig. 7b). These arrays may be indicated as **b**₁, **b**₂ and **b**₃ (since all cations are in the **b** positions). Therefore the full description of the layer sequence (i.e. description that takes into account cation ordering) can be written as $\dots = \text{Ab}_1\text{C} = \text{Cb}_1\text{A} = \text{Ab}_2\text{C} = \text{Cb}_2\text{A} = \text{Ab}_3\text{C} = \text{Cb}_3\text{A} = \dots$

The layer stacking in quintinite- $1M$ (Fig. 8a) can be described as $\dots = \text{AB} = \text{BC} = \text{CA} = \dots$, i.e. it corresponds to a rhombohedral polytype structure typical for most synthetic Mg-Al LDHs. However, because of the cation ordering, the situation becomes more complex and can be deciphered from the analysis of relative position of the 2-D Mg_2Al cation arrays (Fig. 8b–e). First, it is obvious that cations in quintinite- $1M$ are located in all possible sites, **a**, **b**, and **c**, so that the full description of the layer sequence should be written as $\dots = \text{AcB} = \text{BaC} = \text{CbA} = \dots$ In the case of complete Mg-Al disorder, structure with this sequence would have a rhombohedral symmetry (space group $R\text{-}3m$), but cation ordering results in symmetry reduction and formation of superstructure. As can be seen from

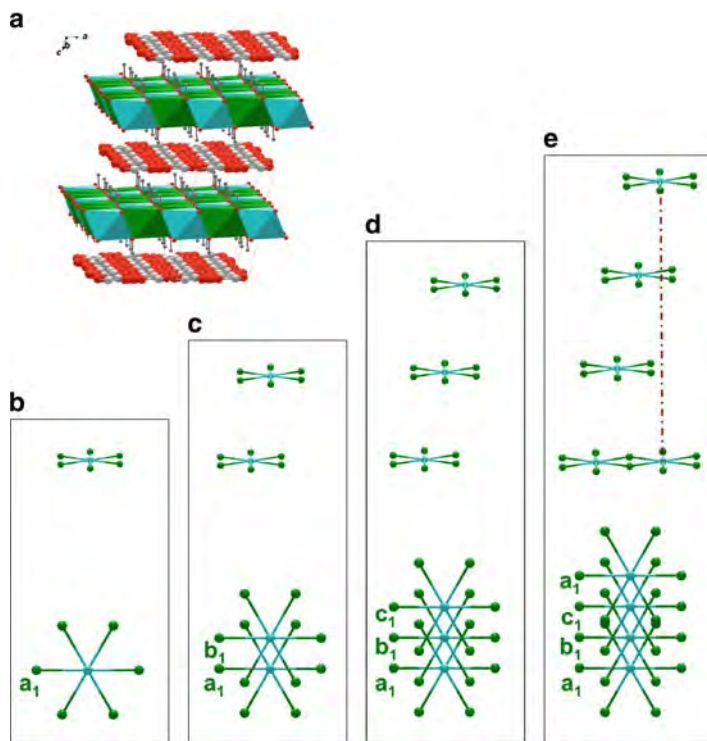


Fig. 8 Crystal structure of quintinite-1*M* (**a**) and schemes of stacking of Mg₂Al cation arrays along the direction perpendicular to the layers (**b–e**)

Fig. 8b–d, Al cations in adjacent Mg₂Al arrays are located in one plane, which is a mirror plane *m* in the space group *C2/m*. This results in disappearance of the threefold symmetry axis perpendicular to the layers and transition from rhombohedral to monoclinic symmetry. In order to distinguish between **a**, **b** and **c** positions occupied by Mg and Al cations in the Mg₂Al array, we identify them as **a**₁, **a**₂, **a**₃, etc. Thus, the complete layer stacking sequence can be described as ... = **A**₁**B** = **B**₁**C** = **C**₁**A** = ... It is of theoretical interest that the sequence ... = **A**₁**B** = **B**₁**C** = **C**₂**A** = ... possesses a trigonal symmetry with Al cations in adjacent layers segregated along a 3₁ screw axis, though this situation has not yet been observed in LDHs. According to the traditional nomenclature of polytypes, sample 2 should be called quintinite-1*M*, since it contains exactly one layer per monoclinic unit cell.

The advantage of single-crystal diffraction is the possibility to analyse electron density distribution in certain areas of a structure. Figure 9a shows electron density distribution map in quintinite-1*M* at the interlayer level of *z* = 0.25. It can be seen that electron density maxima corresponding to the O atoms of carbonate groups are associated into almost continuous toroidal regions, which makes the refinement

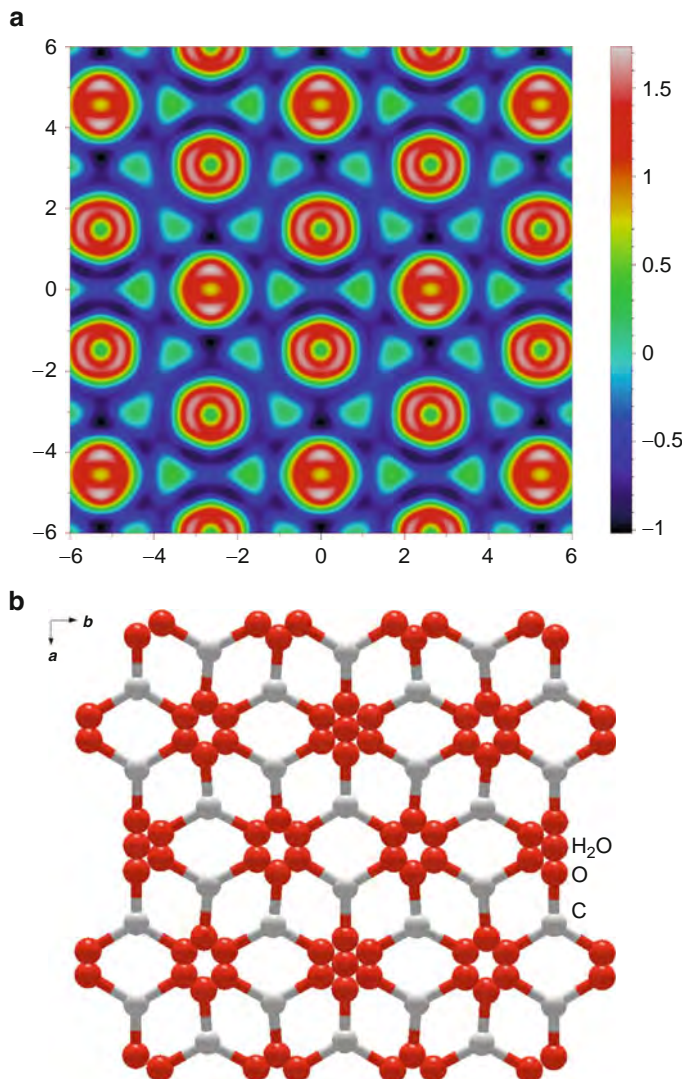


Fig. 9 Electron density Fourier map of interlayer in quintinite-1M (**a**) and model of disordered interlayer arrangement of carbonate anions and water molecules (**b**)

procedure a difficult task. Since there are no indications of any dynamic disorder effects in the structure (e.g., rotation of carbonate triangles), we suppose that the observed continuous character of the tori is due to positional disorder. Figure 9b shows an approximate identification of the electron density peaks as proposed by the refinement.

4 Discussion

The results on cation ordering in natural LDHs with $M^{2+} = Mg^{2+}$ and $M^{3+} = Al^{3+}$, which are by far the most common natural LDHs (we have observed that many samples previously identified as hydrotalcite and manasseite are in fact quintinite polytypes), demonstrate that cation ordering in double hydroxide layers is very conservative and is governed by the tendency to minimize repulsion between the M^{3+} sites. As a result, the arrangement of di- and trivalent cations is controlled by electrostatic forces that would strongly restricts information storage capacity of LDH matrices. The tendency of LDH to periodic arrangement of cations revealed in the recent studies is in disagreement with their role as prebiotic information storage materials (recall the definition of life by Schroedinger as ‘aperiodic crystal’).

In the Greenwell and Coveney’s model of information transfer in LDHs, the crucial role is devoted to the arrangement of interlayer anions. Our experimental results and literature survey indicate that this arrangement is either disordered and not controlled by the cation ordering (in carbonate LDHs) or completely ordered (in sulfate LDHs). In both cases, interlayer anions may not serve as agents in information transfer between adjacent layers.

Thus the role of LDHs as information storage matrices in prebiotic systems is rather doubtful and cannot be used in artificial systems as well.

Acknowledgements This work was supported by the Russian Foundation of Basic research (grant 10-05-00431).

References

- Allmann R, Jepsen HP (1969) Die Struktur des Hydrotalkits. N Jb Mineral Mh 1969:544–551
- Arakcheeva AV, Pushcharovskii DYu, Atencio D, Lubman GU (1996) Crystal structure and Comparative crystal chemistry of $Al_2Mg_4(OH)_{12}(CO_3)·3H_2O$, a new mineral from the hydrotalcite-manasseite group. Crystallogr Rep 41:972–981
- Arrhenius GO (2003) Crystals and life. Helv Chim Acta 86:1569–1586
- Bernal JD (1951) The physicalbasis of life. Routledge and Kegan Paul, London
- Bernal JD (1967) The origin of life. Weidenfeld and Nicolson, London
- Bish DL, Brindley GW (1977) A reinvestigation of takovite, a nickel aluminum hydroxy-carbonate of the pyroaurite group. Am Mineral 62:458–464
- Bish DL, Livingstone A (1981) The crystal chemistry and paragenesis of honessite and hydrohonessite: the sulphate analogues of reevesite. Mineral Mag 44:339–343
- Bonaccorsi E, Merlino S, Orlandi P (2007) Zincalstibite, a new mineral, and cualstibite: crystal chemical and structural relationships. Am Mineral 92:198–203
- Bookin AS, Drits VA (1993) Polytotype diversity of the hydrotalcite-like minerals. I. Possible polytypes and their diffraction patterns. Clays Clay Miner 41:551–557
- Bookin AS, Cherkashin VI, Drits VA (1993) Polytotype diversity of the hydrotalcite-group minerals. II. Determination of the polytypes of experimentally studied varieties. Clays Clay Miner 41:558–564
- Braithwaite RSW, Dunn PJ, Pritchard RG, Paar WH (1994) Iowaite, a re-investigation. Mineral Mag 58:79–85

- Britvin SN, Chukanov NV, Bekenova GK, Yagovkina MA, Antonov AV, Bogdanova AN, Krasnova NI (2008) Karchevskyite, $[\text{Mg}_{18}\text{Al}_9(\text{OH})_{54}][\text{Sr}_2(\text{CO}_3, \text{PO}_4)_9(\text{H}_2\text{O}, \text{H}_3\text{O})_{11}]$, a new mineral species of the layered double hydroxide family. *Geol Ore Deposits* 50:556–564
- Cairns-Smith AG (1982) Genetic takeover and the mineral origins of life. Cambridge University Press, Cambridge
- Chao GY, Gault RA (1997) Quintinite-2H, quintinite-3T, charmarite-2H, charmarite-3T and catesite-3T, a new group of carbonate minerals related to the hydrotalcite/manasseite group. *Can Mineral* 35:1541–1549
- Chukanov NV, Pekov IV, Levitskaya LA, Zadov AE (2009) Droninoite, $\text{Ni}_3\text{Fe}_{34}\text{Cl}(\text{OH})_8 \cdot 2\text{H}_2\text{O}$, a new hydrotalcite-group mineral species from the weathered Dronino meteorite. *Geol Ore Deposits* 51:767–773
- Cooper MA, Hawthorne FC (1996) The crystal structure of shigaite, $[\text{AlMn}_2^{2+}(\text{OH})_6]_3(\text{SO}_4)_2 \text{Na}(\text{H}_2\text{O})_6(\text{H}_2\text{O})_6$, a hydrotalcite-group mineral. *Can Mineral* 34:91–97
- Drits VA, Bookin AS (2001) Crystal structure and X-ray identification of layered double hydroxides. In: Rives V (ed) Layered double hydroxides: present and future. Nova Scientific Publishers, New York, pp 39–92
- Duan X, Evans DG (eds) (2006) Layered double hydroxides, vol 119, Structure and bonding. Springer, Berlin
- Dunn PJ, Peacor DR, Palmer TD (1979) Desautelsite, a new mineral of the pyroaurite [hydrotalcite] group. *Am Mineral* 64:127–130
- Fenoglio M (1938) Ricerche sulla brugnatellite. *Period Mineral* 9:1–13
- Greenwell HC, Coveney PV (2006) Layered double hydroxide minerals as possible prebiotic information storage and transfer compounds. *Orig Life Evol Biosph* 36:13–37
- Grguric BA, Madsen IC, Pring A (2001) Woodallite, a new chromium analogue of iowaite from the Mount Keith nickel deposit, Western Australia. *Mineral Mag* 65:427–435
- Hudson DR, Bussell M (1981) Mountkeithite, a new pyroaurite-related mineral with an expanded interlayer containing exchangeable MgSO_4 . *Mineral Mag* 44:345–350
- Huminicki DMC, Hawthorne FC (2003) The crystal structure of nikischerite, $\text{NaFeAl}_3(\text{SO}_4)_2(\text{OH})_{18}(\text{H}_2\text{O})_{12}$, a mineral of the shigaite group. *Can Mineral* 41:79–82
- Ingram L, Taylor HFW (1967) The crystal structures of sjögrenite and pyroaurite. *Mineral Mag* 36:465–479
- Kashaev AA, Feoktistov GD, Petrova SV (1982) Chlormagaluminit, $(\text{Mg}, \text{Fe}^{2+})_4\text{Al}_2(\text{OH})_{12}(\text{Cl}_2, \text{CO}_3)_2 \cdot 2\text{H}_2\text{O}$ – a new mineral of the manasseite-sjögrenite group. *Zap Vses Miner Obshch* 11:121–127 (in Russian)
- Kim D, Huang C, Lee H, Han I, Kang S, Kwon S, Lee J, Han Y, Kim H (2003) Hydrotalcite-type catalysts for narrow-range oxyethylation of 1-dodecanol using ethyleneoxide. *Appl Catal A: Gen* 249:229–240
- Koritnig S, Suesse P (1975) Meixnerite, $\text{Mg}_6\text{Al}_2(\text{OH})_{18} \cdot 4\text{H}_2\text{O}$, ein neues magnesium-aluminium-hydroxid-mineral. *Tscherm Miner Petrogr Mitt* 22:79–87
- Krivovichev SV, Yakovenchuk VN, Zhitova ES, Zolotarev AA, Pakhomovsky YA, Ivanyuk GY (2010a) Crystal chemistry of natural layered double hydroxides. 1. Quintinite-2H-3c from the Kovdor alkaline massif, Kola peninsula, Russia. *Mineral Mag* 74:821–832
- Krivovichev SV, Yakovenchuk VN, Zhitova ES, Zolotarev AA, Pakhomovsky YA, Ivanyuk GY (2010b) Crystal chemistry of natural layered double hydroxides. 2. Quintinite-1M: First evidence of a monoclinic polytype in $\text{M}^{2+}\text{-M}^{3+}$ layered double hydroxides. *Mineral Mag* 74:833–840
- Kuma K, Paplawsky W, Gedulin B, Arrhenius G (1989) Mixed-valence hydroxides as bioorganic host minerals. *Orig Life Evol Biosph* 19:573–602
- Merlino S, Orlando P (2001) Carraraite and zaccagnaite, two new minerals from the Carrara marble quarries: their chemical compositions, physical properties, and structural features. *Am Mineral* 86:1293–1301
- Mills SJ, Whitfield PS, Wilson SA, Woodhouse JN, Dipple GM, Raudsepp M, Francis CA (2011) The crystal structure of stichtite, re-examination of barbertonite, and the nature of polytypism in MgCr hydrotalcites. *Amer Mineral* 96:179–187

- Morandi N, Dalrio G (1973) Jamborite: a new nickel hydroxide mineral from the Northern Apennines, Italy. *Am Mineral* 58:835–839
- Nickel E (1976) New data on woodwardite. *Mineral Mag* 43:644–647
- Nickel EH, Clarke RM (1976) Carrboydite, a hydrated sulfate of nickel and aluminum: a new mineral from Western Australia. *Amer Mineral* 61:366–372
- Pastor-Rodriguez J, Taylor HFW (1971) Crystal structure of coalingite. *Mineral Mag* 38:286–294
- Piret P, Deliens M (1980) La comblainite, $((\text{Ni}_x^{2+}, \text{Co}_{1-x}^{3+})(\text{OH})_2)(\text{CO}_3)_{(1-x)/2} \cdot y\text{H}_2\text{O}$, nouveau minéral du groupe de la pyroaurite. *Bull Minéral* 103(1):113–117
- Raade G, Elliott CJ, Din VK (1985) New data on glaucocerinit. *Mineral Mag* 49:583–590
- Richardson MC, Braterman PS (2007) Infrared spectra of oriented and nonoriented layered double hydroxides in the range from 4000 to 250 cm^{-1} , with evidence for regular short-range order in a synthetic magnesium-aluminum LDH with Mg: Al = 2: 1 but not with Mg: Al = 3: 1. *J Phys Chem C* 111:4209–4215
- Rius J, Allmann R (1984) The superstructure of the double layer mineral wermlandite $[\text{Mg}_7(\text{Al}_{0.57}\text{Fe}_{0.43}^{3+})_2(\text{OH})_{18}]^{2+}[(\text{Ca}_{0.6}\text{Mg}_{0.4})(\text{SO}_4)_2(\text{H}_2\text{O})_{12}]^{2-}$. *Z Kristallogr* 168:133–144
- Rius J, Plana F (1986) Contribution to the superstructure resolution of the double layer mineral motukoreait. *N Jahrb Mineral Monatsh* 1986:263–272
- Rives V (ed) (2001) Layered double hydroxides: present and future. Nova Science Publishers, New York
- Sideris PJ, Nielsen UG, Gan ZH, Grey CP (2008) Mg/Al ordering in layered double hydroxides revealed by multinuclear NMR spectroscopy. *Science* 321:113–117
- Song Y, Moon HS (1998) Additional data on reevesite and its Co-analogue, as a new member of the hydrotalcite group. *Clay Miner* 33:285–296
- Taylor HFW (1973) Crystal structures of some double hydroxide minerals. *Mineral Mag* 39:377–389
- Trolard F, Bourrie F, Abdelmoula M, Refait P, Feder F (2007) Fougerite, a new mineral of the pyroaurite-iowaite group; description and crystal structure. *Clays Clay Miner* 55:323–334
- Witzke T (1999) Hydrowoodwardite, a new mineral of the hydrotalcite group from Koenigswalde near Annaberg, Saxony/Germany and other localities. *N Jahrb Mineral Monatsh* 1999:75–86
- Witzke T, Raade G (2000) Zincowoodwardite, $[\text{Zn}_{1-x}\text{Al}_x(\text{OH})_2][(\text{SO}_4)_{x/2}(\text{H}_2\text{O})_n]$, a new mineral of the hydrotalcite group. *N Jahrb Mineral Monatsh* 2000:455–465
- Zhitova ES, Yakovenchuk VN, Krivovichev SV, Zolotarev AA, Pakhomovsky YA, Ivanyuk GY (2010) Crystal chemistry of natural layered double hydroxides. 3. The crystal structure of Mg, Al-disordered quintinite-*2H*. *Mineral Mag* 74:841–848

PV

**QUINTINITE-1M FROM BAZHENOVSKOE DEPOSIT (MIDDLE URAL, RUSSIA):
CRYSTAL STRUCTURE AND PROPERTIES
(in Russian)**

The paper “Quintinite-1M from Bazhenovskoe deposit (Middle Ural, Russia): crystal structure and properties” was published in Russian language in Bulletin of Saint-Petersburg State University, Ser. 7, by Krivovichev S.V., Antonov A.A., Zhitova E.S., Zolotarev A.A., Krivovichev V.G., Yakovenchuk V.N.. Reprinted with kind permission of St.Petersburg State University Press.

Concept: Krivovichev S.V., Antonov A.A., Zhitova E.S., Krivovichev V.G.

Sampling and measurement: Antonov A.A., Zhitova E.S., Zolotarev A.A.

Data analysis: Antonov A.A., Zhitova E.S., Zolotarev A.A.

Writing the manuscript: Prof. Dr. S.V. Krivovichev, Zhitova E.S.

Abstract

Krivovichev S.V., Antonov A.A., Zhitova E.S., Zolotarev A.A., Krivovichev V.G., Yakovenchuk V.N. "Quintinite-1M from Bazhenovskoe deposit (Middle Ural, Russia): crystal structure and properties"

The paper reports data on chemical composition, crystal structure and infra-red spectra of quintinite-1M from rodingites of the Bazhenovskoe deposit (Middle Ural). The mineral was found on the walls of cavities in strongly carbonatized rodingites in association with prehnite, shabazite, phillipsite and calcite. Quintinite-1M occurs as intergrowth and druses as well as separate crystals (up to 5 mm across). Pure quintinite is goldish-white and has a nacreous lustre and perfect cleavage on basal pinacoid. Chemical analysis indicated the Mg:Al ratio equal to 2:1. The mineral is monoclinic, space group $C2/m$, $a = 5.283(3)$, $b = 9.151(4)$, $c = 7.758(4)$ Å, $\beta = 103.00(5)^\circ$, $V = 365.4(3)$ Å³. Diffraction patterns are characterized by the presence of diffuse streaks elongated along the c^* axis, which corresponds to the disorder in stacking of the double hydroxide layers. The final structure model had been refined to $R1 = 0.086$ on the basis of 471 independent reflections. The crystal structure is based upon the $[\text{Mg}_2\text{Al}(\text{OH})_6]$ double metal-hydroxide layers with partial order of octahedral cations. The interlayer is occupied by disordered carbonate groups and water molecules. The studied sample of quintinite-1M is the second find of a monoclinic quintinite polytype in the world and in Russia in particular.

Keywords: quintinite, polytype, crystal structure, rodingites, Bazhenovskoe deposit